2003

Process monitoring in end milling

Yong-hoon Choi
Iowa State University

Process monitoring in end milling

by

Yong-hoon Choi

A dissertation submitted to the graduate faculty

in partial fulfillment of the requirements for the degree of

DOCTOR OF PHILOSOPHY

Major: Industrial Engineering

Program of Study Committee:
Ranga Narayanaswami, Major Professor
Douglas Gemmill
Timothy Van Voorhis
Abhijit Chandra
Palaniappa A. Molian

Iowa State University

Ames, Iowa

2003

ProQuest Information and Learning Company
300 North Zeeb Road
P.O. Box 1346
Ann Arbor, MI 48106-1346

Graduate College

Iowa State University

This is to certify that the doctoral dissertation of

Yong-hoon Choi

has met the dissertation requirements of Iowa State University

Signature was redacted for privacy.

Major Professor

Signature was redacted for privacy.

For the Major Program

TABLE OF CONTENTS

LIST OF FIGURES

LIST OF TABLES

ABSTRACT

Monitoring cutting forces in end milling is a necessary step toward the full automation of milling. To monitor the end milling process successfully, the selection of an appropriate signal and signal processing algorithm is very important. In this research, cutting force trends and tool wear effects in ramp cut machining are experimentally observed as machining progresses.

Ramp cuts are unique in the sense that the depth of cut is continuously changing. Traditionally, a series of straight slot cuts are used to machine a deep slot. Ramp cuts in which the depth of cut is continuously changing offers an alternative. Cutting force signals, table motor currents, spindle motor currents, and tool wear in ramp cuts are experimentally observed and compared to the results of straight cuts. Trends in X, Y, and Z cutting forces for straight and ramp cuts are compared.

Tool wear and its identification and estimation are a fundamental problem in machining. With tool wear there is an increase in cutting forces, and leads to deterioration in process stability, part accuracy, and surface finish. Cutting forces using new tools are compared with cutting forces obtained from a progressively wearing tool. The wavelet transform is used for signal processing and is found to be useful for observing cutting force trends.

The Root Mean Square (RMS) value of the wavelet transformed signal and linear regression are used for tool wear estimation. Tool wear is also estimated by measuring a machined slot thickness on a coordinate measuring machine. Picture analysis of the cutting tools using a SEM and microscope are used for tool wear estimation between cutting force and tool worn area.

CHAPTER 1. INTRODUCTION

Monitoring cutting forces and tool wear effects in end milling is a necessary step toward the full automation of milling operations. To monitor the end milling process successfully, the selection of an appropriate signal and signal processing algorithm is very important. Several signals in a milling operation have been considered to monitor tool failure, for example, cutting force, torque, vibration, acoustic emission, and spindle motor current.

This research is concerned with monitoring the cutting forces present during ramp cuts in end milling. The ramp cuts are unique in that they have (i) variation in the depth of cut and (ii) the cutting force trends depend on the feed direction. Extensive experimental results have been observed progressively as new tools are being worn during machining rather than focusing on new and broken (or pre-worn) tools. Cutting force trends in the X, Y, and Z directions of ramp cuts are explained and the measured forces for a new tool and a worn tool are compared.

Machining a deep slot requires a series of cuts. Traditionally straight cuts are used for this purpose. An alternative is ramp cut milling. Ramp cut and straight cut millings are compared experimentally with respect to cutting force and tool wear. A dynamometer, current motor signals, and spindle motor signal are processed for force measurement and analysis. SEM and microscopic pictures are used for observing and estimating tool wear.

For deep slotting, the key difference between ramp and straight cuts lies in contact area between the tool and work-piece. The depth of cut in a ramp cut is continuously

changing. Consequently, contact between the tool and workpiece is twice as large in ramp cuts as it is in straight cuts when removing the same amount of material.

A Computer Numerical Control (CNC) machining center is a multifunction machine that uses a programmable mini-computer with a read–write memory to perform numeric control (NC) functions and control the machine tool. The mini computer provides basic computing capacity and data buffering as a part of the control unit. CNC machines can execute a wide variety of operations, such as milling, drilling, boring, etc., without changing the setup of a component. CNC units also allow combinations of these operations with variable spindle speeds and feed rates. By using the computer numeric control programs, CNC machines can automatically control the tool change, tool path, machining parameters, and coolant usage without complex manipulation.

The multi component dynamometer provides dynamic and quasi-static measurement of the three orthogonal components of a force acting from any direction onto the top plate. The dynamometer has high rigidity and high frequency. The high resolution enables very small dynamic changes to be measured in large force.

Traditional signal processing approaches such as segmental averages and Fourier transform generally assume that the sensor signals are stationary. However, the sensor signals in tool wear monitoring are usually non-stationary. Thus, the approaches that deal with non-stationary signals are more appropriate for process monitoring. The wavelet transform is a convenient tool for processing time varying signals (Wang, Mehrabi, and Kannatey-Asibu, 2001). The wavelet transform is better suited than the Fourier transform for monitoring the cutting force as it provides time-frequency localization of the signal. The

Fourier transform has a problem in that it transforms the signal from a time domain to a frequency domain assuming that the signals are stationary or infinite in nature (Misiti et al, 1996). Namely, it has a difficulty in describing transient components and does not convey any information pertaining to translation of the signal from the time domain to the frequency domain.

Wavelets have proven useful in the analysis of signals that contain transients, image analysis, and image/signal compression. The wavelet transform decomposes a signal into a representation that shows details and trends as a function of time. This representation can be used to characterize transient events, reduce noise, and many other applications. The wavelet transform maintains a constant time resolution regardless of frequency. Accordingly, the wavelet transform is used to analyze the force signal.

The rest of the dissertation is organized as follows. First a background on process monitoring, tool wear, and cutting force modeling is provided in Chapter 2. Observations of cutting force and tool wear effects in ramp cuts are described in Chapter 3. Tool wear monitoring and estimation in ramp cuts are provided in Chapter 4. A comparison of ramp and straight cuts is explained in Chapter 5. Tool wear estimation and monitoring spindle motor current are in Chapter 6. Conclusions are presented in Chapter 7.

CHAPTER 2. BACKGROUND

2.1 Process Monitoring

The monitoring of tool failure and tool wear has been a subject of active research. Tool wear is a complex phenomenon occurring in different ways in metal cutting processes. Generally, worn tools adversely affect the surface finish of the workpiece and therefore there is a need to develop tool wear condition monitoring systems that alert the operator to the state of the tool, and thereby avoiding undesirable consequences.

The cutting force signal is considered to provide rich information for tool failure detection in end milling and drilling operations (Li, 1998). For the purpose of process monitoring, segmental averages and the Fourier transform have been used extensively. However, the wavelet transform is increasingly being used for process monitoring. The wavelet transform has two advantages over segmental averaging (Tansel et al, 1998): first, they represent the system more accurately if the waveform is optimized by considering signal characteristics. Second, wavelet parameters can be used for many other purposes such as identification of tool breakage, run out, and flute deviation. Tansel et al (2000) used both segmental averaging and the wavelet transform as encoding methods for tool wear estimation and found the wavelet transform to be superior. Wavelet transformations require less computation than Fast Fourier Transform (FFT). For example, FFT requires $N \log_2 N$ operations for transformation of a set of N numbers while fast wavelet transformations require N operations (Tansel, Mekdeci, and Mclaughlin, 1995), and the number of operations halves when the transformations are repeated. Tansel, Mekdeci, and

Mclaughlin (1995) studied the characteristics of normal and broken tool signals in end milling operations with wavelet approximation coefficients. They observed that the variation of the estimated parameters of the wavelet transformations is very distinctive at different cutting conditions, and when the tool is broken.

Gong, Obikawa, and Shirakashi (1997) estimated tool wear in turning operations with wavelet transform based on the cutting force. Lee and Tarng (1999) used spindle motor current to monitor tool failure in end milling. They used the wavelet transform to perform a multilevel signal decomposition to extract the tool failure feature and found the four-level wavelet decomposition to be adequate (decomposition up to 4th level). Li et al. (2000) measured feed motor current to estimate the feed cutting force and monitor tool wear in turning. By comparing successive feed cutting force estimates, the onset of the accelerated tool wear was determined. El-Wardany and Elbestawi [2] investigated a stochastic model, for ceramic tools used in the finish turning of case hardened steel materials. Wang, Mehrabi, and Kannatey-Asibu (2001) used a vibration signal and the wavelet transform to monitor tool wear in turning. They observed that the vibration signals from sharp and worn tools showed clear differences.

A recent review on tool wear condition monitoring in turning (Li, 2002) particularly emphasized using the acoustic emission (AE) signal. Li and Wu (2000) used wavelet analysis and AE signals in boring to monitor tool wear.

Li, Dong, and Yuan (1999), devised a tool breakage detection system for drilling based on sensor fusion of AE and electrical current sensors. They found that the discrete wavelet transform could clearly diagnose tool breakage. Mori et al. (1999) remarked that to predict drill bit breakage, it is necessary to detect and distinguish the signal behaviors that

indicate pre-failure phenomena. They proposed a method for extracting pre-failure information from the cutting force to predict breakage of a small drill bit. Li (1999) also used AC servo motor current signal and the wavelet transform to detect breakage of small diameter drill bits. Li, Tso, and Wang (2000) used wavelet transforms and fuzzy techniques to monitor tool breakage and wear conditions according to the measured spindle and feed motor currents.

Tool wear causes increases in cutting forces and vibration. It is important that these effects of tool wear are taken into account. The cutting force models, which mainly model the cutting force under ideal conditions, can then be suitably modified and used in simulation and model based process monitoring. Tool wear estimation can also lead to optimal tool usage by changing the tool at the most appropriate time.

2.2 Modeling of Cutting Forces

The modeling of cutting forces in machining has been extensively studied, and a recent review may be found in (Ehmann et al, 1997). The mechanistic approach for modeling of cutting force has been quite successful. The mechanistic method views the machining process as a combination of chip load-cutting force relationship, cutting tool geometry, cutting process geometry, work-piece geometry and machining conditions.

The end milling process has been modeled mechanistically (Devor, Kline, and Zdeblick, 1980) and EMSIM software (http://mtamri.me.uiuc.edu) simulates forces in end milling. To obtain a complete representation of the forces on the end mill at any given instant of time, the cutter is discretized into thin, disc-like sections, similar to a stack of coins. The location of each flute on each disc is determined, and the elemental force is calculated for

each flute that engages the work-piece. The instantaneous chip thickness, the flute entry angle, and exit angle are needed in order to compute elemental cutting forces. When the feed per tooth is small compared to the radius of the cutter, the instantaneous chip thickness is calculated as

$$t_c(i,j,k) = f_t \sin\beta(i,j,k) \qquad (2.1)$$

Where, β is the wrap around angle due to the helix angle, and *i*, *j*, and *k* refer to the *i*th angular increment, *j*th axial height, and *k*th flute and f_t is the feed per tooth. The expressions for the elemental force acting normal to the rake face dF_N, and the friction force dF_T, are:

$$\begin{aligned} dF_N(i,j,k) &= K_N * dZ * t \\ dF_T(i,j,k) &= \mu * dF_N \end{aligned} \qquad (2.2)$$

Where, dZ is the disk thickness, and the coefficients K_N and μ are determined experimentally by running a series of end milling or turning experiments and measuring forces for each work-piece/tool material combination. Once the normal and friction forces are calculated for a given element, they are transformed from the K_N-μ coordinate system to the X-Y-Z coordinate system. The total force is found by integrating the elemental forces. A comprehensive modeling of end milling forces for arbitrary cutter geometry may be found in (Altintas and Engin, 2001).

Recently, advances have been made in incorporating the effect of tool wear in cutting force modeling. Elanayar and Shin (1996) developed a method to separate the ploughing forces from the shear forces on the shear plane. The forces are decomposed by first separating the shear forces from the total forces and then employing an iterative procedure to calculate the normal forces on the shear plane. The ploughing forces are modeled by taking into account the change in geometry with flank wear. Smithey, Kapoor, and DeVor (2000)

observed experimentally that in three-dimensional cutting operations in which the nose of the tool is engaged, the region of plastic flow grows linearly as the total wearland width increases. Plastic flow occurs at the front of the wearland and elastic contact is assumed at the back of the wearland. The flank of the tool is discretized into small two-dimensional elements and a contact model is used to determine the stresses on the individual elements. These stresses are added to the mechanistic force model for a sharp tool to determine the total cutting force.

2.3 Tool Wear Mechanism

2.3.1 Forms of Wear in Metal Cutting

The progressive wear of a tool takes place in two distinct ways (Boothroyd and Knight, 1989): (1) wear on the tool face characterized by the formation of a crater and resulting from the action of the chip flowing along the face, and (2) wear on the flank where a wear land is formed from the rubbing action of the newly generated workpiece surface.

Crater Wear - The crater formed on the tool face conforms to the shape of the chip underside and is restricted to the chip-tool contact area. In addition, the region adjacent to the cutting edge where sticking friction or a built-up edge occurs is subjected to relatively slight wear. Under high temperature conditions high speed steel tools wear very rapidly because of thermal softening of the tool material. Although carbide-tool materials retain their hardness at these high temperatures, solid-state diffusion can cause rapid wear. Under very high speed cutting conditions, crater wear is often the factor that determines the life of the cutting tool: the cratering becomes so severe that the tool edge is weakened and eventually fractures.

However, when tools are used under economical conditions, the wear of the tool on its flank, known as flank wear, is usually the controlling factor.

Flank Wear – Wear on the flank of a cutting tool is caused by friction between the newly machined workpiece surface and the contact area on the tool flank. Because of the rigidity of the workpiece, the worn area, referred to as the flank wear land, must be parallel to the resultant cutting direction. The width of the wear land is usually taken as a measure of the amount of wear and can be readily determined by means of a toolmaker's microscope.

2.3.2 Types and Wear Mechanism on Cutting Tools

When two moving metallic surfaces are put into sliding contact, there is loss of material from both, although this effect is less damaging to the hardest one. During the chip formation process, there is a strong interaction between the cutting edge, the chip, and the machined surface (on the rake face and on the clearance face, respectively). When this process happens, depending on the cutting conditions, the edge suffers high pressure and high temperature combined with the presence of cutting fluid, which encourages the occurrence of several physical processes and chemical relations. The final result is wear on the cutting edge. The high temperature in the region of chip formation results from the rate of thermal energy generated by the shearing process, which is not fully dissipated. The capacity to dissipate the heat depends on the properties of the tool material and workpiece material. Additionally, other properties, such as hardness, toughness, and chemically stability at cutting temperature, and the capacity to dissipate heat is also important in order to maintain a

relatively low temperature at the cutting edge. The wear on the cutting edge can be attributed to some well-known mechanisms, mainly:

Adhesive wear: Several layers of workpiece material are compressed against the cutting edge at high temperature. After compression, the layers adhere to themselves and to the edge and usually become hard in a manner similar to the process of strength hardening. Some pieces of these layers may break off taking parts of the edge surface away. The process can be more complex than described here, but it usually happens at relatively low cutting speeds associated with a high pressure/high temperature on the cutting edge. The adhesion can also be accelerated depending on the chemical affinity between tool and workpiece materials. A built up edge and notch wear are the more common types of wear related to this mechanism.

Abrasive wear: this occurs where abrasive, or hard particles, are present in the region of interaction between the cutting edge and the workpiece. The resistance to such a wear mechanism is associated with material hardness and melting point. As the cutting speed and federate increase, the temperature in the chip formation region also tends to rise. In such conditions, some hard carbide particles, present in the chip being formed, wear the rake face. Similarly, particles present on surface being machined wear the clearance face of the tool. Using tool materials with a high thermal conductivity may contribute to minimizing the action of the abrasive wear mechanism, because the heat can then be removed rapidly from the chip formation region. Flank and crater wear are the types of wear most frequently associated with this mechanism.

Abrasion is intuitively considered as a major cause of wear and the literature on the subject often describes tool wear in general as abrasive, but this is an area that requires further investigation for normal conditions of cutting. (Trent and Wright, 2000)

Diffusion: This is essentially associated with the chemical affinity between the tool and workpiece materials under the high temperature and pressure occurring during the cutting process. The high temperatures reached during the chip formation create the conditions for diffusion of some of the chemical elements present in both tool and workpiece materials. The most common is the diffusion of the carbon and also the reaction that transforms diamond into graphite. Chemical wear is mainly associated with crater wear and, to a less extent, flank and notch wear.

Fatigue wear: This can be mainly of two kinds: mechanical and thermal fatigue. The first is due to the alternating tensile and compression stresses on the cutting edges. The second can be associated with alternating cycles of heating and cooling. Tool used in milling operations usually present this mechanism. Chipping and catastrophic failure are the main types of wear associated with the fatigue mechanism.

Wear by oxidation: this is a particular type of chemical wear, which occurs when metals and oxygen are in contact. It can be accelerated at high temperatures and/or high pressures. Notch wear is suggested to be caused mainly by this mechanism.

Several, if not all forms of wear, contribute to wear of the tool edge, but there is usually one, which acts predominantly, depending on the cutting conditions. For example, it is suggested that flank wear is caused primarily by abrasive wear and in some cases by

chemical wear and oxidation; crater wear has been mainly associated with chemical diffusion and also with abrasion, depending on the material chemical composition, mechanical properties and microstructure.

Tool failure is usually associated with some form of breakdown of the cutting edge. Under proper operating conditions, this breakdown takes place gradually over a period of time. In the absence of rigidity, or because of improper tool geometry that gives inadequate support to the cutting edge, the tool may fail by mechanical fractures or chipping under the load of the cutting forces. This is not truly a wear phenomenon for it can be eliminated or at least minimized by proper design and application.

Tool wear is a complex phenomenon and is influenced by many factors. The causes of wear do not always behave in the same manner, nor do they always affect wear to the same degree under similar cutting conditions. The causes of wear are not fully understood. Even though there is some disagreement regarding the true mechanisms by which wear actually takes place, most studies agree that most important cause is cutting temperatures. Investigations have also been made on other possible causes such as oxidation and electrochemical reactions in the tool work contact zone.

2.4 Instrumentation

2.4.1 CNC Machining Center

The functions of Computer Numerical Control (CNC) machining center were summarized by Huang (1998). The CNC machining center, such as Fadal VMC15, is a multifunction instrument that uses a programmable mini-computer with a read-write memory to perform NC functions and control the machine tool. It provides basic computing capacity

and data buffering as a part of the control unit. CNC machines can execute a wide variety of operations, such as milling, drilling, boring, etc., without changing the setup of a component. CNC units also allow combinations of these operations with variable spindle speeds and feed rates. By using the CNC programs, CNC machines can automatically control the tool change, tool path, machining parameters, and coolant usage without complex manipulation.

Depending on the direction of cutter spindle, CNC machines can be divided into two types: 1) vertical CNC machines, which have a cutter spindle in the vertical position, lending itself to quick, easy workpiece-setup; or 2) horizontal CNC machines, whose horizontal cutter spindle configuration lends itself to heavy depths of cut on large workpeices. The typical vertical CNC machines provide three axes of movement. The base table offers the movements in X and Y directions and makes the workpiece mounted on the table device move on the horizontal plant. The cutter spindle controls the direction of movement in the Z axis, and moves up and down to cut the workpiece. Because of its accuracy, safety, and easy operation, more and more companies use CNC machines to produce their products to confirm quality and efficiency.

The machine control unit (MCU) is the nucleus of CNC operations in CNC machines. It is responsible for integrating all the function performed by the NC machine, including data input, data processing, data output, and machine I/O interface. It consists of the following six sections:

1. CPU: the central processing unit (CPU) is the central component of any computer system. It controls the various devices throughout the system bus by means of the software loaded into the main memory.

2. Communication: CNC Communication permits information to be sent and received between two components in the system. The system bus is crucial part of CNC communication.
3. Servo drive control: Servo drive control is used to control the axis control motors. This task is carried out by both the servo control interface, which consists of position and velocity of the control loop, and feedback interface, which consists of an interface circuit and D/A converter.
4. Spindle speed control: spindle speed can be controlled by the S-function in most CNC machines. The serial spindle control circuit and spindle feedback interface are used to control the spindle speed.
5. Memory: CNC machines provide memory to store CNC operating programs and processing data. The memory can be classified into two categories: primary and secondary. A primary memory device provides a specific location for each bit and allows the bit to be switched on or off. It can be categorized into read-only memory (ROM) and random-access memory (RAM). The former stores the CNC operation and machine interface programs. And it can not be erased, even when the power-supply is cut. The latter can be read or written by the CPU, and is erased when the power-supply is removed. Secondary memory is provided in the form of magnetic disks. They provide abundant space for storing multiple part programs that must be loaded into RAM for execution.
6. Programmable machine controller: the programmable machine controller (PMC) provides the interface logic to render automatic tool change, automatic coolant, clamping system

control, limit switches interface, timer, counter, emergency interlock, NC I/O interface, machine I/O interface, etc.

2.4.2 Dynamometer

The multi component dynamometer, such as Kistler 9257B, provides dynamic and quasi-static measurement of the three orthogonal components of a force (X, Y, and Z) acting from any direction onto the top plate. The dynamometer has high rigidity and high frequency. The high resolution enables very small dynamic changes to be measured in large forces. The dynamometer can measure the acting cutting force regardless of its application point. The dynamometer is always applied on the cutting force measurements in milling, turning, grinding, and other machining operation.

The cutting force generated on the top plate is measured by four three-component force sensors arranged symmetrically inside the dynamometer. Each sensor has three pairs of quartz plates, one is sensitive to pressure in the Z direction and the other two respond to shear in the X and Y directions. The force components are measured virtually without displacement. The unit of cutting force is the Newton (N) or Pound (lb), and it is transformed to voltage as an output. In these four force sensors, the force is broken down into three components and the collected analog signals are then lead together in the connecting cable and transmitted to the amplifier. Depending on the direction of the force, the collected signals can be generated as positive or negative. However, the positive and negative force will be the same if the magnitude of force is equal.

2.4.3 Current Sensor

Monitoring the motor current of the spindle or table is another method used to detect tool breakage or tool wear. Depending on the cutting force torque, the motor current shows the difference between brand new and worn tools. The motor must supply larger current, which generates larger torque than usual to cut the material if the tool is worn or broken. By applying this principle, a proper threshold of table or spindle motor current can be set to monitor the tool conditions. In this research, shunts with 15 Amp rated current and 50 mV output are used.

2.5 Signal Processing with Wavelet Transform

Wavelets are a class of functions that are the base functions for a wavelet transform. Wavelets have proven useful in the analysis of signals that contain transients, image analysis, and image/signal compression. The wavelet transform decomposes a signal into a representation that shows signal details and trends as a function of time. This representation can be used to characterize transient events, reduce noise, and many other applications. The wavelet transform maintains a constant time resolution regardless of frequency. Comparison between Fourier and wavelet transform is explained by Misiti et al (1996).

Mathematically, the process of Fourier transform is represented by

$$F(\omega) = \int_{-\infty}^{\infty} f(t) e^{-j\omega t} dt \qquad (2.3)$$

Which is the sum over all time of the signal f(t) multiplied by a complex exponential. The results of the transform are the Fourier coefficients F(ω), which when multiplied by a sinusoid of appropriate frequency ω, yield the constituent sinusoidal components of the

original signal. Graphically, the process looks like Figure 2.1. The original signal transformed to the constituent sinusoids of different frequencies.

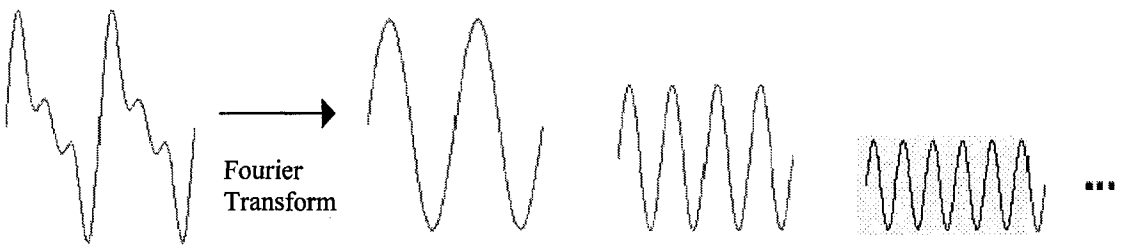

Figure 2.1 Fourier Transform

Similarly, the continuous wavelet transform (CWT) is defined as the sum over all time of the signal multiplied by scaled, shifted versions of the wavelet function ψ:

$$C(scale, position) = \int_{-\infty}^{\infty} f(t)\psi(scale, position, t)dt \qquad (2.4)$$

The results of the CWT are many wavelet coefficients C, which are a function of scale and position. Multiplying each coefficient by the appropriately scaled and shifted wavelet yields the constituent wavelets of the original signal as shown in Figure 2.2.

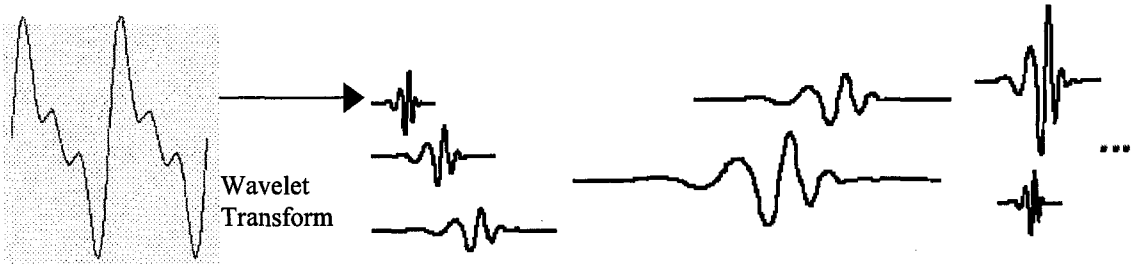

Figure 2.2 Wavelet Transform

The continuous wavelet transform is the sum over all time of the signal multiplied by scaled, shifted versions of the wavelet. This process produces wavelet coefficients that are a

function of scale and position. Shifting a wavelet simply means delaying (or hastening) its onset. Mathematically, delaying a function f(t) by k is represented by f(t-k). The more stretched the wavelet, the longer the portion of the signal with which it is being compared, and thus the coarser the signal features being measured by the wavelet coefficients. Thus, there is a correspondence between wavelet scales and frequency as revealed by wavelet analysis:

- Low scale a > Compressed wavelet > Rapidly changing details > High frequency w.
- High scale a >Stretched wavelet >Slowly changing, coarse features>Low frequency w.

Shift and scale functions of wavelet transform are illustrated in Figure 2.3.

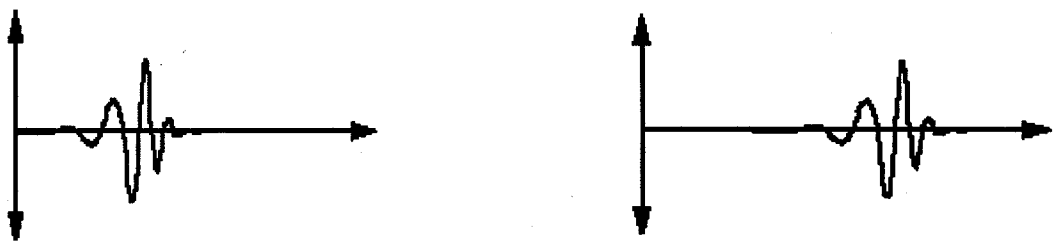

(a) Shift function of wavelet

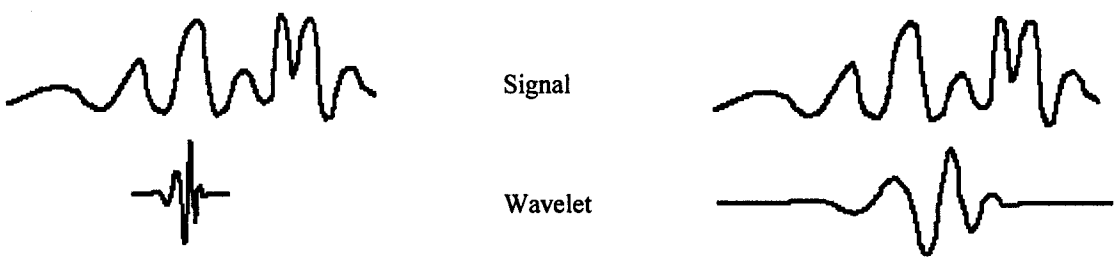

(b) Scale function of wavelet

Figure 2.3 Shift and Scale Function of Wavelet Transform

Any signal processing performed on a computer using real-world data must be performed on a discrete time interval. It is important to know that the continuous wavelet transform is also operating in discrete time. The difference for the continuous wavelet transform from the discrete wavelet transform is the scales at which it operates. Unlike the discrete wavelet transform, the CWT can operate at every scale, from that of the original signal up to some maximum scale which you determine by trading off your need for detailed analysis with available computational horsepower. The CWT is also continuous in terms of shifting: during computation, the analyzing wavelet is shifted smoothly over the full domain of the analyzed function.

Calculating wavelet coefficients at every possible scale is a fair amount of work, and it generates an awful lot of data. Discrete wavelet transform is useful in this matter with the scales and positions based on powers of two and lead much more efficient and accurate analysis.

For many signals, the low-frequency content reflects the general trend, whereas the high-frequency content usually shows details of the process. In discrete wavelet transform used in this research, there are approximations and details. The approximations are the high-scale, (low frequency) components of the signal and the details are the low-scale (high-frequency) components. The low frequency content is the most important part. It is what gives the signal its identity. The high frequency content, on the other hand, imparts flavor or nuance. The human voice can be a good example. If high frequency components are removed, the voice sounds different, but it is still okay to understand. However, if low-frequency components are removed, it is difficult to recognize.

Figure 2.4 shows the decomposition of a signal into approximations and details. The original signal, S, divided by two signals, approximation and detail. The decomposition process can be iterated, with successive approximations being decomposed in turn, so that one signal is broken down into many lower-resolution components as shown in Figure 2.4. These components can be assembled back into the original signal with no loss of information. This process is called reconstruction, or inverse discrete wavelet transform.

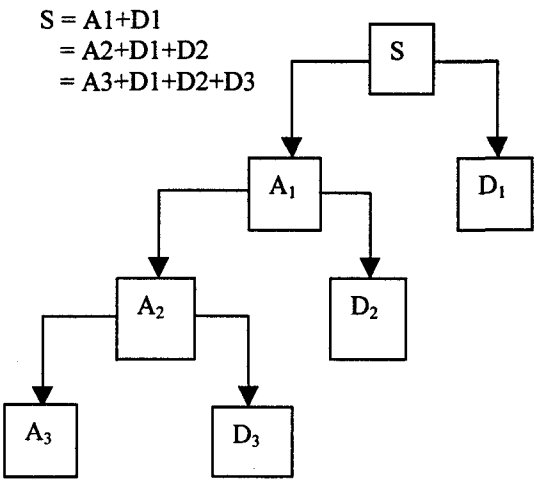

Figure 2.4 Signal Components Using the Wavelet Transform

From the literature it is evident that wavelet based signal analysis has been successful in tool breakage detection and also in estimation of tool wear. Detail wavelet coefficients have been used for breakage detection, particularly in drilling (Li, 1998), (Li, Dong, and Yuan, 1999), (Mori et al., 1999), (Li, 1999), (Li, Tso, and Wang, 2000) and wavelet approximation coefficients have been used in monitoring tool wear in end milling (Tansel et al., 1998), (Tansel et al., 2000), (Tansel, Mekdeci, and Mclaughlin, 1995), and (Lee and Tarng, 1999) . In previous work in the literature, tool wear has been estimated by comparison

with pre-worn tools. There is no documented work on estimation of progressive tool wear using the wavelet transform as the machining cuts are carried out. Further, the depth of cut within a machining cut has usually been taken as a constant, whereas a variable depth of cut is used. Both these features make the research conducted in this dissertation unique. The estimation of tool wear in ramp cuts in end milling is carried out in this research by applying the wavelet transform on the cutting force signal.

CHAPTER 3. EXPERIMENTAL OBSERVATIONS OF CUTTING FORCE AND TOOL WEAR EFFECTS IN RAMP CUTS IN END MILLING

A paper published in the Transactions of NAMRI/SME

Yonghoon Choi and Ranga Narayanaswami

ABSTRACT

Tool wear and its identification is a fundamental problem in machining. With tool wear there is an increase in cutting forces, and leads to deterioration in process stability, part accuracy and surface finish. In this paper, cutting forces in ramp cuts in end milling are experimentally observed. Trends in the X, Y, and Z cutting force for ramp cuts are explained. New tool cutting forces are compared with cutting forces obtained from worn tool. The wavelet transform is used for signal processing and is found to be useful for observing cutting force trends. Preliminary results indicate that tool wear in ramp cuts in end milling may be estimated well using the wavelet transform.

3.1 Introduction

Monitoring cutting forces and tool wear effects in end milling is a necessary step toward the full automation of milling operations. To monitor the end milling process successfully, the selection of an appropriate signal and signal processing algorithm is very important. Several signals in a milling operation have been considered to monitor tool failure, for example, cutting force, torque, vibration, acoustic emission, and spindle motor current.

In this paper we are concerned with monitoring the cutting force in ramp cuts in end milling. The ramp cuts are unique in that they have (i) variation in the depth of cut and (ii) the cutting force trends also depend on the feed direction. Cutting force trends in the X, Y, Z directions in ramp cuts are explained and the measured forces for a new tool and worn tool are compared.

Traditional signal processing approaches such as segmental averages and Fourier Transform generally assume that the sensor signals are stationary. However, the sensor signals in tool wear monitoring are usually non-stationary. Thus, the approaches that deal with non-stationary signals are more appropriate for process monitoring. Wavelet transform is a convenient tool for processing time varying signals [14]. The wavelet transform is better suited than the Fourier transform for monitoring the cutting force as it provides time-frequency localization of the signal. The Fourier transform has a problem in that it transforms the signal from a time domain to a frequency domain assuming that the signals are stationary or infinite in nature [9]. Namely, it has a difficulty in describing transient components, and does not convey any information pertaining to translation of the signal from the time domain to the frequency domain. Accordingly, we use the wavelet transform to analyze the force signal.

The rest of the paper is organized as follows. First a brief background on cutting force modeling, process monitoring and tool wear is provided. The experimental setup used to conduct the ramp cuts is described next. A short section on the wavelet transform for signal processing is included next. The experimental data and explanation of cutting force trends is provided next. Conclusions and future research directions are presented finally.

3.2 Background

The modeling of cutting forces in machining has been extensively studied, and a recent review may be found in [3]. The mechanistic approach for modeling of cutting force has been quite successful. The mechanistic method views the machining process as a combination of chip load-cutting force relationship, cutting tool geometry, cutting process geometry, work-piece geometry and machining conditions.

The end milling process has been modeled mechanistically [2] and EMSIM software [5] simulates forces in end milling. To obtain a complete representation of the forces on the end mill at any given instant of time, the cutter is discretized into thin, disc-like sections, similar to a stack of coins. The location of each flute on each disc is determined, and the elemental force is calculated for each flute that engages the work-piece. The instantaneous chip thickness, and the flute entry angle, and exit angle, are needed in order to compute elemental cutting forces. For small feed per tooth compared to the radius of the cutter, the instantaneous chip thickness is calculated as

$$t_c(i,j,k) = f_t \sin\beta(i,j,k)$$

Where, β is the wrap around angle due to the helix angle, and i, j, k refer to the ith angular increment, jth axial height, and kth flute and f_t is the feed per tooth. The expressions for the elemental force acting normal to the rake face dF_N, and the friction force dF_T, are:

$$dF_N(i,j,k) = K_N * dZ * t$$
$$dF_T(i,j,k) = \mu * dF_N$$

Where, dZ is the disk thickness, and the coefficients K_N and μ are determined experimentally by running a series of end milling or turning experiments and measuring forces for each work-piece/tool material combination. Once the normal and friction forces are calculated for

a given element, they are transformed from the K_N-μ coordinate system to the X-Y-Z coordinate system. The total force is found by integrating the elemental forces. A comprehensive modeling of end milling forces for arbitrary cutter geometry may be found in [1].

Recently, advances have been made in incorporating the effect of tool wear in cutting force modeling. Shin and Elanayar [4] developed a method to separate the ploughing forces from the shear forces on the shear plane. The forces are decomposed by first separating the shear forces from the total forces and then employing an iterative procedure to calculate the normal forces on the shear plane. The ploughing forces are modeled by taking into account the change in geometry with flank wear. Smithey, Kapoor, and DeVor [10] observed experimentally that in three-dimensional cutting operations in which the nose of the tool is engaged, the region of plastic flow grows linearly as the total wearland width increases. Plastic flow occurs at the front of the wearland and elastic contact is assumed at the back of the wearland. The flank of the tool is discretized into small two-dimensional elements and a contact model is used to determine the stresses on the individual elements. These stresses are added to the mechanistic force model for a sharp tool to determine the total cutting force.

The monitoring of tool failure has also been a subject of active research. The cutting force signal is considered to provide rich information for tool failure detection in end milling operations and in drilling [8]. For the purpose of process monitoring, segmental averages and the Fourier transform have been used extensively. However, the wavelet transform is increasingly being used for process monitoring. The wavelet transform has two advantages over segmental averaging [13]: first, they represent the system more accurately if the waveform is optimized by considering the characteristics of the signal. Second, wavelet

parameters can be used for many other purposes such as identification of tool breakage, run out, and flute deviation. Tansel et al. [11] used both segmental averaging and the wavelet transform as encoding methods for tool wear estimation found the wavelet transform to be superior. Wavelet transformations require less computation than FFT. For example, FFT requires $N \log_2 N$ operations for transformation of a set of N numbers while fast wavelet transformations require N operations [12], and the number of operations halves when the transformations are repeated.

Gong, Obikawa and Shirakashi [6] estimated tool wear in turning operations with wavelet transform based on the cutting force. Lee and Tarng [7] used spindle motor current to monitor tool failure in end milling. They used the wavelet transform to perform a multilevel signal decomposition to extract the tool failure feature and found the four-level wavelet decomposition to be adequate (decomposition up to 4th level). Wang, Mehrabi and Kannatey-Asibu [14] used a vibration signal and the wavelet transform to monitor tool wear in turning. They found the vibration signals from sharp and worn tools showed clear differences.

3.3 Experimental Setup

As shown in Figure 3.1, a dynamometer is mounted on the table of a three-axis Fadal CNC machining center. The work-piece is fixtured in the vise, which is bolted on top of the dynamometer. The DAQ card has 16 channels and (-10V~10V) range to display. The amplifier has 3 channels to send the data to the DAQ card for each X, Y, and Z force signals. The sampling rate is set at 500/sec.

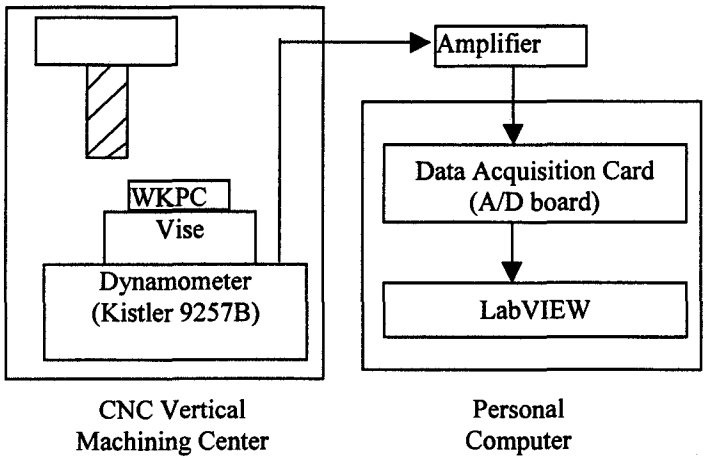

Figure 3.1 Schematic Diagram of Experimental Setup

Table 3.1 Experimental Conditions

Work-piece	AISI1018 steel 1" X 1.25" X 3"
Tool	High Speed Steel (0.5in diameter flat end mill with 4 flutes)
Depth of Cut	0 to 0.1inch for ramp cut
Feed Rate	7 in/min
Spindle Speed	2,000 rpm (CW)

Ramp cut machining was carried out with a high-speed steel end mill on an AISI1018 steel work-piece (see Table 3.1). The work-piece and cut configuration is shown in Figure 3.2. Four types of ramp cuts are possible. These are shown in Figure 3.3 and are referred to as 1) low to high forward, 2) low to high backward, 3) high to low forward and 4) high to low backward. The terms low and high refer to the axial depth of cut and the terms forward and backward refer to the tool feed direction.

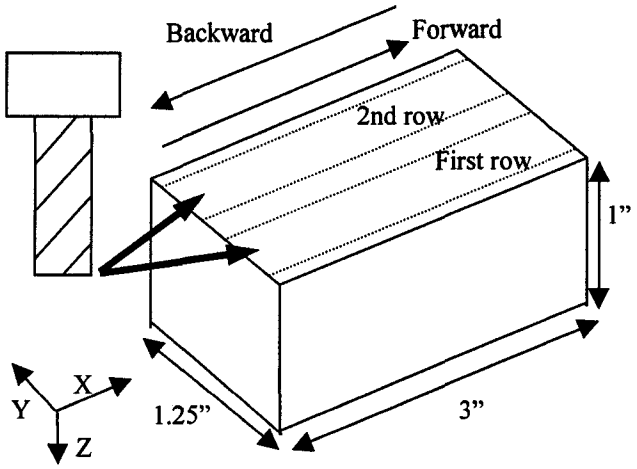

Figure 3.2 Schematic Diagram of Machining

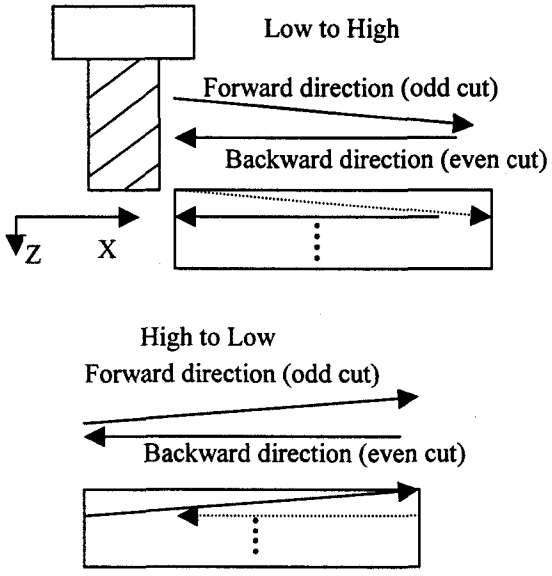

Figure 3.3 Four Types of Ramp Cuts

As shown in Figure 3.2, at first the tool moves in the forward direction, then it moves in the backward direction to its original position (X and Y) after recording data for the first cut. Repeated cuts are made until the bottom of the work-piece is reached. 18 cuts in each row are made for a total of 36 cuts in one work-piece. Two work-pieces are used to generate all cutting data.

3.4 Wavelet Transform

Wavelets are a class of functions that are the basis functions for a wavelet transform. Wavelets have proven useful in the analysis of signals that contain transients, image analysis, and image/signal compression. The wavelet transform decomposes a signal into a representation that shows signal details and trends as a function of time. This representation can be used to characterize transient events, reduce noise, and many other applications. The wavelet transform maintains a constant time resolution regardless of frequency [9].

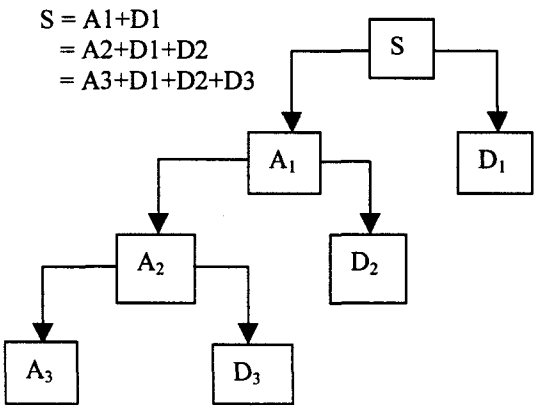

Figure 3.4 Signal Components Using the Wavelet Transform

For many signals, the low-frequency content reflects the general trend, whereas the high-frequency content usually shows nuance. In wavelet transform, there are approximations and details. The approximations are the high-scale, (low frequency) components of the signal and the details are the low-scale (high-frequency) components. Figure 3.4 shows the decomposition of a signal into approximations and details.

3.5 Experimental Data

Experimental data is presented for all four types of ramp cuts. 36 cuts are made on each work-piece. The tool is assumed to be rotating in a clockwise direction. Cutting forces with a new tool ($1^{st}/2^{nd}$ cut) are compared with those of a worn tool ($35^{th}/36^{th}$ cut). The raw data for cutting force in X, Y, Z direction is shown first. The +X direction is the forward feed direction. The +Z direction points downward. The Y- axis forms a left-handed coordinate system. The Daubechies wavelet transform is applied to the raw data.

3.5.1 Low to High Forward Ramp Cut

Figure 3.5 shows the cutting force data. 3.5(a) shows the raw X force data followed by the approximation A5 and detail D1. A5 clearly shows the increasing trend in the X force. 3.5(b) shows the Y force data. The approximation (A5) shows that the Y-force starts at a positive value and drops to a negative value (with respect to the mean line) at the end of the cut. The Z-force data is shown in 3.5(c). The A5 wavelet approximation clearly shows the decreasing trend in the Z-force. Figures 3.5(d), (e), (f) show the X, Y, Z force with a worn tool. It is clearly observed that the magnitude of force has increased in each case.

3.5.2 Low to High Backward Ramp Cut

Figure 3.6(a) shows the X cutting force magnitude to be increasing as the cut progresses. 3.6(b) shows the Y-force to be increasing and 3.6(c) shows the Z-force to be crossing the axis (mean line). Figures 3.6(d), (e), (f) show the effect of tool wear. All force magnitudes have increased.

3.5.3 High to Low Forward Ramp Cut

Figure 3.7(a) shows the X-force to be decreasing as the cut progresses. 3.7(b) shows the Y-force magnitude to be decreasing. 3.7(c) shows the Z-force starts from a negative value and switches to a positive value at the end of the cut (crosses the mean line).

3.5.4 High to Low Backward Ramp Cut

Figure 3.8(a) shows the X-force to be decreasing in magnitude as the cut progresses. 3.8(b) shows the Y-force to be decreasing and 3.8(c) shows the Z-force to be crossing the axis (mean line).

3.6 Cutting Force Explanation

The new features in this research are to understand the mechanics of ramp cuts. Four types of geometrical cases occur. Two cases arise due to depth of cut, one is increasing depth of cut (low to high) and the other is decreasing depth of cut (high to low) and the other two cases arise from feed direction that can be either forward or backward. Figure 3.9 shows the difference in terms of cutting configuration.

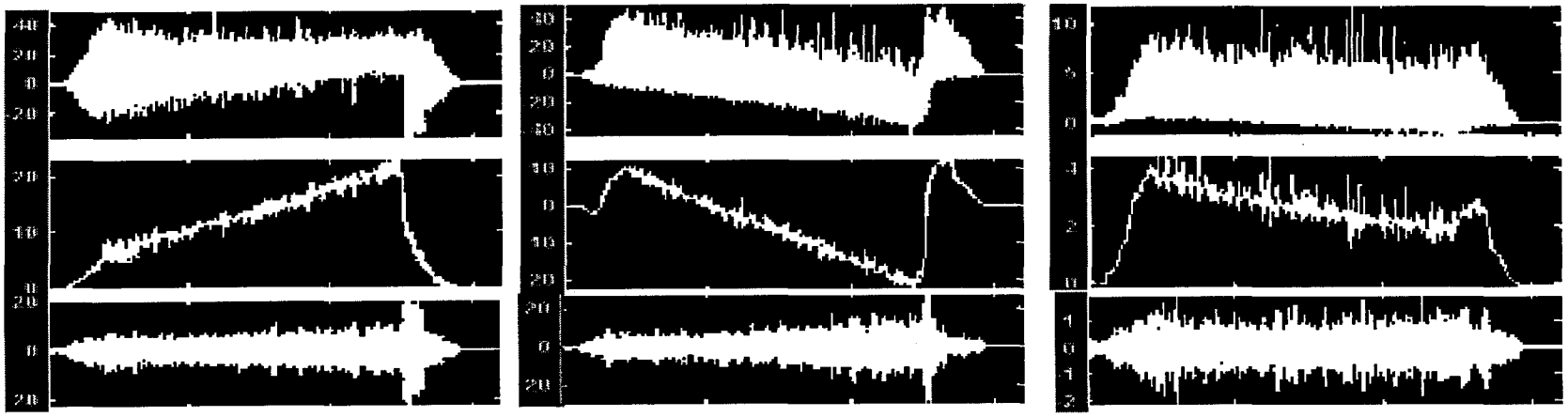

(a) 1st X signal and its A5 and D1 (b) 1st Y signal and its A5 and D1 (c) 1st Z signal and its A5 and D1

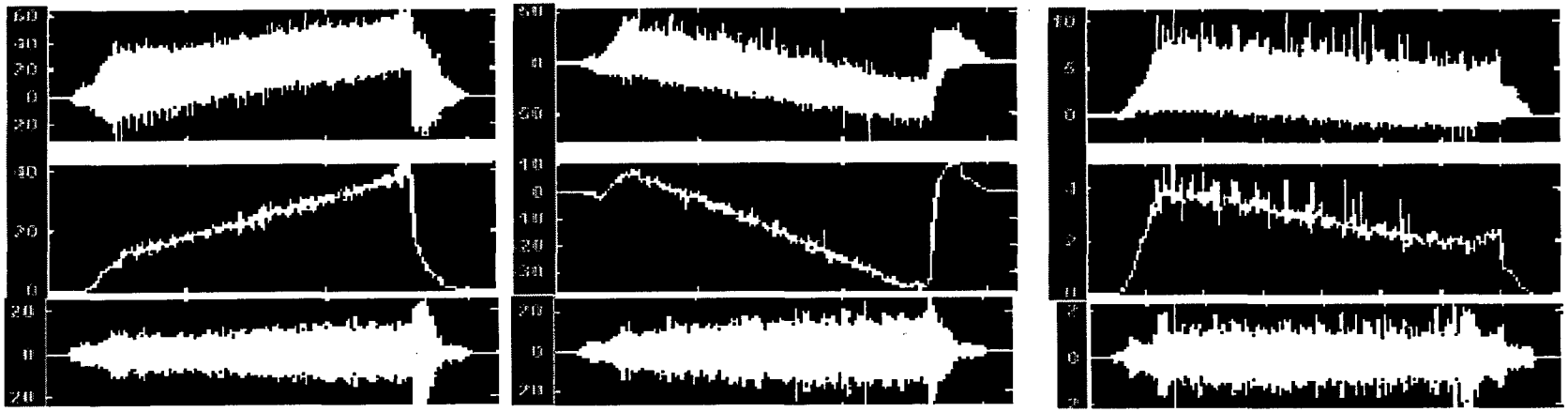

(d) 35th X signal and its A5 and D1 (e) 35th Y signal and its A5 and D1 (f) 35th Z signal and its A5 and D1

Figure 3.5 1st and 35th Low to High Forward Ramp Cuts (force in lbs)

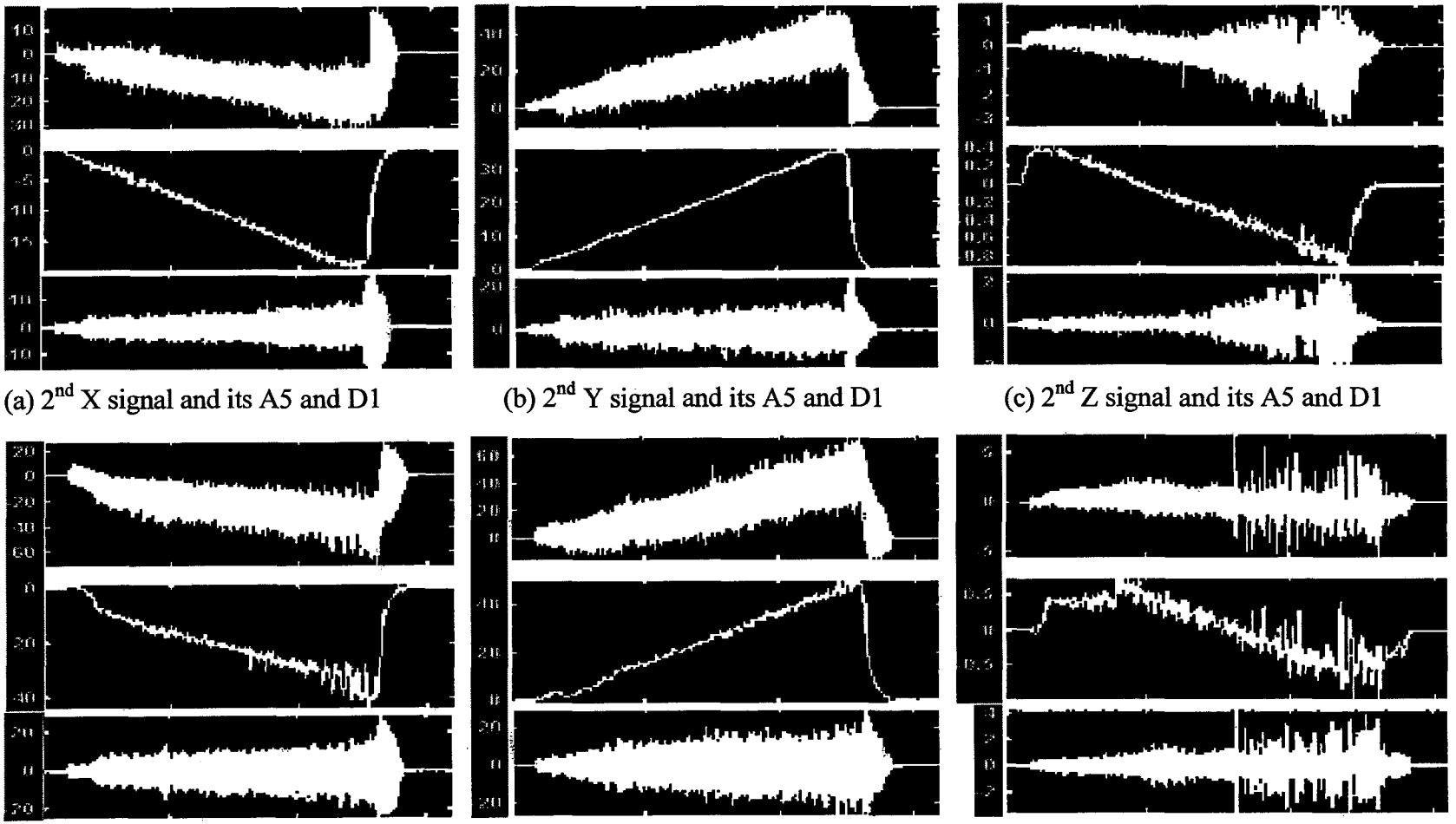

(a) 2nd X signal and its A5 and D1 (b) 2nd Y signal and its A5 and D1 (c) 2nd Z signal and its A5 and D1

(d) 36th X signal and its A5 and D1 (e) 36th Y signal and its A5 and D1 (f) 36th Z signal and its A5 and D1

Figure 3.6 2nd and 36th Low to High Backward Ramp Cuts (force in lbs)

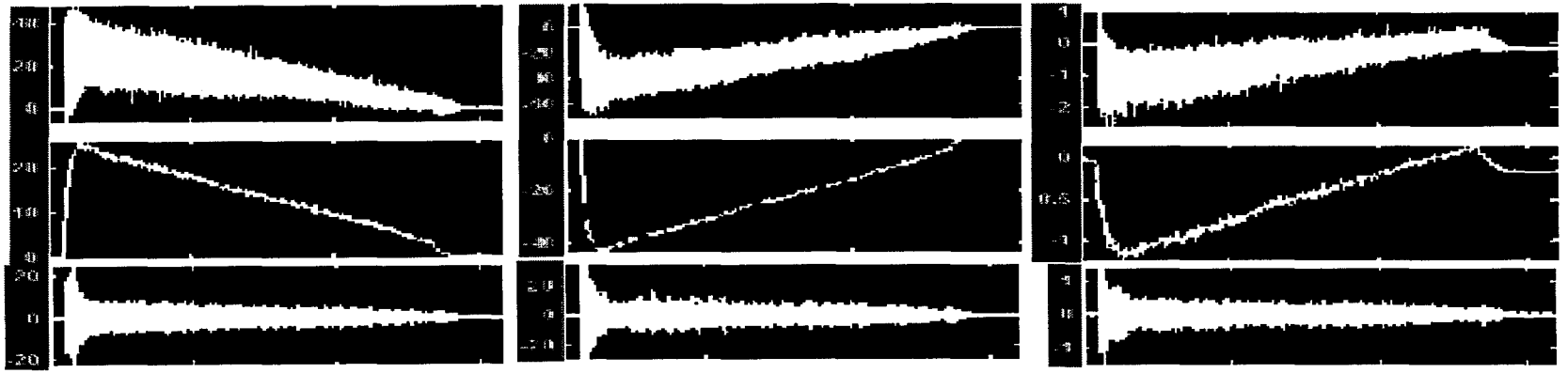

(a) 1st X signal and its A5 and D1 (b) 1st Y signal and its A5 and D1 (c) 1st Z signal and its A5 and D1

Figure 3.7 1st High to Low Forward Ramp Cut (force in lbs)

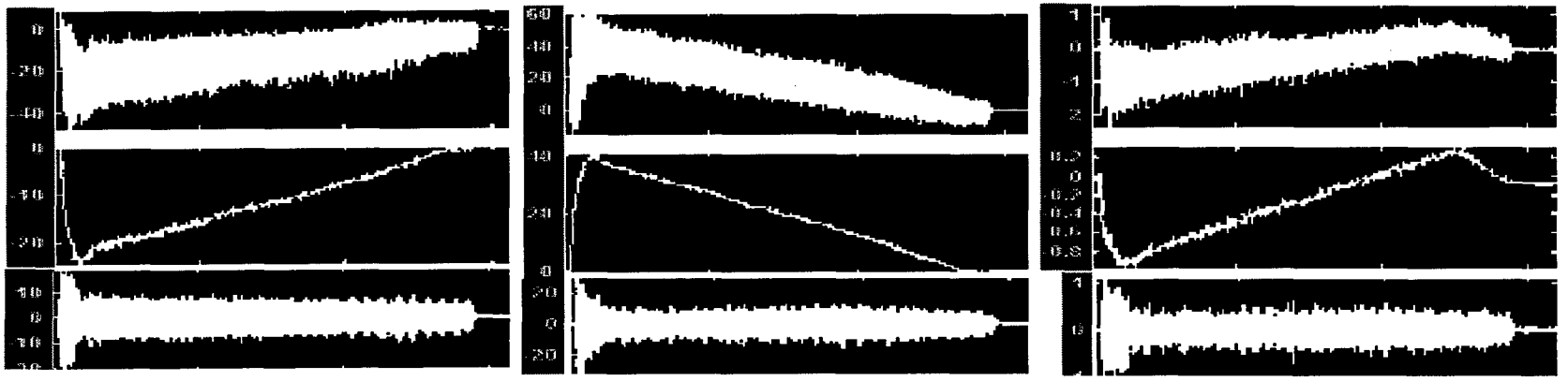

(a) 2nd X signal and its A5 and D1 (b) 2nd Y signal and its A5 and D1 (c) 2nd Z signal and its A5 and D1

Figure 3.8 2nd High to Low Backward Ramp Cut (force in lbs)

As can be seen from Figure 3.9, on the bottom of the tool, both front and rear teeth (rear teeth with unit depth of cut) are engaged in machining for the low to high forward ramp cut while only front teeth are contacting for the high to low forward ramp cut. This contributes to the difference in force signals. EMSIM simulates only the high to low forward ramp cut and our results match their simulation.

In Figure 3.5 (low to high forward ramp cut) the X force continuously increases with increasing axial depth of cut. The Y force signals for (1^{st} and 35^{th} cut) are in positive side of the axis at the first stage and it tends to go to the negative side after the tool moves into the second half of the work-piece. This trend can be explained with the contact area shown in Figure 3.9(a). All 4 teeth of the tool are engaged in machining. The key point to be noted is that teeth at the backside are cutting only a unit amount of volume (principally at the bottom of the teeth), while the teeth at the front side are removing more amount of chips with both sides and bottoms of the teeth as the tool moves down. The rear teeth provide the positive Y-force and the front teeth provide the negative Y-force. Therefore, as the depth of cut increases, the negative Y force exceeds the positive Y force. The Y signals therefore show the trend of crossing the axis to the negative side.

The X forces for all the cuts are easy to understand. The direction of the X-force is along the feed direction, and increases with increasing axial depth of cut, or decreases with decreasing axial depth of cut. The Y-force in Figures 3.6, 3.7, and 3.8 does not cross the axis. This is because there is no significant cutting at the backside of the end mill.

The Z-force needs some more explanation. In each case of ramp cut, the Z-force has the potential to cross the axis (mean line). In Figure 3.10, we can see that 'I' is the force acting from the tool to the top surface of the work-piece. As the tool comes down, the bottom

teeth exert a uniform downward pressure on the work-piece. The axial depth of cut is increasing and this is the negative Z force (II). The net Z force is I+II. So "I + II" can cross the axis depending on the depth of cut. In the data of 1st and 35th cut in Figure 3.5, Z signal did not cross the axis because 'I' was sufficiently big enough. A similar trend is noticed for the Z signals for the low to high backward ramp cut. In the cases of 2nd and 36th cuts (Figure 3.6), the cutter is moved along -X and the axial depth of cut is increasing because of the slope of the work-piece. In this case, the Z axis crosses the mean line and allows one to deduce that the downward pressure (I) is smaller in this case than the corresponding forward ramp cut because the tool does not keep pressing the work-piece (Figure 3.11).

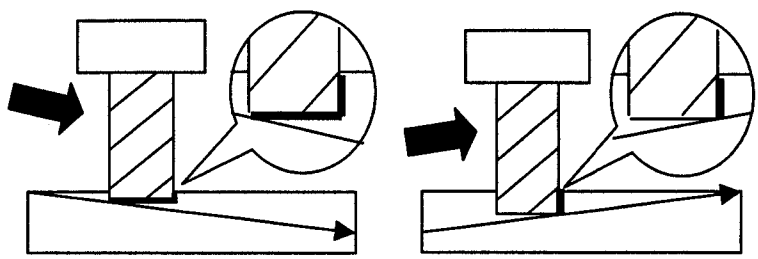

(a) low to high (b) high to low

Figure 3.9 Contact Area between Tool and Workpiece for Forward Ramp Cuts

For the high to low ramp cuts, as the cut progresses, the negative Z force is decreasing. The downward pressure (positive) is uniform across the cut. Therefore as the cut progresses the net Z force goes from a negative to positive value. In general, the Z forces are smaller than the X and Y force and subject to noise. The wavelet transform is effective at removing this noise and signal approximations show good force trends for the cutting signal.

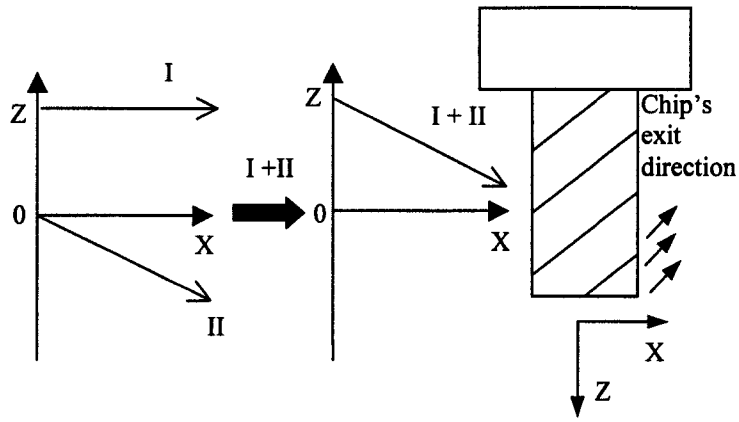

Figure 3.10 Explanation of Z Force Signal for Low to High Forward Ramp Cut

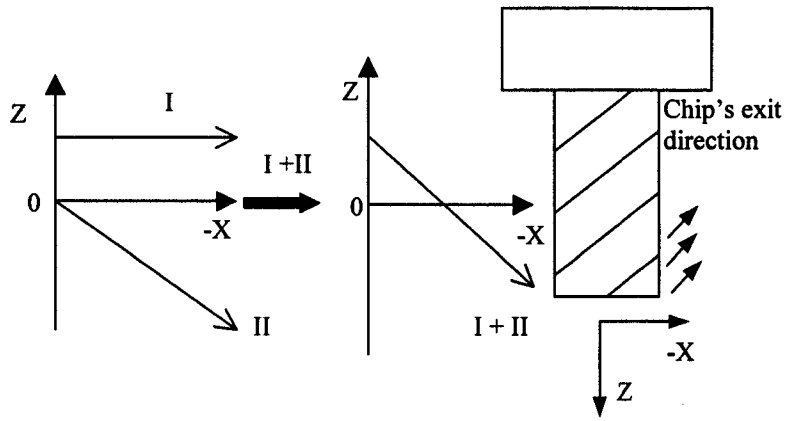

Figure 3.11 Explanation of Z Force Signal for Low to High Backward Ramp Cut

The importance of maintaining details in the wavelet transform is to capture any discontinuities in frequency that occurs in the time domain. Discontinuities may occur in the event of a cutting edge being chipped or broken for example. The details will show these phenomena, while approximations will still reflect tool wear. Other process faults such as run out and flute deviation can further complicate the signal and the entire set of wavelet

coefficients will be necessary to handle the multiple process faults, tool wear and the possibility of tool chipping or breakage to establish a reliable process monitoring system.

3.7 Tool Wear

As seen from experimental data in Figures 3.5 – 3.8, repeated machining with the same tool leads to tool wear and increase in the cutting force. The wavelet approximations show an increase in the mean force. The wavelet details show more oscillations implying that the process is less stable. The maximum values (magnitude) of cutting force for very first and last cut, for each type of ramp cut are compared (Table 3.2).

Table 3.2 Percentage Increase in Force Magnitude with Tool Wear Based on Wavelet Approximation

	X	Y	Z
Low to High Forward Ramp Cut	86	40	19
Low to High Backward Ramp Cut	115	35	38
High to Low Forward Ramp Cut	125	53	28
High to Low Backward Ramp Cut	144	55	30

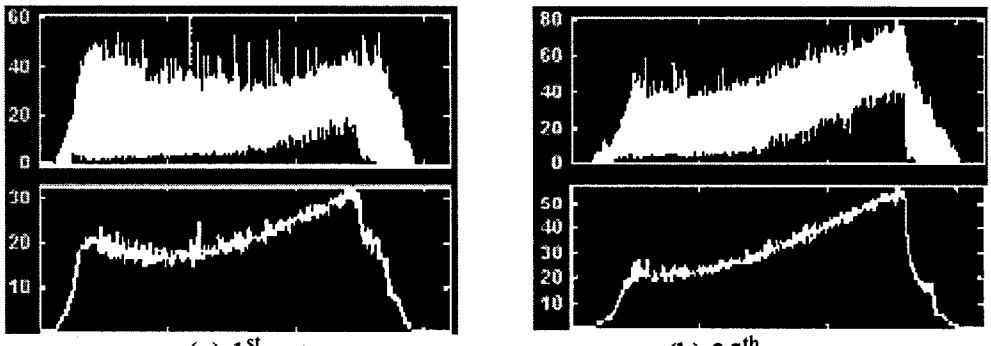

(a) 1st cut (b) 35th cut

Figure 3.12 Resultant Force Signals (top) and A5 (below) in Low to High Forward Ramp Cuts

The resultant cutting force can be wavelet transformed at scale A5 and the Root Mean Square (RMS) value of this approximated signal may be calculated for a more reliable estimate of increased cutting force due to tool wear. As an example, the RMS value increases from 18.95 to 29.62 (Figure 3.12).

3.8 Conclusion and Future Work

Experimental cutting force data in ramp cuts in end milling were explained for the trends in the X, Y and Z force signals. Wavelet transforms were used to generate an accurate and compact representation with multilevel signal decomposition. The wavelet transform approximations were useful in conveying information on the general non-stationary time varying force trends. The worn tool signals showed significant increase in the magnitude of the force. The X forces increased the most, followed by the Y forces and the Z forces increased the least. The high frequency component of the force signal increased with tool wear showing increased vibration and in some cases jumped instantly indicating possible tool edge chipping and the wavelet details show these important trends. The next phase of the work will involve measurement and estimation of the tool wear, and modeling work to include the effect of tool wear in force models for end milling. This will result in an effective model-based tool monitoring system for end milling, and be useful in the industry.

3.9 Acknowledgement

This research is supported by the National Science Foundation under grant No. DMI 9970083. Any opinions, findings, and conclusions or recommendations expressed in this

material are those of the authors and do not necessarily reflect the views of the National Science Foundation. The authors gratefully acknowledge help from Jim Dautremont in Mechanical Engineering and Kevin Brownfield in Industrial and Manufacturing Systems Engineering for assistance with the experiments.

3.10 References

[1] Altintas, Y. and Engin, S. (2001), "Generalized Modeling of Mechanics and Dynamics of Milling Cutters", *Annals of the CIRP*, Vol. 50, no. 1, pp. 25-30.

[2] Devor, R.E., Kline, W. A. and Zdeblick, W. J. (1980), "A Mechanistic Model of the Force System in End Milling with Application to Machining Airframe Structures," *Proceedings of the 8th North American Metalworking Research Conference*, pp. 297-303.

[3] Ehmann, K. F., Kapoor, S. G., DeVor, R. E., and Lazoglu, I. (1997), "Machining Process Modeling: A Review", *Journal of Manufacturing Science and Engineering*, Vol. 119, Nov., pp. 655-663.

[4] Elanayar, S. and Shin, Y. C. (1996), "Modeling of Tool Forces for Worn Tools: Flank Wear Effects", *Journal of Manufacturing Science and Engineering,* Vol. 118, No. 3, pp. 359-366.

[5] "EMSIM" (2002), http://mtamri.me.uiuc.edu, simulation software at University of Illinois at Urbana-Champaign, accessed on Jan. 2002.

[6] Gong, W., Obikawa, T., and Shirakashi, T. (1997), " Monitoring of Tool Wear States in Turning Based on Wavelet Analysis", *JSME International Journal*, Vol. 40, No. 3, pp. 447-453.

[7] Lee, B. Y. and Tarng, Y. S. (1999), "Application of the Discrete Wavelet Transform to the Monitoring of Tool Failure in End Milling Using the Spindle Motor Current", *International Journal of Advanced Manufacturing Technology*, Vol. 15, pp. 238-243.

[8] Li, X. (1998), "Real-time Detection of the Breakage of Small Diameter Drills with Wavelet Transform", *International Journal of Advanced Manufacturing Technology*, Vol. 14, pp. 539-543.

[9] Misiti, M., Misiti, Y., Oppenheim, G., and Poggi, J. (1996), "Wavelet Toolbox", *The Mathworks. Inc.*

[10] Smithey, D. W., Kapoor, S. G., and DeVor, R. E. (2000), "A Worn Tool Force Model for Three-Dimensional Cutting Operations", *International Journal of Machine Tools and Manufacture*, Vol. 40, pp. 1929-1950.

[11] Tansel, I. N., Arkan, T. T., Bao, W. Y., Mahendrakar, N., Shisler, B., Smith, D., and McCool, M., (2000), "Tool Wear Estimation in Micro-Machining. Part II: Neural-Network-Based Periodic Inspector for Non-Metals", Vol. 40, pp. 609-620.

[12] Tansel, I. N., Mekdeci, C., and Mclaughlin C. (1995), "Detection of Tool Failure in End Milling with Wavelet Transformations and Neural Networks", *International Journal of Machine Tools and Manufacture*, Vol. 35, No. 8, pp. 1137-1147.

[13] Tansel, I., Rodriguez, O., Trujillo, M., Paz, E., and Li, W. (1998), "Micro-end-milling - I. Wear and Breakage", *International Journal of Machine Tools and Manufacture*, Vol. 38, pp. 1419-1436.

[14] Wang, L., Mehrabi, M. G., and Kannatey-Asibu, E., Jr. (2001), "Tool Wear Monitoring in Machining Processes Through Wavelet Analysis", *Transactions of NAMRI/SME*, Vol. 29, pp. 399-406.

CHAPTER 4. TOOL WEAR MONITORING IN RAMP CUTS IN END MILLING USING THE WAVELET TRANSFORM

A paper accepted by the International Journal of Advanced Manufacturing Technology

Yonghoon Choi[1], Ranga Narayanaswami[1], and Abhijit Chandra[2]

ABSTRACT

Tool wear and its identification and estimation are a fundamental problem in machining. With tool wear there is an increase in cutting forces, and leads to deterioration in process stability, part accuracy, and surface finish. In this paper, cutting force trends and tool wear effects in ramp cut machining are experimentally observed as machining progresses. The ramp cuts are unique in the sense that the depth of cut is continuously changing. New tool cutting forces are compared with cutting forces obtained from a progressively wearing tool as a result of machining. The wavelet transform is used for signal processing and is found to be useful for observing resultant cutting force trends. The Root Mean Square (RMS) value of the wavelet transformed signal and linear regression are used for tool wear estimation. Tool wear is also estimated by measuring slot thickness on a coordinate measuring machine.

Key words: Tool Wear, Cutting Forces, Wavelet Transform, Ramp Cuts, and Signal Processing

---

[1]Industrial and Manufacturing Systems Engineering

[2]Mechanical Engineering

4.1 Introduction

Monitoring cutting forces and tool wear effects in end milling is a necessary step toward the full automation of milling operations. To monitor the end milling process successfully, the selection of an appropriate signal and signal processing algorithm is very important. Several signals in a milling operation have been considered to monitor tool failure, for example, cutting force, torque, vibration, acoustic emission, and spindle motor current.

In this paper we are concerned with monitoring the cutting force in ramp cuts in end milling. The ramp cuts are unique in that they have (i) variation in the depth of cut and (ii) the cutting force trends also depend on the feed direction [1]. Extensive experimental results have been observed progressively as new tools are being worn during machining rather than focusing on new and broken (or pre-worn) tools.

Traditional signal processing approaches such as segmental averages and Fourier Transform generally assume that the sensor signals are stationary. However, the sensor signals in tool wear monitoring are usually non-stationary. Thus, the approaches that deal with non-stationary signals are more appropriate for process monitoring. The wavelet transform is a convenient tool for processing time varying signals [2]. The wavelet transform is better suited than the Fourier transform for monitoring the cutting force as it provides time-frequency localization of the signal. The Fourier transform has a problem in that it transforms the signal from a time domain to a frequency domain assuming that the signals are stationary or infinite in nature [3]. Namely, it has a difficulty in describing transient components, and does not convey any information pertaining to translation of the signal from the time domain

to the frequency domain. Accordingly, we use the wavelet transform to analyze the force signal.

The rest of the paper is organized as follows. First a brief background on process monitoring, tool wear, and cutting force modeling is provided. The experimental setup used to conduct the ramp cuts is described next. A short section on the wavelet transform for signal processing is included next. The experimental data, explanation of trends in cutting force, the effect of tool wear and its estimation with linear regression and metrology with a coordinate measuring machine (CMM) are provided next. Conclusion and future research directions are presented finally.

4.2 Related Work

The monitoring of tool failure and tool wear has been a subject of active research. Tool wear is a complex phenomenon occurring in different and varied ways in metal cutting processes. Generally, worn tools adversely affect the surface finish of the workpiece and therefore there is a need to develop tool wear condition monitoring systems that alert the operator to the state of tool, thereby avoiding undesirable consequences.

The cutting force signal is considered to provide rich information for tool failure detection in end milling operations and in drilling [4]. For the purpose of process monitoring, segmental averages and the Fourier transform have been used extensively. However, the wavelet transform is increasingly being used for process monitoring. The wavelet transform has two advantages over segmental averaging [5]: first, they represent the system more accurately if the waveform is optimized by considering signal characteristics. Second, wavelet parameters can be used for many other purposes such as identification of

tool breakage, run out, and flute deviation. Tansel et al. [6] used both segmental averaging and the wavelet transform as encoding methods for tool wear estimation found the wavelet transform to be superior. Wavelet transformations require less computation than FFT. For example, FFT requires $N \log_2 N$ operations for transformation of a set of N numbers while fast wavelet transformations require N operations, and the number of operations halves when the transformations are repeated. Tansel, Mekdeci, and Mclaughlin [7] studied the characteristics of normal and broken tool signals in end milling operations with wavelet approximation coefficients. They observed that the variation of the estimated parameters of the wavelet transformations is very distinctive at different cutting conditions, and when the tool is broken.

Gong, Obikawa and Shirakashi [8] estimated tool wear in turning operations with wavelet transform based on the cutting force. Wang, Mehrabi and Kannatey-Asibu [2] used a vibration signal and the wavelet transform to monitor tool wear in turning. They found the vibration signals from sharp and worn tools showed clear differences. A recent review on tool wear condition monitoring in turning with particular emphasis on using the acoustic emission (AE) signal may be found in [9]. Lee and Tarng [10] used spindle motor current to monitor tool failure in end milling. They used the wavelet transform to perform a multilevel signal decomposition to extract the tool failure feature and found the four-level wavelet decomposition to be adequate (decomposition up to 4th level). Li and Wu [11] used wavelet analysis and AE signals in boring to monitor tool wear state.

Li, Dong, and Yuan [12], devised a tool breakage detection system for drilling based on sensor fusion of AE and electrical current sensors. They found that the discrete wavelet transform could clearly diagnose tool breakage. Mori et al. [13] remarked that to predict drill

bit breakage, it is necessary to detect and distinguish the signal behaviors that indicate pre-failure phenomena. They proposed a method for extracting pre-failure information from the cutting force to predict breakage of a small drill bit. Li [14] also used AC servo motor current signal and the wavelet transform to detect breakage of small diameter drills. Li, Tso, and Wang [15] used wavelet transforms and fuzzy techniques to monitor tool breakage and wear conditions according to the measured spindle and feed motor currents.

Tool wear estimation under different cutting conditions is important to accommodate for increases in cutting force and other effects such as vibration. The cutting force models, which mainly model the cutting force under ideal conditions, can then be suitably modified and used in simulation and model based process monitoring. Tool wear estimation can also lead to optimal tool usage by changing the tool at the most appropriate time.

The modeling of cutting forces in machining has been extensively studied, and a recent review may be found in [16]. The mechanistic approach for modeling of cutting force has been quite successful. The mechanistic method views the machining process as a combination of chip load-cutting force relationship, cutting tool geometry, cutting process geometry, work-piece geometry and machining conditions.

The end milling process has been modeled mechanistically [17] and EMSIM software [18] simulates forces in end milling. To obtain a complete representation of the forces on the end mill at any given instant of time, the cutter is discretized into thin, disc-like sections, similar to a stack of coins. The location of each flute on each disc is determined, and the elemental force is calculated for each flute that engages the work-piece. The instantaneous chip thickness, and the flute entry angle, and exit angle, are needed in order to compute

elemental cutting forces. For small feed per tooth compared to the radius of the cutter, the instantaneous chip thickness is calculated as

$$t_c(i,j,k) = f_t \sin\beta(i,j,k) \qquad (1)$$

Where, β is the wrap around angle due to the helix angle, and *i*, *j*, and *k* refer to the *i*th angular increment, *j*th axial height, and *k*th flute and f_t is the feed per tooth. The expressions for the elemental force acting normal to the rake face dF_N, and the friction force dF_T, are:

$$\begin{aligned} dF_N(i,j,k) &= K_N * dZ * t \\ dF_T(i,j,k) &= \mu * dF_N \end{aligned} \qquad (2)$$

Where, dZ is the disk thickness, and the coefficients K_N and μ are determined experimentally by running a series of end milling or turning experiments and measuring forces for each work-piece/tool material combination. Once the normal and friction forces are calculated for a given element, they are transformed from the K_N-μ coordinate system to the X-Y-Z coordinate system. The total force is found by integrating the elemental forces. A comprehensive modeling of end milling forces for arbitrary cutter geometry may be found in [19].

Recently, advances have been made in incorporating the effect of tool wear in cutting force modeling. Elanayar and Shin [20] developed a method to separate the ploughing forces from the shear forces on the shear plane. The forces are decomposed by first separating the shear forces from the total forces and then employing an iterative procedure to calculate the normal forces on the shear plane. The ploughing forces are modeled by taking into account the change in geometry with flank wear. Smithey, Kapoor, and DeVor [21] observed experimentally that in three-dimensional cutting operations in which the nose of the tool is engaged, the region of plastic flow grows linearly as the total wearland width increases.

Plastic flow occurs at the front of the wearland and elastic contact is assumed at the back of the wearland. The flank of the tool is discretized into small two-dimensional elements and a contact model is used to determine the stresses on the individual elements. These stresses are added to the mechanistic force model for a sharp tool to determine the total cutting force.

From the literature it is evident that wavelet based signal analysis has been successful in tool breakage detection and also in estimation of tool wear. Detail wavelet coefficients have been used for breakage detection, particularly in drilling [4], [12-15] and wavelet approximation coefficients have been used in monitoring tool wear in end milling [5-7], [10]. In previous work in the literature, tool wear has been estimated by comparison with pre-worn tools. There is no documented work on estimation of progressive tool wear using the wavelet transform as the machining cuts are carried out. Further, the depth of cut within a machining cut has usually been taken as a constant, whereas we use a variable depth of cut. Both these features make the research conducted in this paper unique. The estimation of tool wear in ramp cuts in end milling is carried out in this paper by applying the wavelet transform on the resultant cutting force signal. The incorporation of progressive tool wear effects into a mechanistic model for cutting force modeling is a rich area that we are beginning to explore.

4.3 Experimental Setup

As shown in Figure 4.1(a), a dynamometer is mounted on the table of a three-axis Fadal CNC machining center. The work-piece is fixtured in the vise, which is bolted on top of the dynamometer. The DAQ card has 16 channels and (-10V ~ +10V) display range. The amplifier has 3 channels to send data to the DAQ card for each X, Y, and Z force signals. The sampling rate is set at 500 Hz.

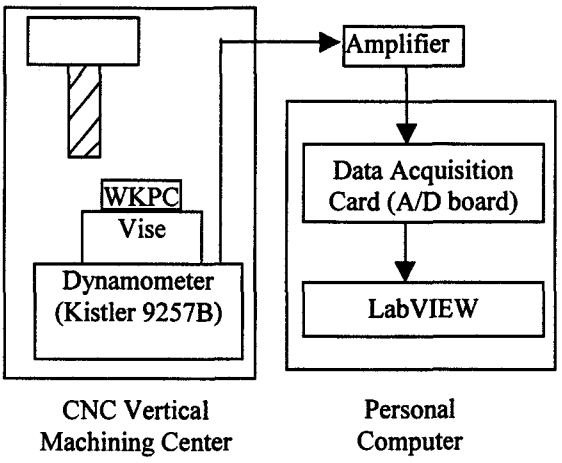

(a) Schematic diagram of experimental set up

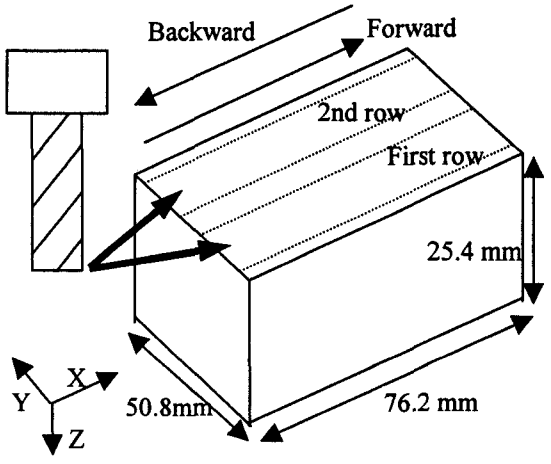

(b) Schematic diagram of machining

Figure 4.1 Experimental Setup and Machining

Ramp cut machining was carried out with a high-speed-steel end mill on an AISI1018 steel work-piece (see Table 4.1). The work-piece and cut configuration is shown in Figure 4.1(b). Two types of ramp cuts were machined as shown in Figure 4.2 and referred to as 1) low to high forward and 2) low to high backward. The terms low and high refer to the axial depth of cut and the terms forward and backward refer to the tool feed direction.

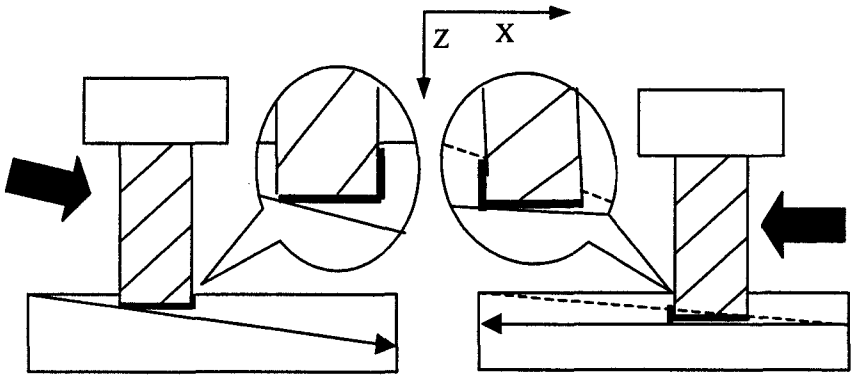

(a) Forward (odd) cut (b) Backward (even) cut

Figure 4.2 Two Types (low to high) of Ramp Cuts and Their Contact Area between Tool and Workpiece

Table 4.1 Experimental Conditions

Work piece	AISI 1018 Steel 50.8mm X 76.2mm X 25.4mm
Tool	High Speed Steel (12.7mm/0.5in diameter flat end mill with 4 flutes)
Depth of Cut	0 to 1.27 mm, 0 to 2.54 mm, and 0 to 3.81 mm for ramp cut
Feed Rate	25.4 and 50.8 cm/min
Spindle Speed	1,000 and 2,000 rpm (CW)

As shown in Figure 4.1(b), at first the tool moves in the forward direction to create the forward ramp cut. Cutting force data is recorded and then the tool is moved in the backward direction to create the backward ramp cut. Repeated forward and backward cuts are made until the bottom of the work-piece is reached. Experimental conditions used for the ramp cuts are shown in Table 4.1. Specific cutting conditions and parameters used for the

ramp cuts are displayed in Table 4.2. Three choices of DOC (Depth of Cut), two valued of feed rate, and two values for the RPM were tried.

Table 4.2. Machining Parameter Sets.

Cutting Conditions	Depth of Cut (mm)	Feed Rate (cm/min)	Spindle Speed (rpm)
1	0 to 1.27	25.4	1000
2	0 to 1.27	50.8	1000
3	0 to 2.54	25.4	1000
4	0 to 2.54	50.8	2000
5	0 to 3.81	25.4	1000

The target is to make 12 rectangular slots/6 work-pieces (2 slots in each work-piece) by making ramp cuts. The size of each slot is 12.7mm X 76.2mm X 22.9mm. To achieve this target with conditions mentioned above, the required machining time and cut numbers are different. Cutting conditions 1 and 2 require 432 cuts to machine 12 slots (36 cuts in each slot) while cutting conditions 3 and 4 require 216 cuts (18 cuts in each slot) and cutting condition 5 needs 144 cuts (12 cuts in each slot). Required machining time for cutting conditions 2 and 4 is half of that for cutting conditions 1, 3, and 5 due to the feed rate being faster by a factor of two. It is noted that the cutting forces shown in this paper are all in lbs.

4.4 Wavelet Transform

Wavelets are a class of functions that are the basis functions for a wavelet transform. Wavelets have proven useful in the analysis of signals that contain transients, image analysis,

and image/signal compression. The wavelet transform decomposes a signal into a representation that shows signal details and trends as a function of time. This representation can be used to characterize transient events, reduce noise, and many other applications. The wavelet transform maintains a constant time resolution regardless of frequency [3].

For many signals, the low-frequency content reflects the general trend, whereas the high-frequency content usually shows details of the process. In a wavelet transform, there are approximations and details. The approximations are the high-scale, (low frequency) components of the signal and the details are the low-scale (high-frequency) components. Figure 3 shows the decomposition of a signal into approximations and details.

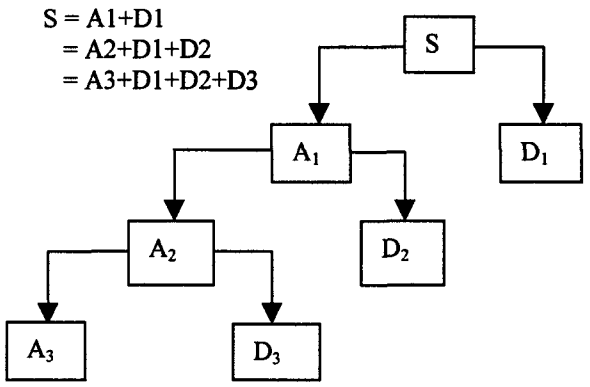

Figure 4.3 Wavelet Decomposition of a Signal

4.5 Experimental Data and Observations

Experimental data are presented for all five machining parameter sets for each forward and backward ramp cut. Cutting forces in the X, Y and Z direction are measured. The +X direction is the forward feed direction. The +Z direction points downward. The +Y axis forms a left-handed coordinate system. The resultant cutting force is obtained as shown

in Equation 3. The Daubechies wavelet transform is applied to the force data. The tool is assumed to be rotating in a clockwise direction.

$$Resultant\ Force = \sqrt{X^2 + Y^2 + Z^2} \qquad (3)$$

In each machining set the forward ramp cuts have odd numbers and the backward ramp cuts have even numbers. The process for forward and backward machining is repeated until 12 slots are machined in each machining condition.

Figure 4.4 shows the X, Y and Z and the resultant cutting force for both the forward and backward ramp cut for a particular machining condition. All signals show either increasing or decreasing trends in cutting force, since the DOC in ramp cuts is either increasing or decreasing. These trends are not noticed in straight slot machining as the DOC is fixed. The cutting force trends for forward and backward cuts tend to be different as noted by Choi and Narayanaswami in [1].

For the forward ramp cut, the X force continuously increases with increasing axial depth of cut. The Y force signal shows a downward sloping trend. It starts from the positive side of the axis at the first stage and tends to go to the negative side after the tool moves into the second half of the work-piece. The Z force is downward sloping and also has the potential to cross the axis.

For the backward ramp cut, the X force continuously decreases (increases in negative direction). The Y force signal shows an upward sloping trend (tool feed direction reversed). The Z force is downward sloping and crossing the axis.

The difference in cutting force trend between Figure 4.4(a) and 4.4(e) is obvious. The crossing of the axis for the Y force in Figure 4.4(b) needs some explanation. As can be seen from Figure 4.2(a) and with respect to the bottom tool surface, both front and rear teeth

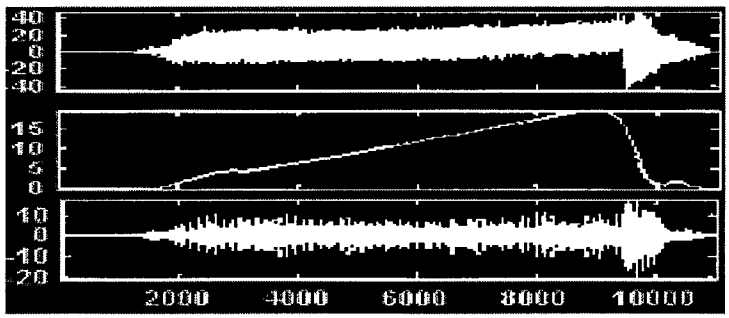

(a) X force signal and its A9 and D1 (cut no. 3)

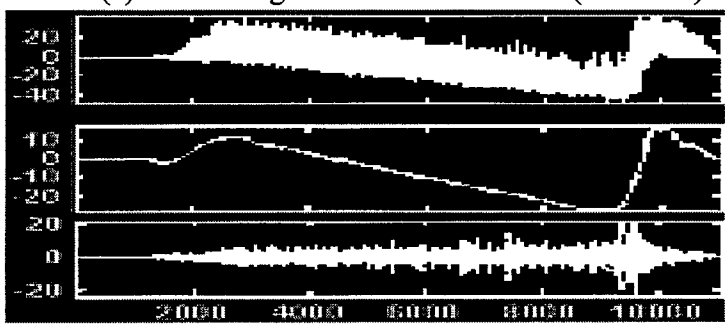

(b) Y force signal and its A9 and D1 (cut no. 3)

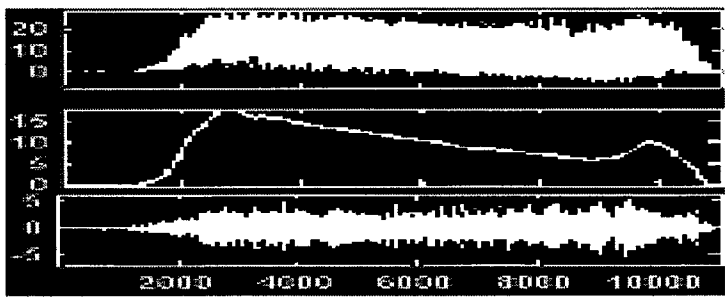

(c) Z force signal and its A9 and D1 (cut no. 3)

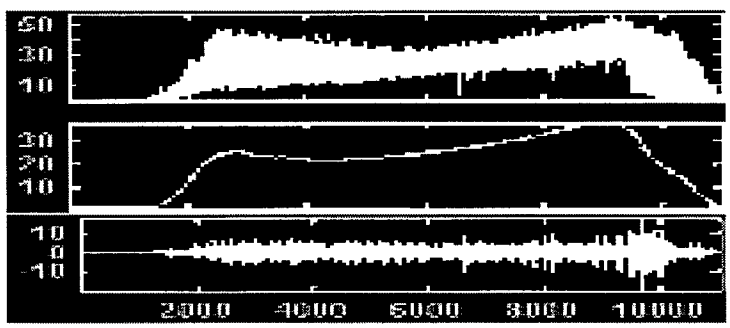

(d) Resultant force signal and its A9 and D1 (cut no. 3)

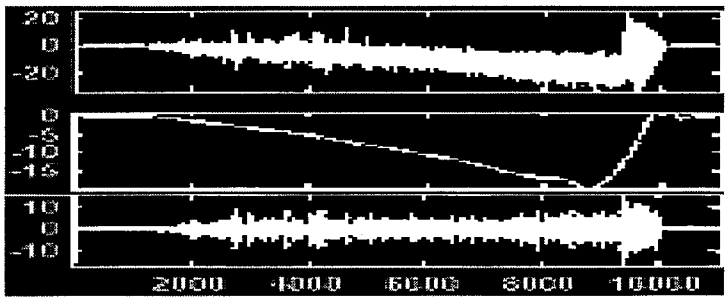

(e) X force signal and its A9 and D1 (cut no. 4)

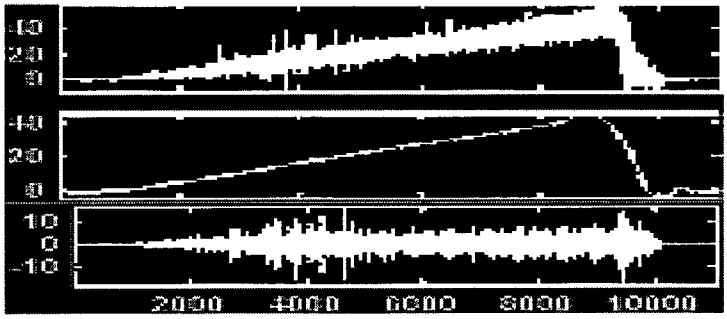

(f) Y force signal and its A9 and D1 (cut no. 4)

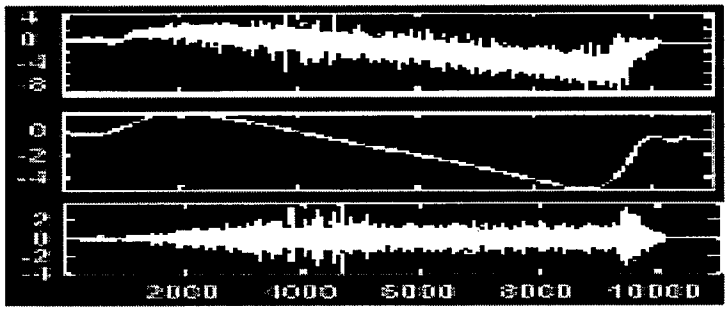

(g) Z force signal and its A9 and D1 (cut no. 4)

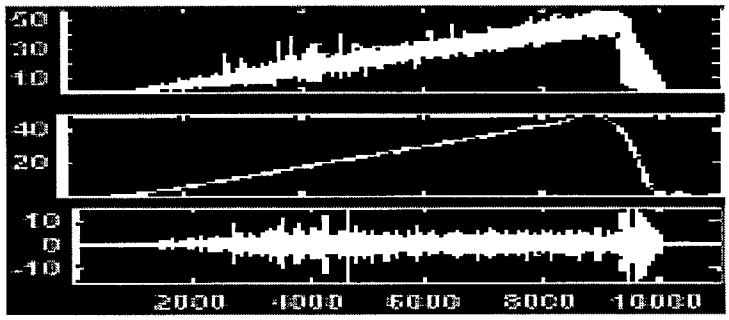

(h) Resultant force signal and its A9 and D1 (cut no. 4)

Figure4.4 X, Y, Z, and Resultant Force Signals (lbs) for Forward and Backward Machining (machining parameters of 0 to 1.27 mm DOC, 25.4 cm/min feed rate, 1000 rpm, and total 432 cuts)

(rear teeth with unit depth of cut) are engaged in machining for the forward ramp cut. For the backward ramp cut however, only front teeth are engaged in machining and rear teeth are contacting the work-piece surface without any active machining. Based on tool contact for the forward ramp cut, the key point to be noted is that teeth at the backside are cutting only a unit amount of volume (principally at the bottom of the teeth). However, the teeth at the front side are removing more chips with both sides and bottoms of the teeth as the tool moves down. The rear teeth provide the positive Y-force and the front teeth provide the negative Y-force. Therefore, as the depth of cut increases, the negative Y force exceeds the positive Y force. The Y signals therefore show the trend of crossing the axis to the negative side

The Z-force trend for both forward and backward cuts needs some more explanation as well. In Figure 4.5(a), we can see that 'I' is the force due to uniform downward pressure exerted by the bottom teeth of the tool and is independent of the depth of cut. The side cutting teeth on the front of the cutter are exerting an upward force (direction of chip exit), and as the axial depth of cut increases, the magnitude of this force increases. This is the negative Z force (II) in Figure 4.5(a). The net Z force is the summation I + II. So "I + II" can cross the axis depending on the depth of cut. In Figure 4.4(c), the Z signal did not cross the axis because 'I' was sufficiently big enough. In Figure 4.4(g) the Z force crosses the axis and allows one to deduce that the downward pressure (I) is smaller in this case than the corresponding forward ramp cut because the tool does not keep pressing the work-piece (Figure 4.5(b)).

In summary, the forward and backward ramp cuts have different trends in cutting force because of differences in tool contact. In the case of the forward ramp cut, the back teeth on the bottom surface of the cutting tool are performing some cutting. Moreover, the

downward thrust force or pressure exerted by the cutting tool is greater in case of the forward ramp cut as the tool is pressing down in the +Z direction. So the resultant cutting force (RMS or mean) in forward machining is higher than the cutting force in backward machining particularly for larger depths of cut.

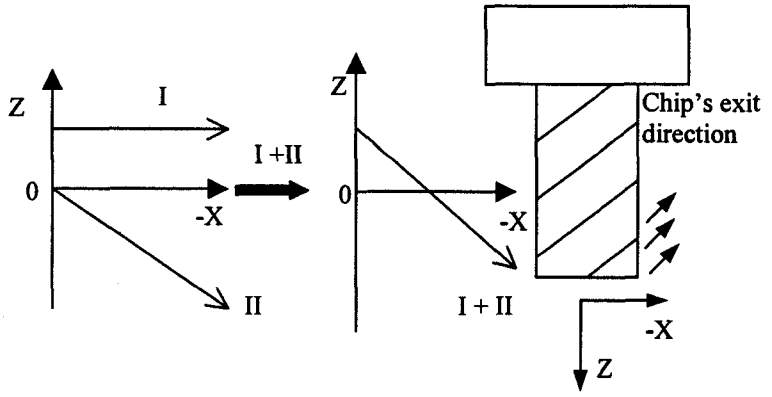

(a) Forward machining

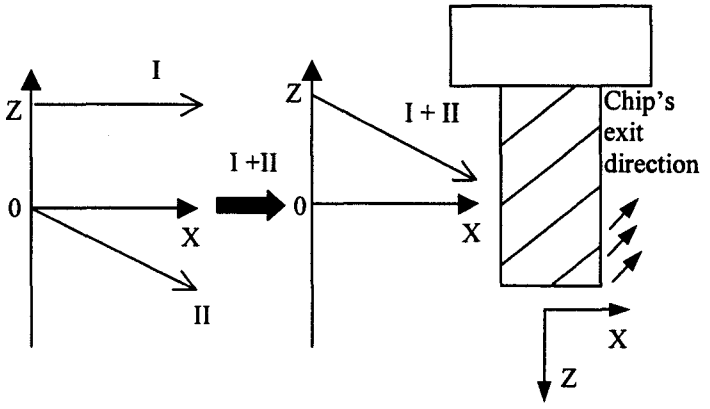

(b) Backward machining

Figure 4.5 Explanation of Z Force Signal for Ramp Cut

4.6 Wavelet Based Signal Processing of Cutting Force

First, the signal for one revolution of the tool is shown in Figure 4.6. 30 data points correspond to one revolution of the tool with a sampling rate of 500 Hz and a spindle RPM of

1000 rev/min. The figure displays two graphs of cutting force each with four peaks and four valleys corresponding to a four-fluted end mill. The graph with the lower magnitude peaks corresponds to the entry region of the cut (lower depth of cut) and the graph with the higher magnitude peaks corresponds to the exit region of the cut (higher depth of cut). As the depth of cut increases it is observed that both the mean cutting force (approximation) and its oscillation (detail) increase.

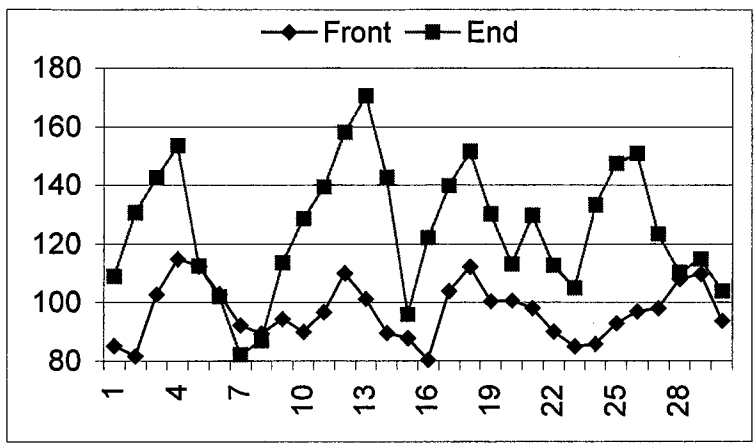

Figure 4.6 Sample Resultant Force Signal (lbs) for One Revolution of the Tool with Scan Rate of 500 Hz and Spindle RMP of 1000 (cut number 215 of cutting condition 3)

4.6.1 Approximation Coefficients

Figure 4.7 shows the resultant cutting force (RF) and its wavelet approximation coefficients at approximation level 9 (A9) as an example. A clear comparison is shown between a beginning cut, cut number 4, (Figure 4.7(a)) when the tool is new and the last cut, cut number 432 (Figure 4.7(b)) when the tool is worn. From Figure 4.7 it is clear that the cutting force increases within each cut and also the cutting force magnitude increases considerably with tool wear. The wavelet approximation A9 clearly shows the cutting force

trend by filtering out the oscillations. The oscillations are captured by the detail wavelet coefficients.

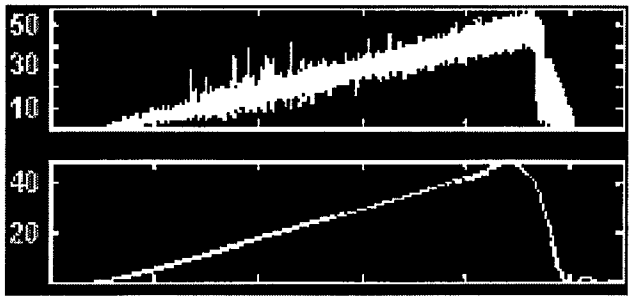

(a) Signal and A9 of cut number 4

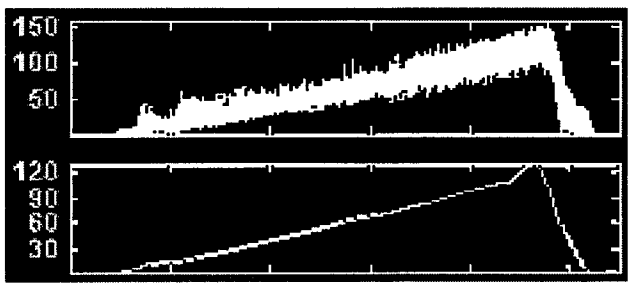

(b) Signal and A9 of cut number 432

Figure 4.7 Sample Resultant Force Signals (lbs) for Ramp Cuts and Their A9s (machining parameters of 0 to 1.27 mm DOC, 25.4 cm/min feed rate, 1000 rpm, and total 432 cuts)

The Root Mean Square (RMS) value of the A9 coefficients within each cut is calculated as shown in Equation 4. The RMS value of A9 within each cut is posted in Figure 4.8 along with a linear regression fit. Figure 4.8 has 10 sub graphs covering forward and backward machining cuts for all 5 experimental conditions.

$$RMS = \sqrt{\frac{\sum_{i=1}^{n} x_i^2}{n}}$$
$$x = values\ of\ A9s \qquad (4)$$
$$n = number\ of\ data$$

In Figure 4.8, the X-axis represents the cut number and the Y-axis represents the RMS value of the resultant cutting forces at A9 at each graph. Data marked on the graphs are for cut number 3 or 4 (depending on forward or backward) and bottom cuts at each slot for both forward and backward cuts. The range of cut numbers in each sub plot in Figure 4.8 is accordingly different.

In all cases except two, (g) and (i), the measured data fit into the linear equations well. Cases (g) and (i) are both forward machining cuts with higher DOC compared to machining parameter sets 1 and 2 making them somewhat severe machining conditions. As explained earlier, the forward ramp cuts generate more cutting force, and with larger DOC a linear regression is not appropriate. For high DOC forward ramp cuts, the cutting force is expected to have a non-smooth trend (locally) as shown in Figure 4.8(g) and (i), and with an increasing trend overall as machining goes on.

The graphs in Figure 4.8 can be compared with respect to changes in the machining conditions. Graphs for forward machining, (a), (e), and (i), show that maximum and minimum values of RMS clearly increased with increased DOC while maintaining other cutting conditions to be the same. The same trend is also noticed for backward machining cuts as shown in Figures 4.8 (b), (f), and (j) where the depth of cut is increased and other cutting conditions are held the same.

The effect of feed rate is another important parameter to be observed. Comparison between Figure 4.8 (a) and (c) for forward cuts and between Figure (b) and (d) for backward cuts, where the feed rate is doubled indicates that cutting forces have increased with increase in feed rate.

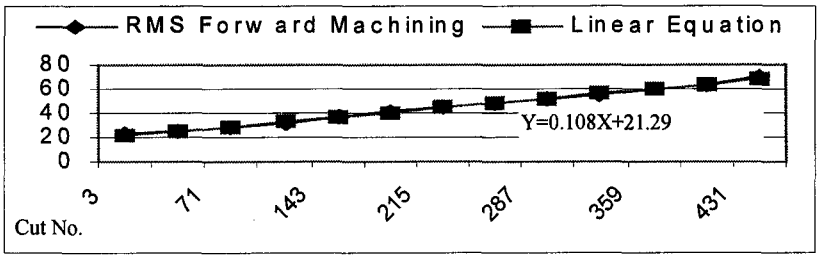

(a) 0.05 inch DOC, 10 ipm feed rate, 1000 rpm, and total 432 cuts (Forward data)

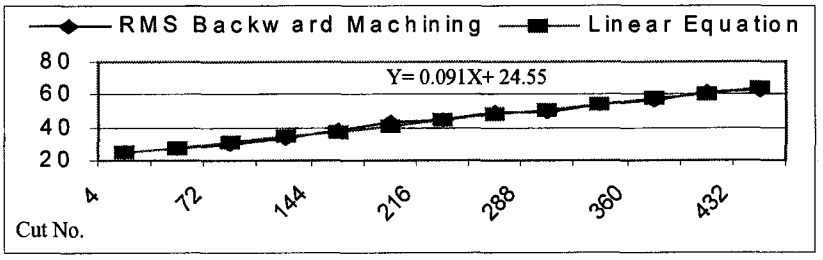

(b) 0.05 inch DOC, 10 ipm feed rate, 1000 rpm, and total 432 cuts (Backward data)

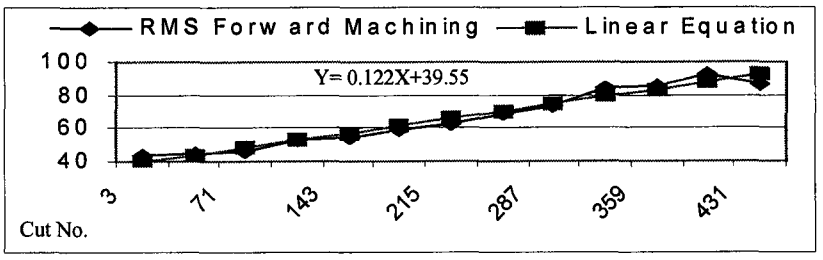

(c) 0.05 inch DOC, 20 ipm feed rate, 1000 rpm, and total 432 cuts (Forward data)

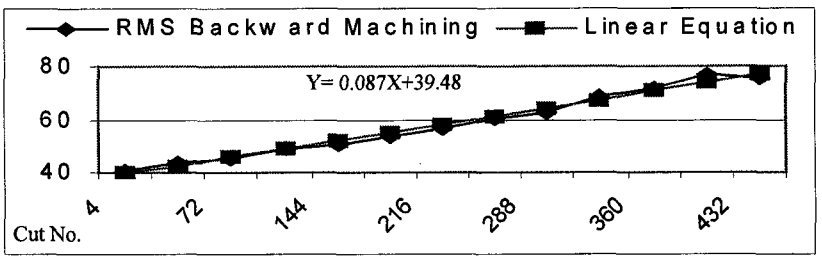

(d) 0.05 inch DOC, 20 ipm feed rate, 1000 rpm, and total 432 cuts (Backward data)

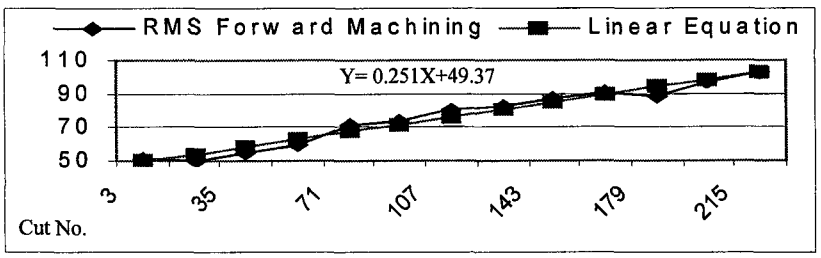

(e) 0.1 inch DOC, 10 ipm feed rate, 1000 rpm, and total 216 cuts (Forward data)

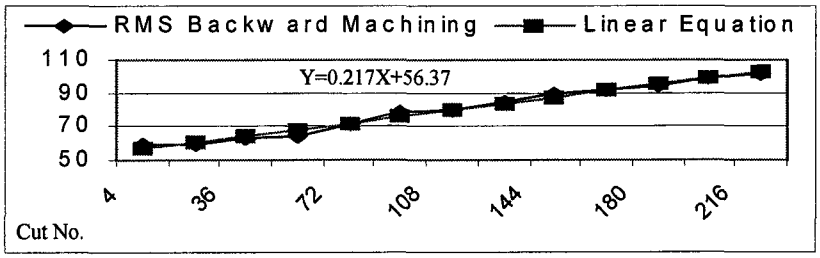

(f) 0.1 inch DOC, 10 ipm feed rate, 1000 rpm, and total 216 cuts (Backward data)

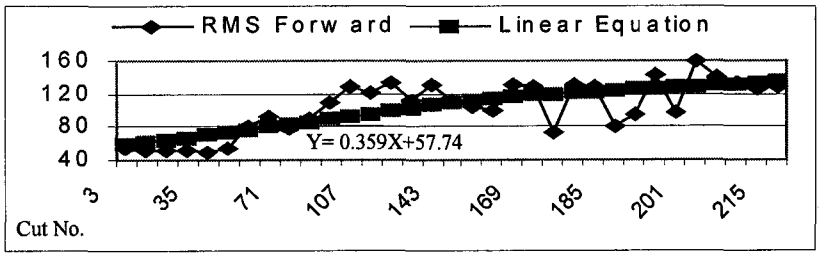

(g) 0.1 inch DOC, 20 ipm feed rate, 2000 rpm, and total 216 cuts (Forward data)

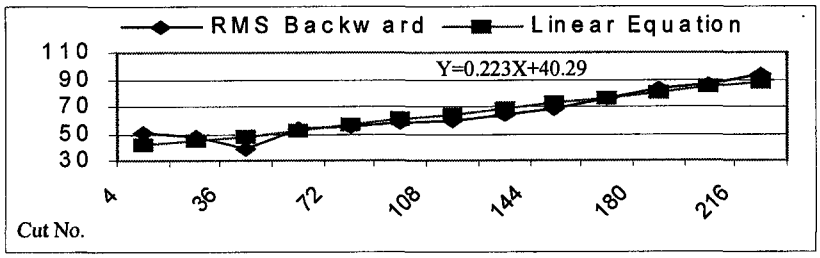

(h) 0.1 inch DOC, 20 ipm feed rate, 2000 rpm, and total 216 cuts (Backward data)

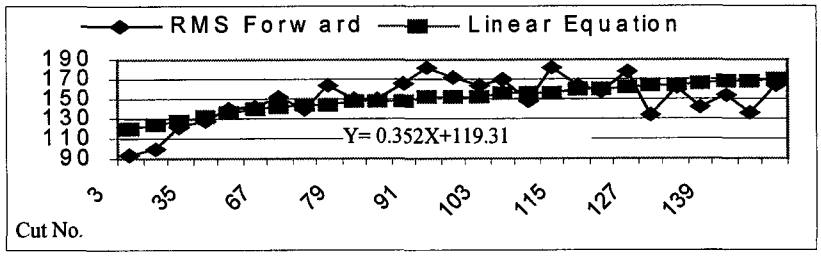

(i) 0.15 inch DOC, 10 ipm feed rate, 1000 rpm, and total 144 cuts (Forward data)

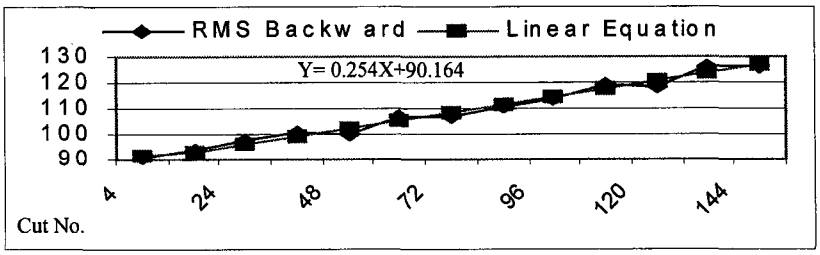

(j) 0.15 inch DOC, 10 ipm feed rate, 1000 rpm, and total 144 cuts (Backward data)

Figure 4.8 Linear Regression of Root Mean Square of A9's of Resultant Cutting Forces (lbs)

Cases shown in Figure 4.8(g) and (h) are difficult to compare directly to other graphs since they have changes in two different conditions (increased rpm) and feed rate as compared to other graphs.

4.6.2 Detail Coefficients

The importance of maintaining details in the wavelet transform is to capture any discontinuities in frequency that occurs in the time domain. Discontinuities may occur in the event of a cutting edge being chipped or broken for example. The details will show these phenomena, while the approximations will still reflect tool wear. Other process faults such as run out and flute deviation can further complicate the signal and the entire set of wavelet coefficients will be necessary to handle the multiple process faults, tool wear and the possibility of tool chipping or breakage to establish a reliable process monitoring system [1].

The RMS values of the detail coefficients at level 1 are displayed in Figure 4.9. The X-axis shows cut numbers at each machining condition and the Y-axis shows the RMS value of the detail coefficient. Each sub - figure has two graphs for forward and backward machining. One obvious trend to notice is that detail coefficients are getting higher with increased feed rate or DOC. A higher detail value means higher oscillation of an original signal. In Figures 4.9(a), (b) and (d) there is a gradual increase in the value of the detail coefficient. This is suggestive of larger cutting force oscillation as a result of tool wear. These trends are not so noticeable in Figures 4.9(c) and (e).

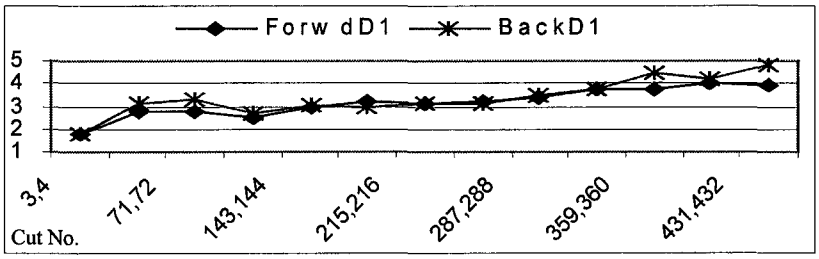

(a) 0.05 inch DOC, 10 ipm feed rate, 1000 rpm, and total 432 cuts

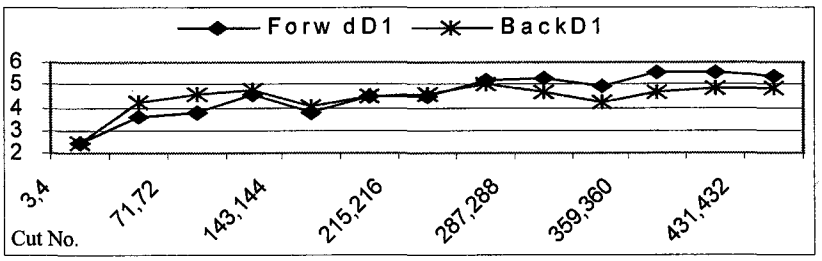

(b) 0.05 inch DOC, 20 ipm feed rate, 1000 rpm, and total 432 cuts

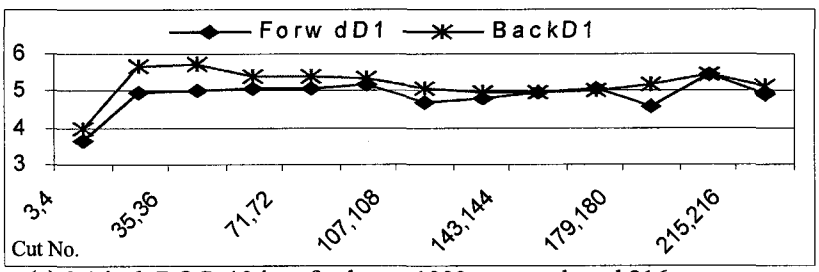

(c) 0.1 inch DOC, 10 ipm feed rate, 1000 rpm, and total 216 cuts

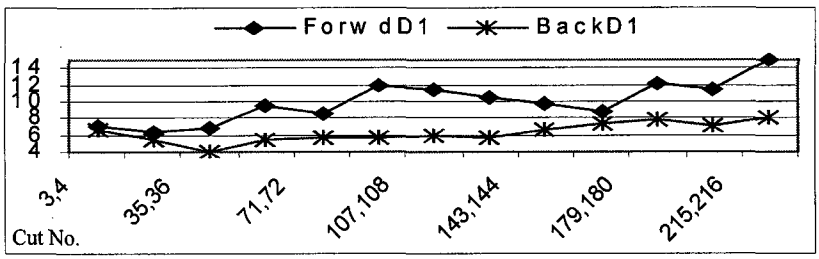

(d) 0.1 inch DOC, 20 ipm feed rate, 2000 rpm, and total 216 cuts

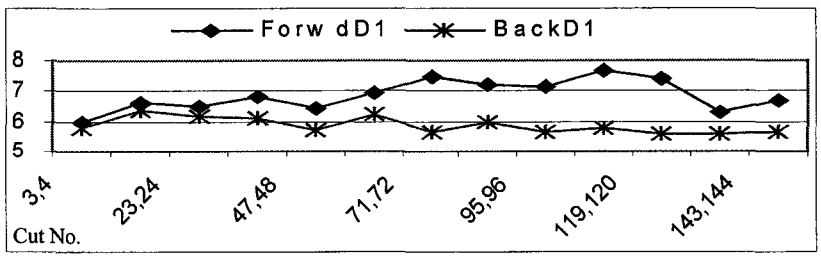

(e) 0.15 inch DOC, 10 ipm feed rate, 1000 rpm, and total 144 cuts

Figure 4.9 RMS of D1 for Each Machining Set (lbs)

4.7 Tool Wear

Figure 4.8 shows that repeated machining with the same tool leads to increase in the cutting force as a result of tool wear. The wavelet approximations of resultant forces show an increase in the mean force of ramp cuts as shown in Figure 4.7. A sample SEM picture of one side flute of worn tool is shown in Figure 4.10. The amount of tool wear may be estimated using linear regression as well as metrology of the machined slot. Both of these are considered below.

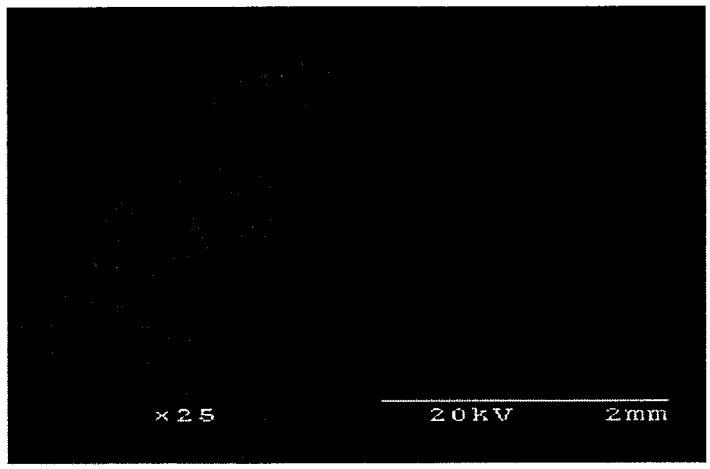

Figure 4.10 Sample SEM Photograph of a Single Flute of a Worn 4 Fluted End Mill

4.7.1 Tool Wear Estimation with Linear Regression

1.0 minus residual variance is referred to as R-square or the coefficient of determination. The R-square value is an indicator of how well the model fits the data (e.g., an R-square close to 1.0 indicates that we have accounted for almost all of the variability with the variables specified in the model). Table 4.3 shows all R-squares of the linear regression in Figure 4.8. All values are close to 1.0 except for cases (g) and (i) where linear regression is not appropriate.

As can be seen from Table 4.4, each linear equation fits well to the measured value of RMS. Only machining parameter sets 1, 2, and 3 have been tested since sets 4 and 5 are considered somewhat severe conditions. Maximum difference between measured and linear equation of RMS is 5.38 %. 2 cut numbers for both forward and backward cuts for each machining parameter sets were selected randomly and tested.

Table 4.3. R-Squares of Linear Regressions in Figure 4.8

Cutting Conditions	Sub Figures	R-square
1.27 mm, 25.4 cm/min, 1000 rpm, and 432 cuts	(a)	0.993
	(b)	0.991
1.27 mm, 50.8 cm/min, 1000 rpm, and 432 cuts	(c)	0.964
	(d)	0.985
2.54 mm, 25.4 cm/min, 1000 rpm, and 216 cuts	(e)	0.969
	(f)	0.985
2.54 mm, 50.8 cm/min, 2000 rpm, and 216 cuts	(g)	0.578
	(h)	0.900
3.81 mm, 25.4 cm/min, 1000 rpm, and 144 cuts	(i)	0.407
	(j)	0.983

Table 4.4 Comparison of Measured RMS of Resultant Force at A9 and Linear Regression Models

		Cut no.	Measured	Lin. Eq.	Diff. in %
DOC: 1.27 mm	Forward	63	27.4868	28.094	2.21
Feed: 25.4 cm/min		235	47.5376	46.67	-1.83
Speed: 1,000 rpm	Backward	100	33.2808	33.65	1.11
Total 432 cuts		280	50.0618	50.03	-0.06
DOC: 1.27 mm	Forward	119	54.4915	54.068	-0.78
Feed: 50.8 cm/min		379	87.9340	85.788	-2.44
Speed: 1,000rpm	Backward	208	58.0055	57.576	-0.75
Total 432 cuts		416	75.7522	75.672	-0.11
DOC: 2.54 mm	Forward	31	54.6216	57.151	4.63
Feed: 25.4 cm/min		115	81.5575	78.235	-4.07
Speed: 1,000rpm	Backward	140	91.6803	86.75	-5.38
Total 216 cuts		190	100.2500	97.6	-2.64

4.7.2 Metrology

The Coordinate Measuring Machine (CMM) has also been used to estimate the tool wear. For each machining set, first the slot width at the top part of the first workpiece is measured (very first machining), and then slot width at the bottom of the cut for each work-piece in consecutive order is measured next. These slot sizes are compared relatively to the initial size of the first measurement (at the top of the first workpiece). Results are shown in Table 4.5.

For each machining parameter set the slot width is reduced from the first cut to the last cut. This is indicative of tool wear. It can be noticed that as the machining conditions get more severe with higher feed rate or DOC, the amount of tool wear is getting bigger (slot size is become smaller). Machining parameter set 5 is the most severe machining condition (highest tool wear). The measured slot width can therefore also serve as an indicator of tool wear and can be used as a strategy for tool changing.

Table 4.5 Measurements of Relative Slot Thickness (mm) Using a CMM

Cutting Conditions	Locations	Relative Slot Thickness
1.27 mm, 25.4 cm/min,	Bottom at 3rd wkpc	-0.0457
1000 rpm, and 432 cuts	Final size	-0.0483
1.27 mm, 50.8 cm/min,	Bottom at 3rd wkpc	-0.0559
1000 rpm, and 432 cuts	Final size	-0.0940
2.54 mm, 25.4 cm/min,	Bottom at 3rd wkpc	-0.1397
1000 rpm, and 216 cuts	Final size	-0.2388
2.54 mm, 50.8 cm/min,	Bottom at 3rd wkpc	-0.1575
2000 rpm, and 216 cuts	Final size	-0.2718
3.81 mm, 25.4 cm/min,	Bottom at 3rd wkpc	-0.1829
1000 rpm, and 144 cuts	Final size	-0.2921

4.8 Conclusions and Future Work

Experimental cutting force data in ramp cuts in end milling were generated and analyzed for tool wear effects. The ramp cuts are unique in that they have a changing depth

of cut. The wavelet transform was used to generate a multilevel decomposition of the cutting force signal. Cutting force trends have been observed progressively as new tools are being worn with different cutting parameters. The RMS value of the approximation coefficients of the resultant cutting force signal was used to model and estimate tool wear. For smaller depth of cut a linear regression fit of the RMS value of the approximation coefficients was obtained. Under these conditions tool wear was estimated within an error of 6%. Metrology was also used to estimate the tool wear. The slot thickness is continuously reduced as the tool is worn and can serve as another indicator for tool wear estimation.

The estimation of tool wear can be used to plan optimal tool replacement. The modeling of tool wear into existing cutting force models presents an interesting future research direction. The next phase of the work will involve mechanistic modeling of cutting force including the effect of tool wear. This will result in an effective model-based tool monitoring system for end milling, and be useful in the industry. The new mechanistic model of cutting force may be used in simulations and in planning optimal tool replacement.

4.9 Acknowledgement

This research is supported by the National Science Foundation under grant No. DMI 9970083. Any opinions, findings, and conclusions or recommendations expressed in this material are those of the authors and do not necessarily reflect the views of the National Science Foundation. The authors gratefully acknowledge help from Jim Dautremont in Mechanical Engineering and Kevin Brownfield in Industrial and Manufacturing Systems Engineering for assistance with the machining experiments.

4.10 References

[1] Choi, Y. and Narayanaswami, R. (2002), "Experimental Observations of Cutting Force and Tool Wear Effects in Ramp Cuts in End milling," *Transactions of NAMRI/SME*, Vol. 30, May. (Accepted)

[2] Wang, L., Mehrabi, M. G., and Kannatey-Asibu, E., Jr. (2001), "Tool Wear Monitoring in Machining Processes Through Wavelet Analysis," *Transactions of NAMRI/SME*, Vol. 29, pp. 399-406.

[3] Misiti, M., Misiti, Y., Oppenheim, G., and Poggi, J. (1996), "Wavelet Toolbox," *The Mathworks. Inc.*

[4] Li, X. (1998), "Real-time Detection of the Breakage of Small Diameter Drills with Wavelet Transform," *International Journal of Advanced Manufacturing Technology*, Vol. 14, pp. 539-543.

[5] Tansel, I., Rodriguez, O., Trujillo, M., Paz, E., and Li, W. (1998), "Micro-end-milling - I. Wear and Breakage," *International Journal of Machine Tools and Manufacture*, Vol. 38, pp. 1419-1436.

[6] Tansel, I. N., Arkan, T. T., Bao, W. Y., Mahendrakar, N., Shisler, B., Smith, D., and McCool, M., (2000), "Tool Wear Estimation in Micro-Machining. Part II: Neural-Network-Based Periodic Inspector for Non-Metals," *International Journal of Machine Tools and Manufacture,* Vol. 40, pp. 609-620.

[7] Tansel, I. N., Mekdeci, C., and Mclaughlin, C. (1995), "Detection of Tool Failure in End Milling with Wavelet Transformations and Neural Networks," *International Journal of Machine Tools and Manufacture*, Vol. 35, No. 8, pp. 1137-1147.

[8] Gong, W., Obikawa, T., and Shirakashi, T. (1997), "Monitoring of Tool Wear States in Turning Based on Wavelet Analysis," *JSME International Journal*, Vol. 40, No. 3, pp. 447-453.

[9] Li, X. (2002), "A brief review: Acoustic Emission Method for Tool Wear Monitoring during Turning", *International Journal of Machine Tools and Manufacture*, Vol. 42, pp. 157-165.

[10] Lee, B. Y. and Tarng, Y. S. (1999), "Application of the Discrete Wavelet Transform to the Monitoring of Tool Failure in End Milling Using the Spindle Motor Current," *International Journal of Advanced Manufacturing Technology*, Vol. 15, pp. 238-243.

[11] Li, X. and Wu, J. (2000), "Wavelet Analysis of Acoustic Emission Signals in Boring", *Proceedings of the Institution of Mechanical Engineers, Part B: Journal of Engineering Manufacture*, Vol. 214, no. 5, pp. 421-424.

[12] Li, X., Dong, S., and Yuan, Z. (1999), "Discrete Wavelet Transform for Tool Breakage Monitoring", *International Journal of Machine Tools and Manufacture*, Vol. 39, pp. 1935-1944.

[13] Mori, K., Kasashima, N., Fu, J.C., and Muto, K. (1999), "Prediction of Small Drill Bit Breakage by Wavelet Transforms and Linear Discriminant Functions" *International Journal of Machine Tools and Manufacture*, Vol. 39, pp. 1471-1484.

[14] Li, X. (1999), "On-Line Detection of the Breakage of Small Diameter Drills using Current Signature Wavelet Transform", *International Journal of Machine Tools and Manufacture,* Vol. 39, pp. 157-164.

[15] Li, X., Tso, S., and Wang, J. (2000), "Real-Time Tool Condition Monitoring using Wavelet Transforms and Fuzzy Techniques", *IEEE Transactions on Systems, Man, and Cybernetics - Part C: Applications and Reviews*, Vol. 30, no. 3, pp. 352-357.

[16] Ehmann, K. F., Kapoor, S. G., DeVor, R. E., and Lazoglu, I. (1997), "Machining Process Modeling: A Review," *Journal of Manufacturing Science and Engineering*, Vol. 119, Nov., pp. 655-663.

[17] Devor, R.E., Kline, W. A. and Zdeblick, W. J. (1980), "A Mechanistic Model of the Force System in End Milling with Application to Machining Airframe Structures," *Proceedings of the 8th North American Metalworking Research Conference*, pp. 297-303.

[18] "EMSIM" (2002), http://mtamri.me.uiuc.edu, simulation software at University of Illinois at Urbana-Champaign, accessed on Jan. 2002.

[19] Altintas, Y. and Engin, S. (2001), "Generalized Modeling of Mechanics and Dynamics of Milling Cutters," *Annals of the CIRP*, Vol. 50, no. 1, pp. 25-30.

[20] Elanayar, S. and Shin, Y. C. (1996), "Modeling of Tool Forces for Worn Tools: Flank Wear Effects," *Journal of Manufacturing Science and Engineering*, Vol. 118, No. 3, pp. 359-366.

[21] Smithey, D. W., Kapoor, S. G., and DeVor, R. E. (2000), "A Worn Tool Force Model for Three-Dimensional Cutting Operations," *International Journal of Machine Tools and Manufacture*, Vol. 40, pp. 1929-1950.

CHAPTER 5. COMPARISON OF STRAIGHT AND RAMP CUTS IN END MILLING

A paper to be submitted to the Journal Publication

Yonghoon Choi and Ranga Narayanaswami

ABSTRACT

Traditionally, a series of straight slot cuts are used to machine a deep slot. Ramp cuts in which the depth of cut is continuously changing offers another possibility. In this paper, cutting force signals, table motor currents and tool wear in straight and ramp cuts in end milling are experimentally observed and compared. Trends in X, Y, Z cutting force for straight and ramp cuts are explained. Cutting force trends are also analyzed for tool wear. In addition, SEM pictures are presented to show differences in tool wear for these two types of cuts.

5.1 Introduction

Machining a deep slot requires a series of cuts. Traditionally straight cuts are used for this purpose. An alternative is ramp cut milling. In this paper, we compare these two methods experimentally with respect to cutting force and tool wear. Dynamometry and current signals are processed for force measurement and analysis. SEM pictures are used for observing tool wear.

The ramp cuts are unique in that they have (i) variation in the depth of cut and (ii) the cutting force trends also depend on the feed direction. Cutting force trends in the X, Y, Z directions in ramp cuts were explained previously by the authors in [1].

For deep slotting, the key difference between ramp and straight cuts lies in contact area between the tool and work-piece. The depth of cut in a ramp cut is continuously changing. Consequently, tool contact in ramp cuts is twice that for straight cuts while removing the same amount of volume.

Several signals have been considered for monitoring the milling process and include cutting force, torque, vibration, acoustic emission, and spindle motor current. In this paper we are concerned with monitoring the cutting force and table motor current in ramp and straight cuts in end milling. The selection of an appropriate signal processing algorithm is important. Traditional signal processing approaches such as segmental averages and Fourier Transform generally assume that the sensor signals are stationary. However, the sensor signals in tool wear monitoring are usually non-stationary. Thus, the approaches that deal with non-stationary signals are more appropriate for process monitoring.

The wavelet transform is a convenient tool for processing time varying signals. The wavelet transform is better suited than the Fourier transform for monitoring the cutting force as it provides time-frequency localization of the signal. The Fourier transform has a problem in that it transforms the signal from a time domain to a frequency domain assuming that the signals are stationary or infinite in nature. Namely, it has a difficulty in describing transient components, and does not convey any information pertaining to translation of the signal from the time domain to the frequency domain. Accordingly, we use the wavelet transform to analyze the force signal.

The rest of the paper is organized as follows. First a brief background on process monitoring and tool wear is provided. The experimental setup used for ramp and straight cut machining and the measurement of cutting force and current signals is described next. Experimental results from force signals, current signals, and tool wear observation with SEM and microscope pictures are shown next. Conclusions are presented finally.

5.2 Background

The monitoring of tool failure and wear has been a subject of active research. Segmental averages and the Fourier transform have been used extensively for signal processing. However, the wavelet transform is increasingly being used for process monitoring. The wavelet transform has two advantages over segmental averaging [7]: first, they represent the system more accurately if the waveform is optimized by considering the characteristics of the signal. Second, wavelet parameters can be used for many other purposes such as identification of tool breakage, run out, and flute deviation.

Li [5] used the wavelet transform to detect tool breakage in small diameter drills using the cutting force signal. Lee and Tarng [4] used spindle motor current to monitor tool failure in end milling. They used the wavelet transform to perform a multilevel signal decomposition to extract the tool failure feature and found the four-level wavelet decomposition to be adequate.

Gong, Obikawa and Shirakashi [3] estimated tool wear in turning operations with wavelet transform based on the cutting force. Li et al. [6] measured feed motor current to estimate the feed cutting force and monitor tool wear in turning. By comparing successive feed cutting force estimates, the onset of the accelerated tool wear was determined. Wang,

Mehrabi and Kannatey-Asibu [8] used a vibration signal and the wavelet transform to monitor tool wear in turning. They found the vibration signals from sharp and worn tools showed clear differences. El-Wardany and Elbestawi [2] investigated a stochastic model, for ceramic tools used in the finish turning of case hardened steel materials.

It is clear that the literature supports the use of wavelets for signal processing. The cutting force and current signals have also been successfully utilized for tool wear monitoring. The literature however has not addressed the monitoring of ramp cuts other than the work by the authors [1].

5.3 Experimental Setup

The experimental setup consists of a dynamometer mounted on the table of a three-axis Fadal CNC machining center and current sensors to measure the table motor current. The work-piece is fixtured in the vise, which is bolted on top of the dynamometer. The DAQ card has 16 channels and (-10V~10V) range to display. The amplifier has 3 channels to send the data to the DAQ card for each X, Y, and Z force signals. The sampling rate is set at 500/sec and the tool is assumed to be rotating in a clockwise direction.

Table 5.1 Experimental Conditions

Work-piece	AISI1018 steel 1" X 2" X 3"
Tool	High Speed Steel (0.5in diameter flat end mill with 4 flutes) 30° Helix Angle and 10° Radial Rake Angle
Depth of Cut	0 to 0.1inch for ramp cut 0.05 inch for straight cut
Feed Rate	10 in/min
Spindle Speed	1,000rpm (CW)

Machining was carried out with a high-speed steel end mill on an AISI1018 steel work-piece (see Table 5.1). The geometric difference between straight and ramp cuts is shown in Figure 5.1. The work-piece and cut configuration is shown in Figure 5.2.

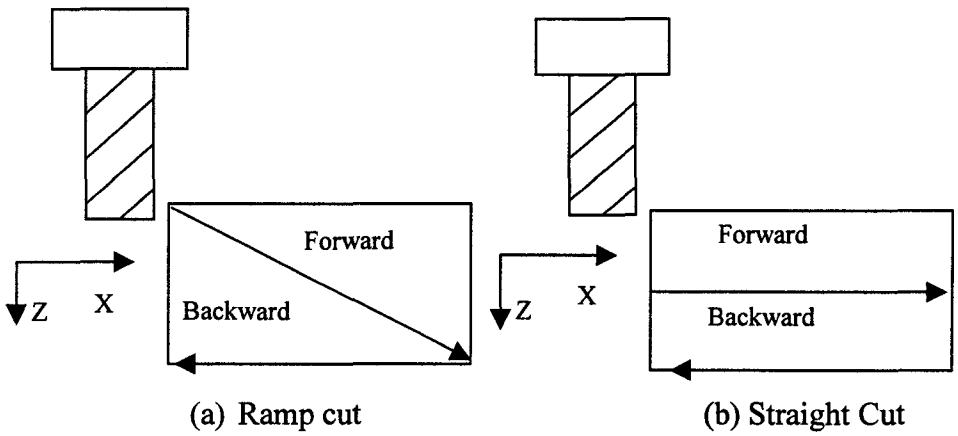

Figure 5.1 Geometric Difference in Ramp and Straight Cut

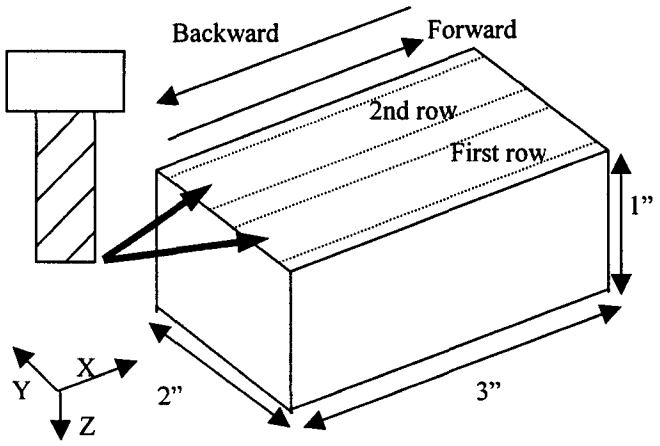

Figure 5.2 Schematic Diagram of Machining

As shown in Figure 5.2, at first the tool moves in the forward direction, and then it moves in the backward direction to its original position (X and Y) after recording data for the

first cut. Repeated cuts are made until the bottom of the work-piece is reached, then the tool moves to the 2nd row. The +X direction is the forward feed direction. The +Z direction points downward. 18 cuts in each row are made for a total of 36 cuts in one work-piece. Six work-pieces are used to generate all cutting data on each ramp and straight cut. Consequently, the tool cuts 216 times to remove specified volumes in each case.

To compare ramp and straight cuts in another way, current sensors are used to measure table motor currents and the signals gained through multi-meters.

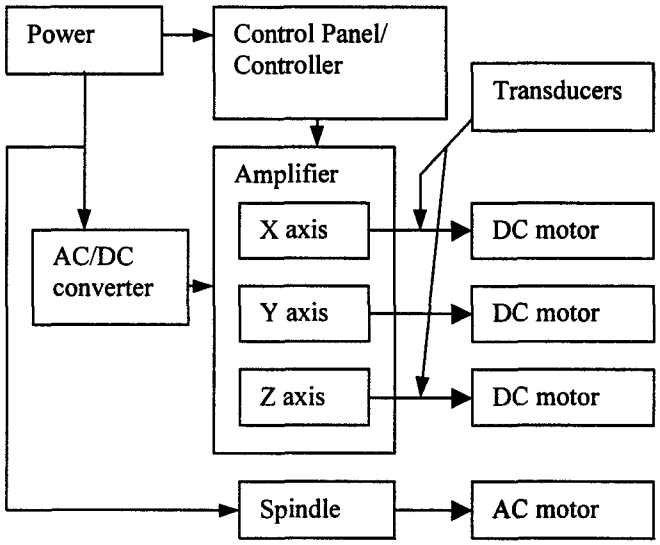

Figure 5.3 Schematic Control Diagram of CNC Machining Center

As shown in Figure 5.3, transducers are used to measure current signals for table motors. X axis motor signal is crucial to be measured because X is feeding direction. Z axis motor signal needs to be measured for ramp cuts as the depth of cut changes continuously while it might not be needed for straight cut since the depth of cut does not change. Y axis motor was not measured because it does not move during machining. In this set of

experiments, both ramp and straight cuts were performed alternately and repeatedly. As shown in Figure 5.4 the tool cuts a set of ramp cuts followed by a set of straight cuts.

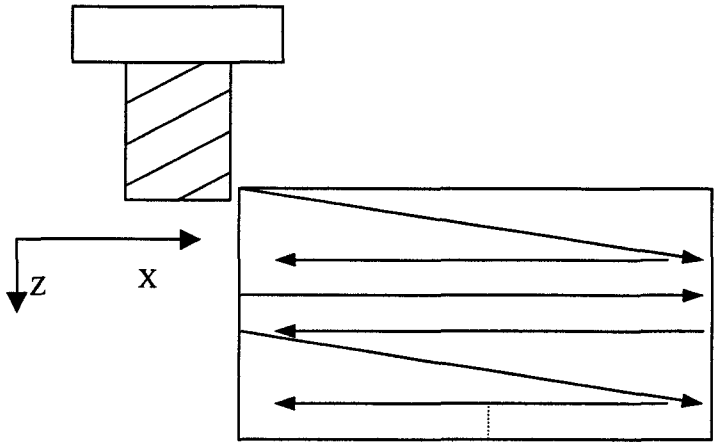

Figure 5.4 Alternate Ramp and Straight Cut

5.4 Cutting Force Signals

The tool contact area, the changing depth of cut and the unit pressing load because of downward motion of the tool are the key factors in explaining cutting force trends in ramp cuts [1]. Cutting force trends in straight cuts are easy to understand. Constant forces are recorded as there is no variation in depth of cut while the tool is engaged in machining. Figure 5.5 shows the cutting force trends in ramp and straight cuts for forward direction machining. For each cut, X, Y, and Z force signals and the corresponding wavelet transformed signal at approximation 9 (A9) are shown. The cutting force trends in backward machining are similar to forward machining.

The Root Mean Square (RMS) value of the A9 coefficients within each cut is calculated as

$$RMS = \sqrt{\frac{\sum_{i=1}^{n} x_i^2}{n}}$$

$x = values\ of\ A9s$

$n = number\ of\ data$

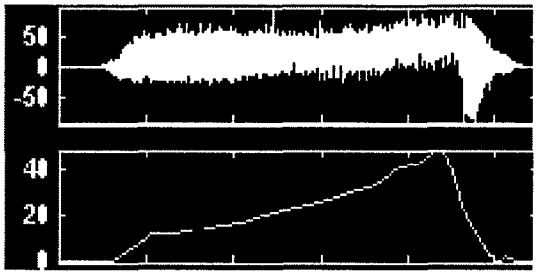

(a) X forward ramp cut

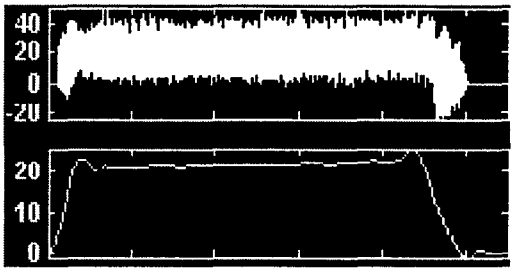

(d) X forward straight cut

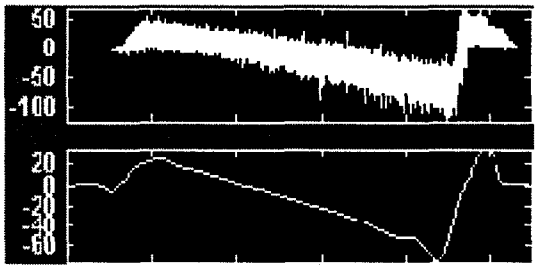

(b)Y forward ramp cut

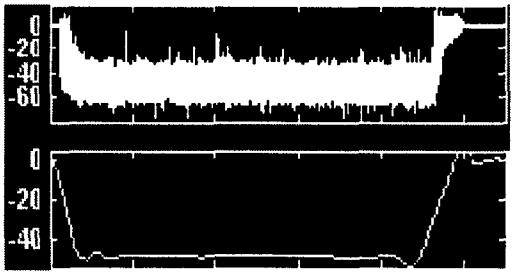

(e) Y forward straight cut

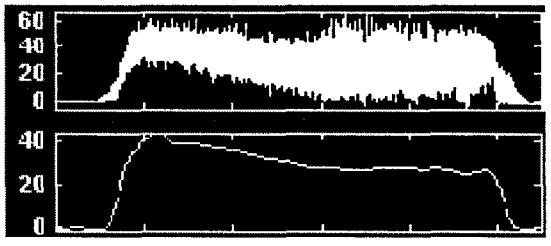

(c) Z forward ramp cut

(f) Z forward straight cut

Figure 5.5 X, Y, and Z Force Trends in Ramp and Straight Cuts

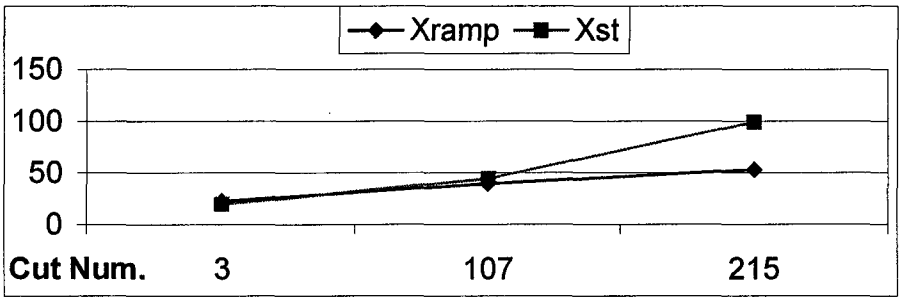

(a) X forward comparison

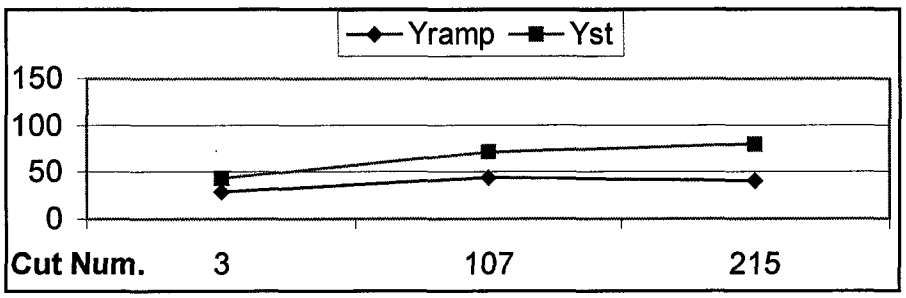

(b) Y forward comparison

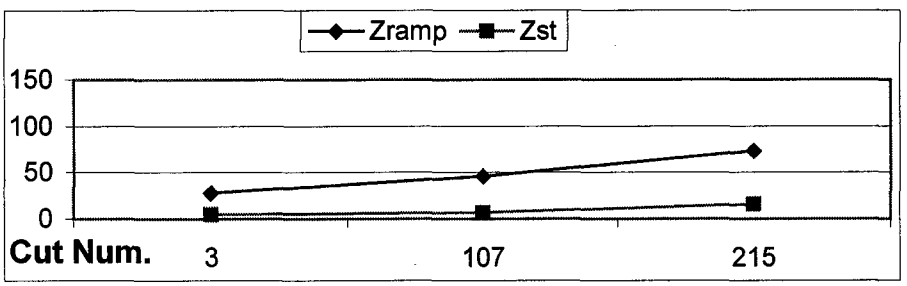

(c) Z forward comparison

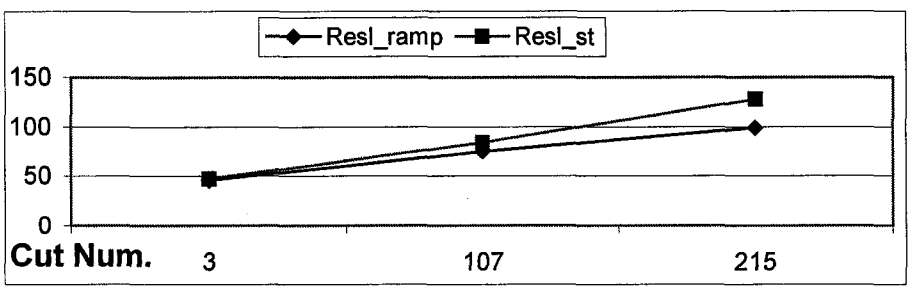

(d) Resultant forward comparison

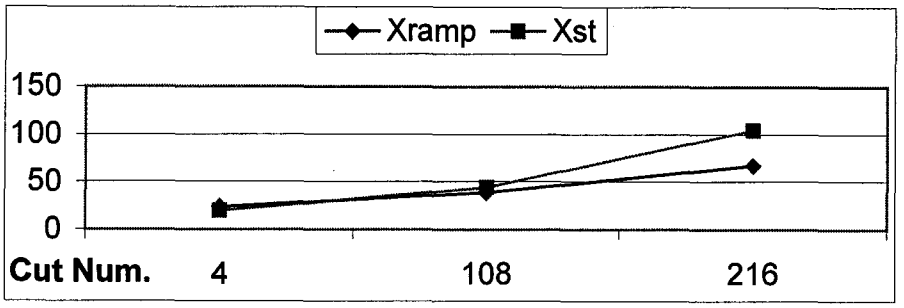

(e) X backward comparison

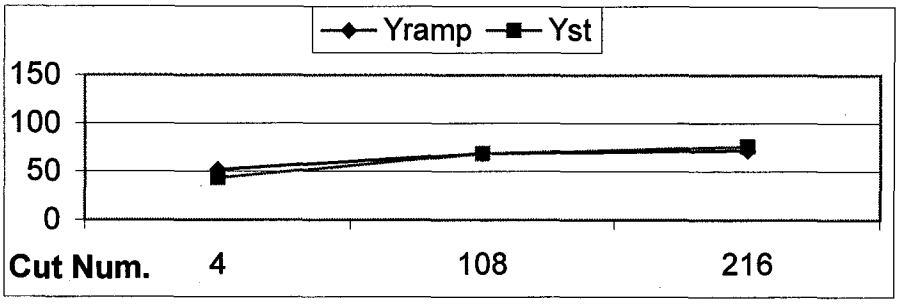

(f) Y backward comparison

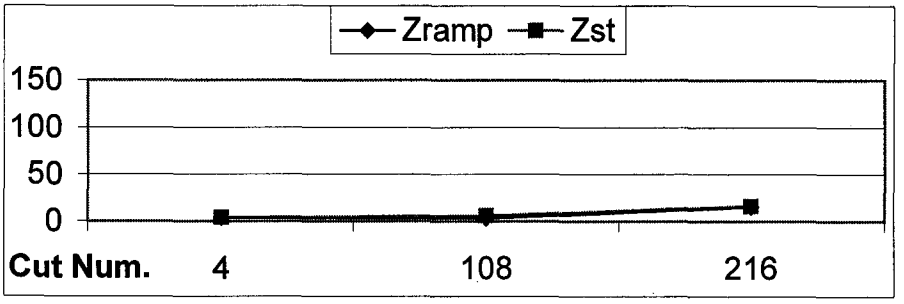

(g) Z backward comparison

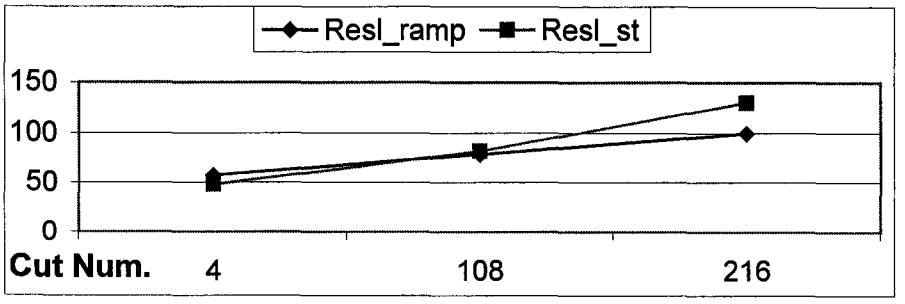

(h) Resultant backward comparison

Figure 5.6 RMS Comparison Between Ramp and Straight Cuts

Figure 5.6 shows RMS comparison between ramp and straight cut for each X, Y, Z, and resultant force, where the resultant force is calculated as

$$Resultant\ Force = \sqrt{X^2 + Y^2 + Z^2}$$

216 ramp and straight cuts were machined (6 work-pieces and 36 cuts on each work-piece). Odd cut numbers correspond to forward cuts and even cut numbers are for backward cuts. X axis represents cut number (first, middle and last are marked) and Y axis represents force magnitude in lbs.

As machining goes on in all cases except Z forward, RMS values of straight cuts show higher force values. In case of Z forward, ramp cut results in higher force because the tool presses down on the work-piece as machining goes on. The resultant force for forward cuts is however still lower than for straight cuts. The trends observed in this comparison suggest that the ramp cut requires less force than straight cuts.

Table 5.2 shows percentage differences of RMS at the last cut between ramp and straight cuts. Negative sign for Z forward indicates that the RMS value of ramp cut is higher than straight cut. Resultant force shows that the straight cut results in higher RMS values than the ramp cut by about 30 % for both forward and backward cases.

To further investigate in detail, the middle value at A9 in each cut, where the depth of cut for ramp and straight cuts are the same is compared. Mid point comparison is shown in Figure 5.7. X axis represents cut number and y axis represents force in lbs.

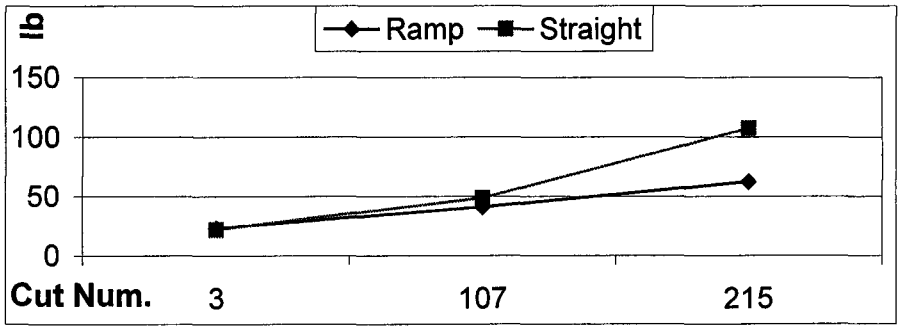

(a) X forward comparison

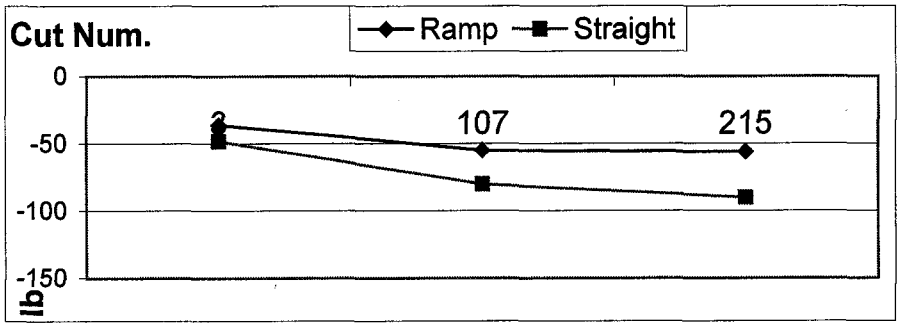

(b) Y forward comparison

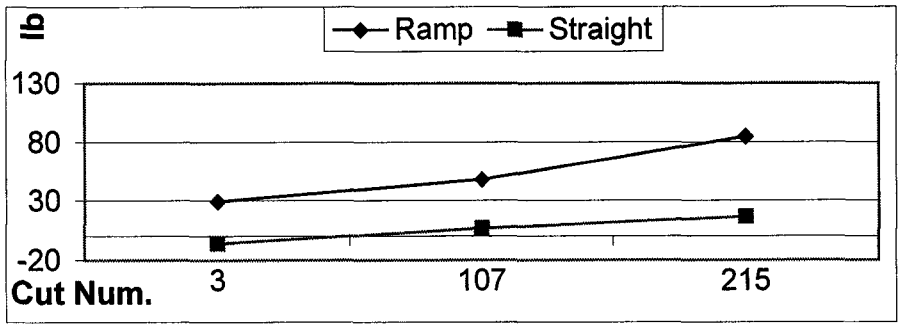

(c) Z forward comparison

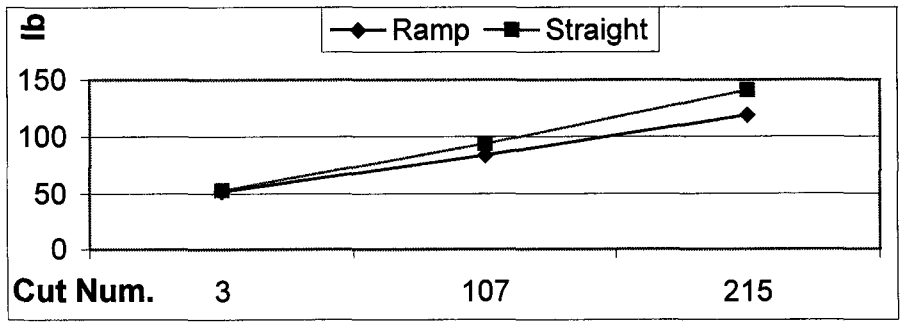

(d) Resultant forward comparison

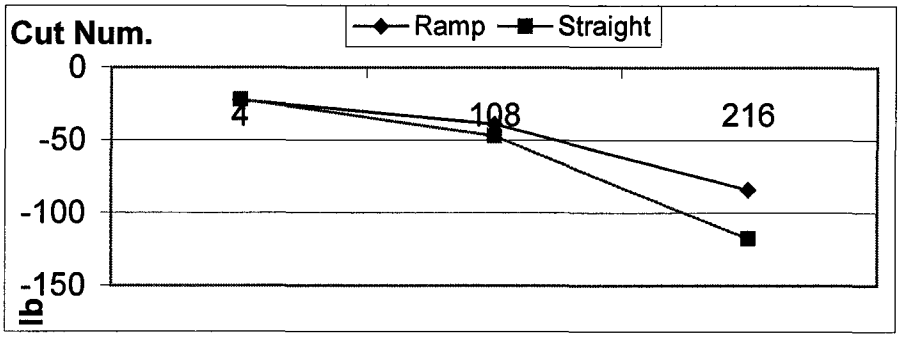

(e) X backward comparison

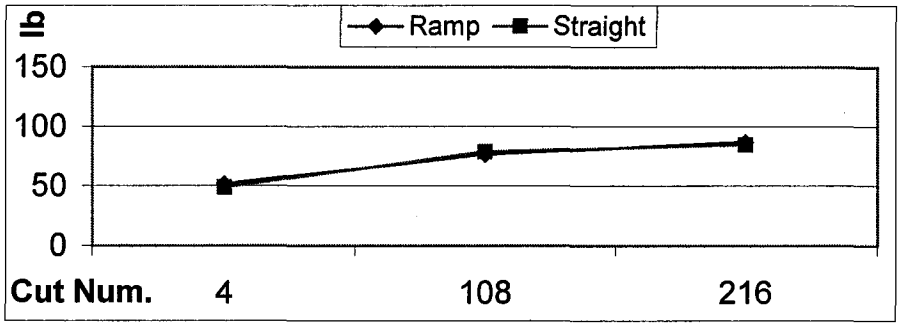

(f) Y backward comparison

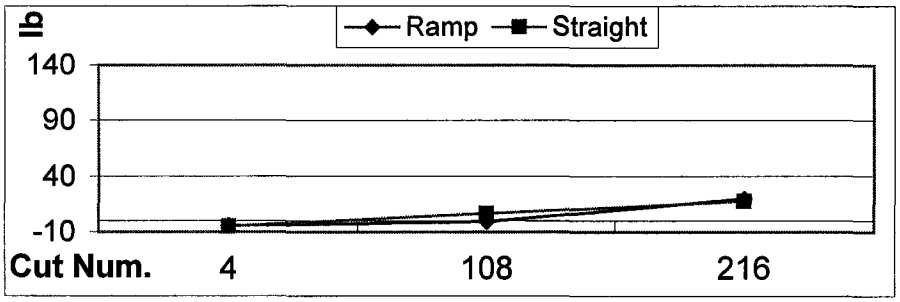

(g) Z backward comparison

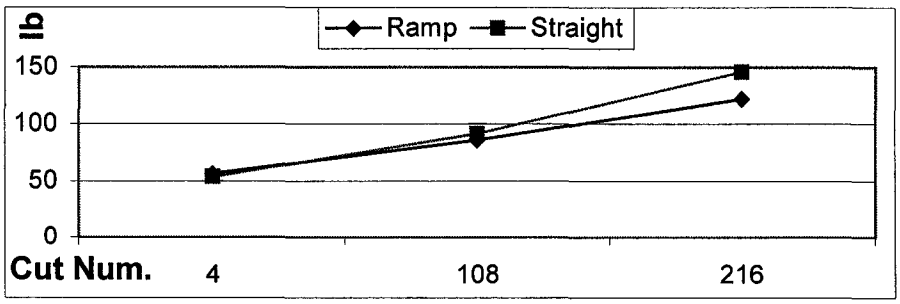

(h) Resultant backward comparison

Figure 5.7 Mid Point Value Comparison Between Ramp and Straight Cuts

Table 5.2 Percentage Difference of RMS at the Last Cut Between Ramp and Straight Cuts

Forward	X	Y	Z	Resultant Force
% difference	86	97	-78	29
Backward	X	Y	Z	Resultant Force
% difference	55	5	3	30

Table 5.3 Percentage Difference of Cutting Force at the Middle of the Last Cut Between Ramp and Straight Cuts

Forward	X	Y	Z	Resultant Force
% difference	72	62	-81	18
Backward	X	Y	Z	Resultant Force
% difference	40	-3	-12	20

As seen from Figure 5.7, cutting force in ramp cut is lower than straight cut at the mid point of each cut except only for Z forward. Again Z forward can be explained in the same way as RMS comparison. The tool in forward ramp cut presses does and results in a higher value of force magnitude. Table 5.3 indicates the percentage differences and is more or less consistent with results in Table 5.2.

5.5 Feed Current Signals

Current sensor signal is used to compare ramp and straight cuts in another way. The current sensor is used to measure current signals from X and Z table motors. Voltage values measured during machining is almost constant at 30 volts. To ensure experimental setup consistency alternate ramp and straight cut are made repeatedly.

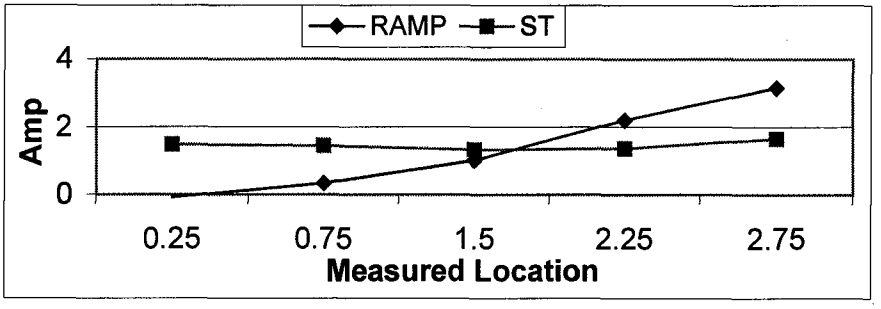

(a) X forward comparison

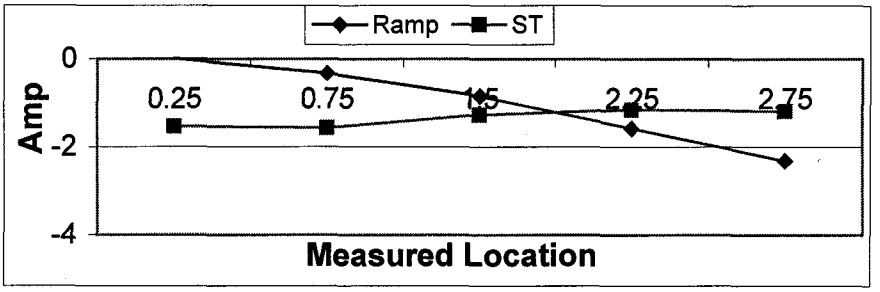

(b) X backward comparison

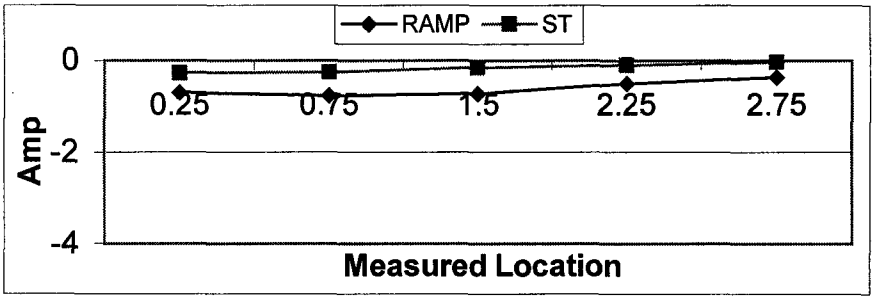

(c) Z forward comparison

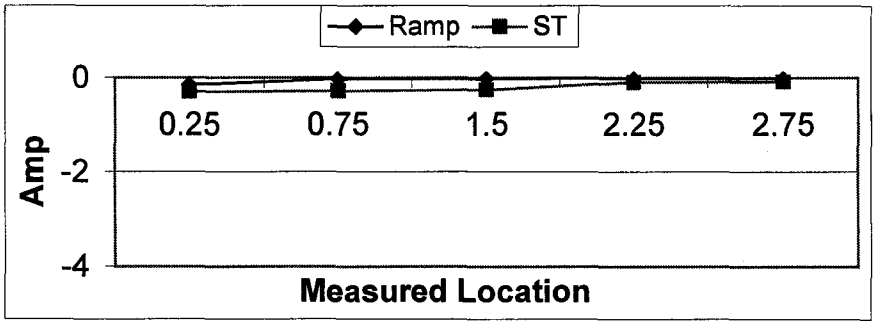

(d) Z backward comparison

Figure 5.8 Comparison of Ramp and Straight Cut Current Sensor Signals

In each cut, data was measured at 5 locations. Since the length of workpiece is 3 inches, measured locations were decided at 0.25, 0.75, 1.5, 2.25, and 2.75 inches at the center of the tool. In Figure 8 ramp and straight cut signals are plotted for X and Z current signals.

Table 5.4 Percentage Difference of Area of X Current Signals Between Ramp and Straight Cuts

	Fwd ramp	Fwd st.	Bwd ramp	Bwd st.
Area	3.18	3.56	2.4	3.34
% diff.		10.7%		28%

In Figure 5.8, it is noticed that the ramp cuts show lower values of current for the X motor at the middle of the cut for both forward and backward cuts. In case of Z forward, ramp cut shows a higher value of current since the tool presses down on the work-piece. In addition, an almost constant trend is noticed because the bottom teeth of the end mill removes only unit amount of chips. Straight Z forward, straight Z backward, and ramp Z backward signals show almost zero values during machining since the tool remains at the same height. Table 5.4 shows area calculations for X current signals to compare ramp and straight cuts for forward as well as backward cuts. The area is less by about 10 % and 28 % for ramp cuts compared to straight cuts. Consequently, the power consumption for straight cuts is expected to be higher than ramp cuts since power is multiplication of voltage and current.

5.6 Tool Wear

Pictures are taken in an SEM to see the teeth from top view and with a microscope to view the side teeth. The worn tool after 216 cuts is compared with a brand new tool for both ramp and straight cuts. Figure 5.9 shows tool edges from top view with SEM and Figure 5.10 shows side teeth with microscope.

It is evident from Figure 5.1 and also observed from Figure 5.9 that the contact area between the tool and work-piece for ramp cut is twice longer than the straight cut for removing the same amount of volume. Therefore, there is more stress concentration in straight cuts than in ramp cuts and this leads to increased tool wear in straight cuts. Worn area for the ramp cut is 1.94 mm^2 and 3.32 mm^2 for the straight cut.

Figure 5.10 shows side view of the teeth of the cutting tools. It indicates clearly that the tool for the straight cut is worn more than the one for ramp cut.

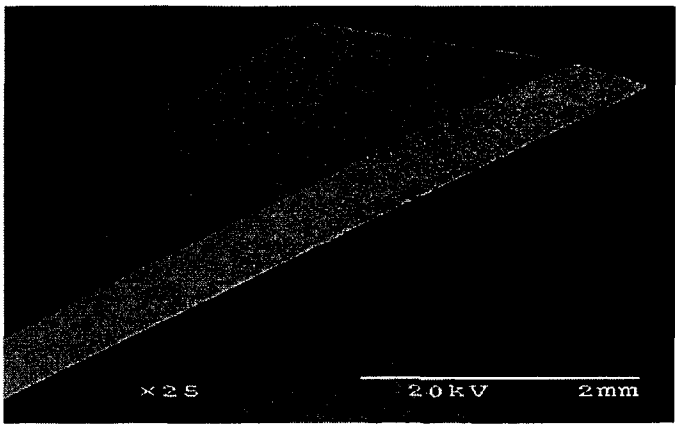

(a) Brand new tool

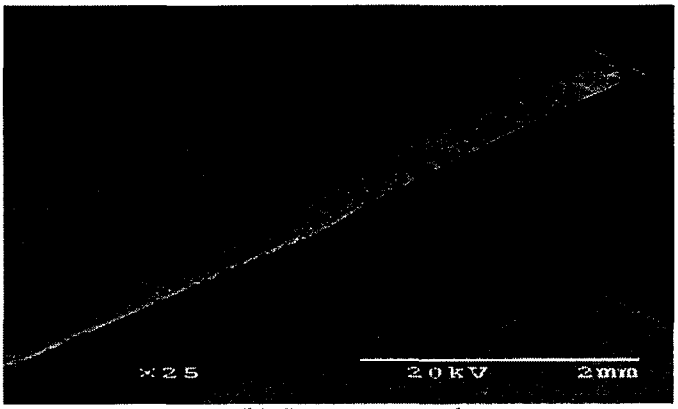

(b) Ramp cut tool

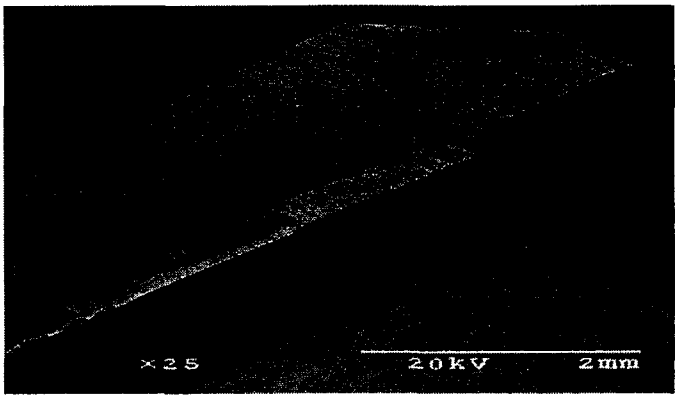

(c) Straight cut tool

Figure 5.9 SEM Pictures of the Tools

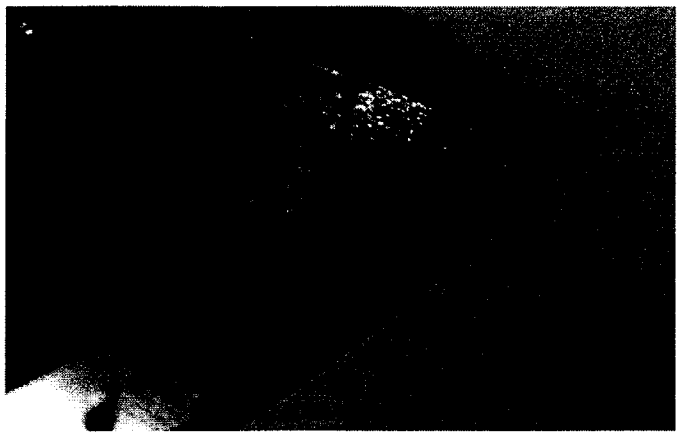

(a) Brand new tool

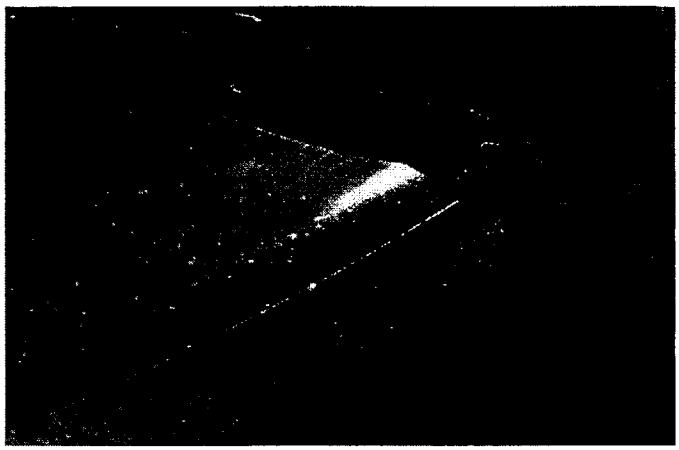

(b) Ramp cut tool

(c) Straight cut tool

Figure 5.10 Side Views of the Teeth with Microscope

5.7 Conclusion

Experimental cutting force data in ramp and straight cuts in end milling measured with dynamometer and current sensors were compared for the trends in the X, Y and Z signals. The wavelet transform was used to generate an accurate and compact representation with multilevel signal decomposition of cutting forces. It was observed that ramp cuts needed less cutting forces and power consumption than straight cuts. Ramp cut shows less RMS values than straight cut except for the forward Z force attributed to geometric reasons. However, X and Y forces are lower and consequently the resultant force is lower for ramp cuts. In the mid point comparison, ramp cut also shows less or about same values of forces compared to the straight cut. Comparing table motor currents also shows that ramp cuts use less cutting force than straight cuts. Picture analysis with SEM and microscope also shows clearly that the tool for straight cut has worn more than the one for ramp cut.

5.8 Acknowledgement

This research is supported by the National Science Foundation under grant No. DMI 9970083. Any opinions, findings, and conclusions or recommendations expressed in this material are those of the authors and do not necessarily reflect the views of the National Science Foundation. The authors gratefully acknowledge help from Jim Dautremont in Mechanical Engineering and Kevin Brownfield in Industrial and Manufacturing Systems Engineering for assistance with the experiments.

5.9 References

[1] Choi, Y. and Narayanaswami, R. (2002), "Experimental Observations of Cutting Force and Tool Wear Effects in Ramp Cuts in End milling", *Transactions of NAMRI/SME*, Vol. 30, pp. 191-198.

[2] El - Wardany, T. I. and Elbestawi, M. A. (1997), "Prediction of Tool Failure Rate in Turning Hardened Steels", *International Journal of Advanced Manufacturing Technology*, Vol. 13, pp. 1-16.

[3] Gong, W., Obikawa, T., and Shirakashi, T. (1997), "Monitoring of Tool Wear States in Turning Based on Wavelet Analysis", *JSME International Journal*, Vol. 40, No. 3, pp. 447-453.

[4] Lee, B. Y. and Tarng, Y. S. (1999), "Application of the Discrete Wavelet Transform to the Monitoring of Tool Failure in End Milling Using the Spindle Motor Current", *International Journal of Advanced Manufacturing Technology*, Vol. 15, pp. 238-243.

[5] Li, X. (1998), "Real-time Detection of the Breakage of Small Diameter Drills with Wavelet Transform", *International Journal of Advanced Manufacturing Technology*, Vol. 14, pp. 539-543.

[6] Li, X., Djordjevich, A., and Venuvinod, P.K. (2000), "Current Sensor Based Feed Cutting Force Intelligent Estimation and Tool Wear Condition Monitoring", IEEE Transactions of Industrial Electronics, Vol. 47, No. 3, pp. 697-701.

[7] Tansel, I., Rodriguez, O., Trujillo, M., Paz, E., and Li, W. (1998), "Micro-end-milling - I. Wear and Breakage", *International Journal of Machine Tools and Manufacture*, Vol. 38, pp. 1419-1436.

[8] Wang, L., Mehrabi, M. G., and Kannatey-Asibu, E., Jr. (2001), "Tool Wear Monitoring in Machining Processes Through Wavelet Analysis", *Transactions of NAMRI/SME*, Vol. 29, pp. 399-406.

CHAPTER 6. TOOL WEAR ESTIMATION AND MONITORING SPINDLE MOTOR CURRENT

6.1 Tool Wear Estimation

In order to investigate tool wear estimation for both ramp and straight cut, the same cutting condition is chosen as shown in Chapter 5 (spindle speed: 1,000 rpm, feed rate: 10 inch/min, and depth of cut: 0 to 0.1 inch for ramp cut and 0.05 inch for straight cut). 3 tools are used for each ramp and straight cut. At first, brand new tools machined 2 workpieces (72 cuts for each case), second another set of new tools machined 4 workpieces (144 cuts for each case), and finally the last set of new tools machined 6 workpieces (216 cuts for each case).

Repeatability of data in the range of cut number 1 to 72 and 1 to 144 has been checked and shown in Figure 6.1 and 6.2. Figure 6.1 and 6.2 show RMS values of wavelet approximation coefficients at approximation level 9 (A9) as cut number increases for each ramp and straight cut. Figure 6.1(c) and 6.2(c) show the machining of 6 workpieces (216 cuts, 36 cuts/workpiece). The data have been analyzed with linear regression that shows about 0.97 ~ 0.99 R-squares.

Figure 6.3 and 6.4 show top views of the tool using the SEM and side views using a microscope for each ramp and straight cuts as machining progresses. It is noticed that the tools are getting worn progressively. The contact area between the tool and work-piece for the ramp cut is twice as long as the contact area between the tool and workpiece for the straight cut when removing the same amount of materials. Therefore, there is more stress concentration in straight cuts than in ramp cuts and this leads to increased tool wear in straight cuts.

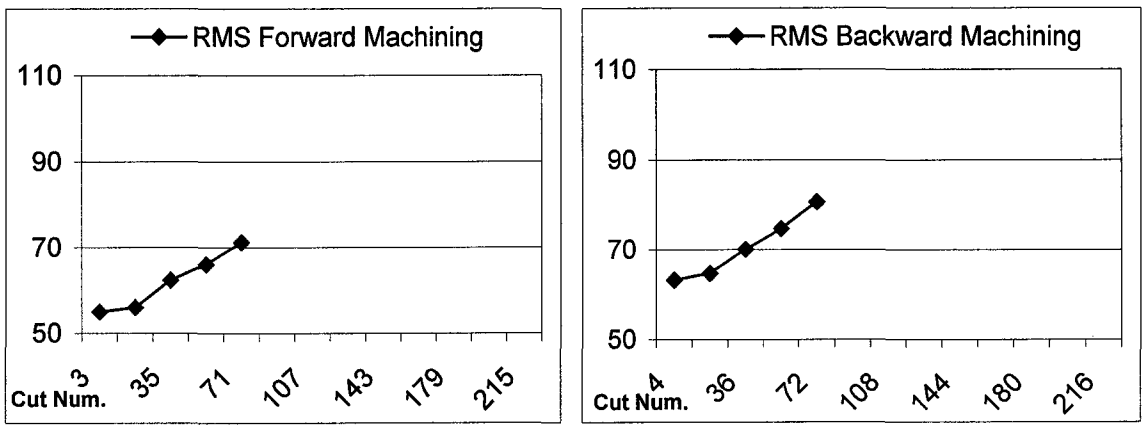

(a) Forward and backward cuts with 2 workpieces

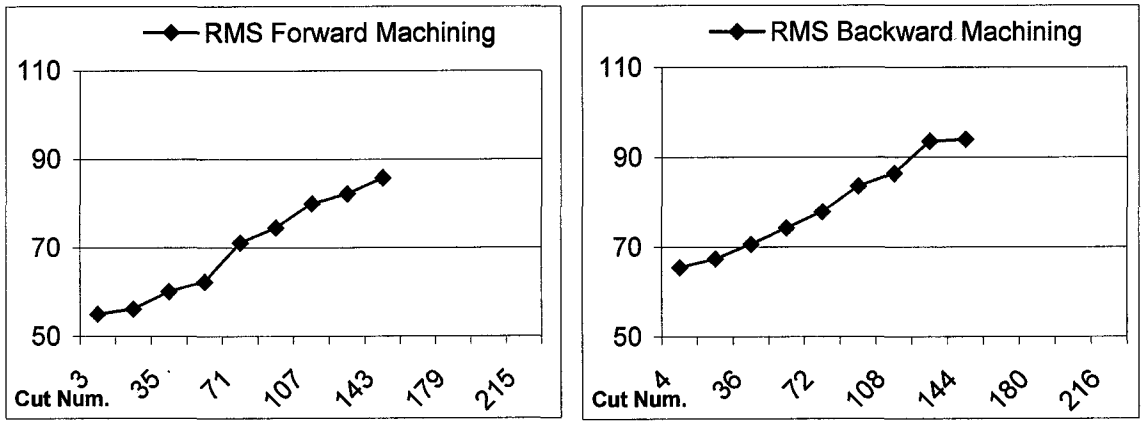

(b) Forward and backward cuts with 4 workpieces

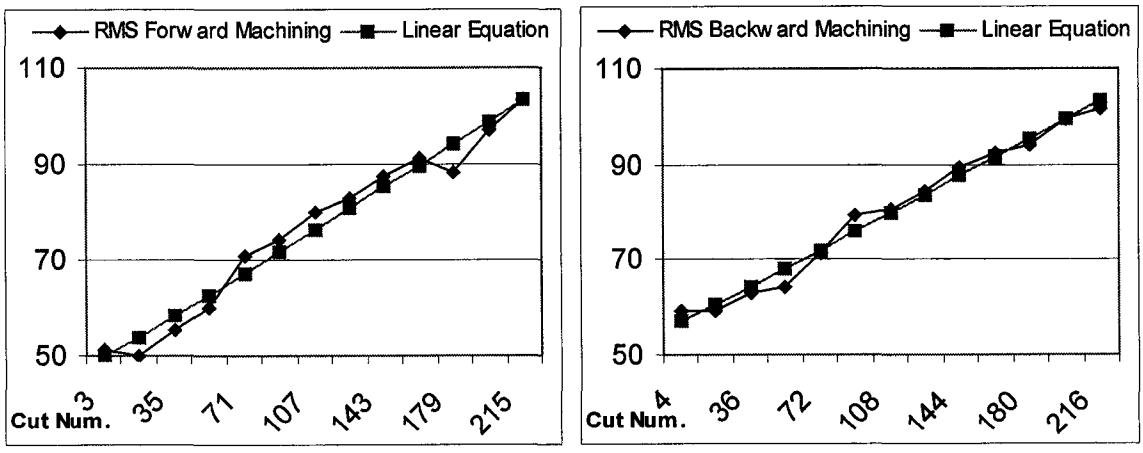

(c) Forward and backward cuts with 6 workpieces

Figure 6.1 Repeatability of Cutting Forces in Ramp Cut with Various Cut Numbers

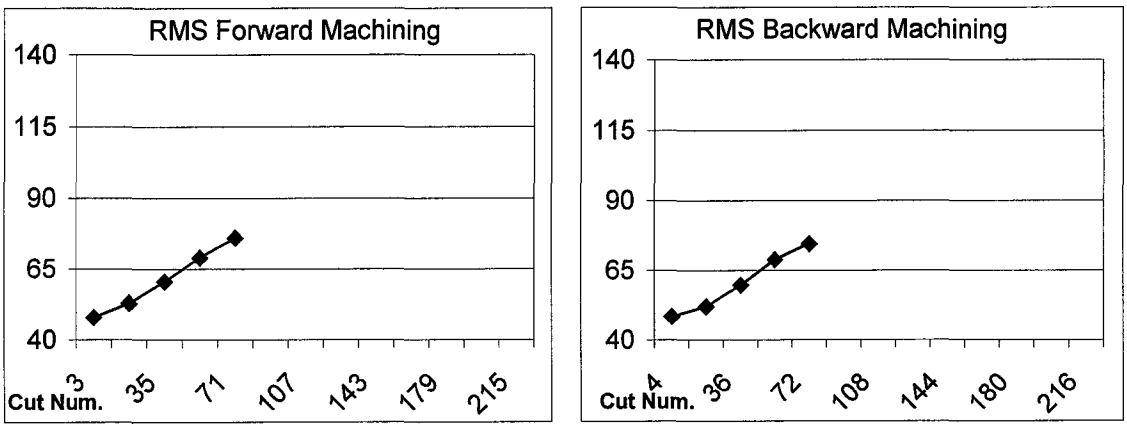

(a) Forward and backward cuts with 2 workpieces

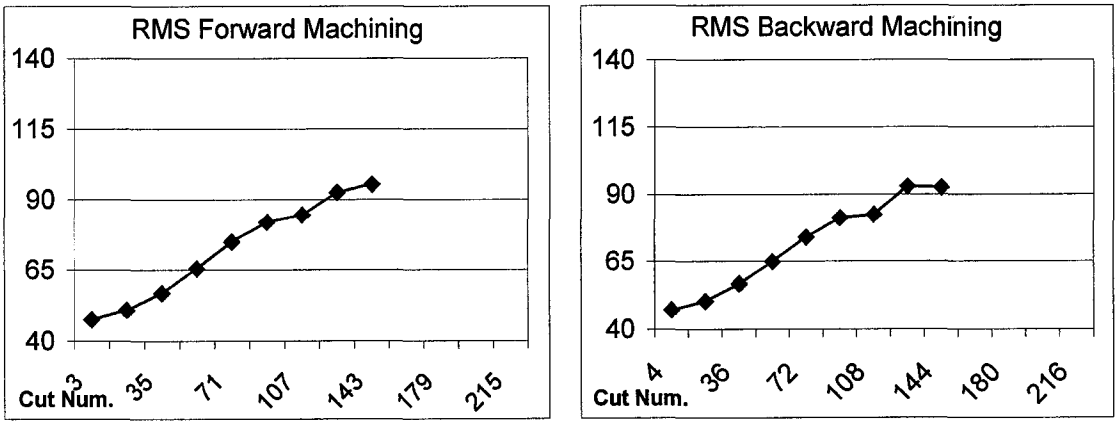

(b) Forward and backward cuts with 4 workpieces

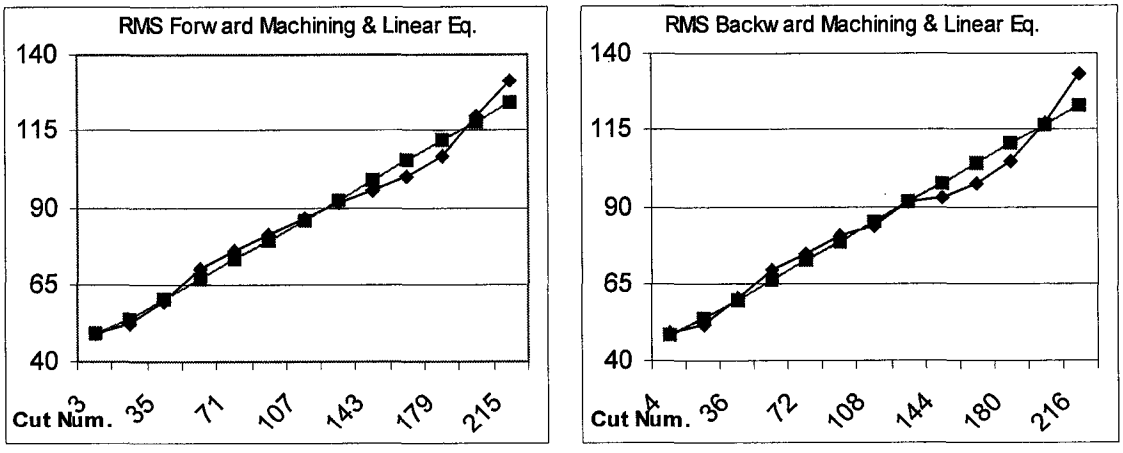

(c) Forward and backward cuts with 6 workpieces

Figure 6.2 Repeatability of Cutting Forces in Straight Cut with Various Cut Numbers

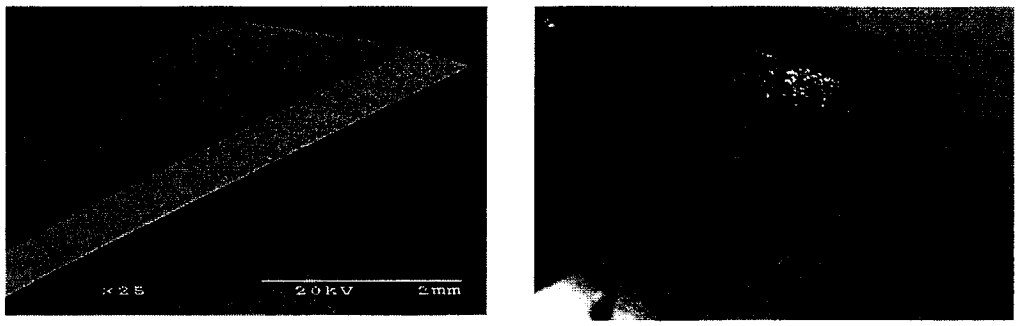

(a) Brand new tool

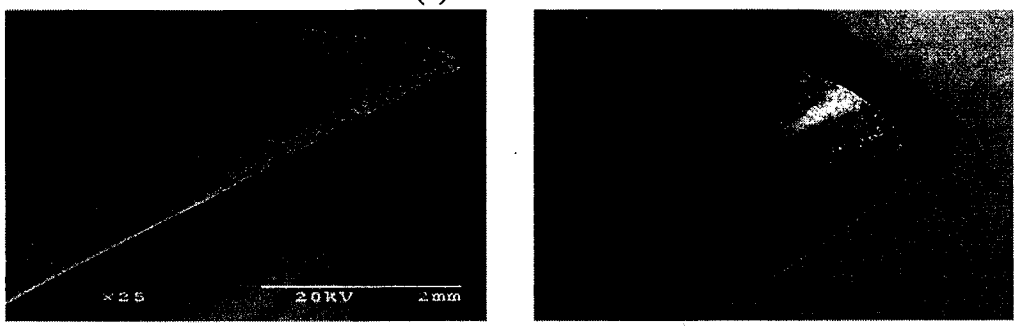

(b) Tool after machining 2 workpieces (72 cuts)

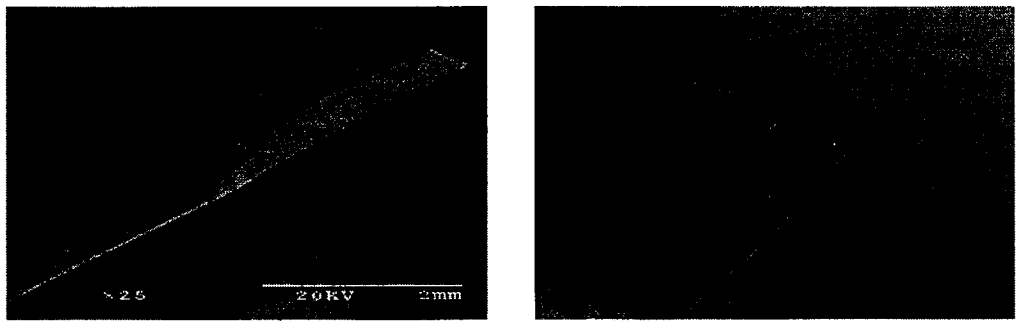

(c) Tool after machining 4 workpieces (144 cuts)

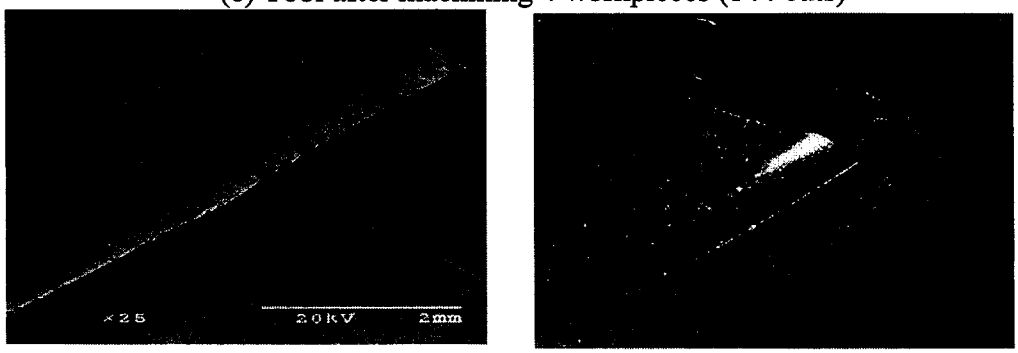

(d) Tool after machining 6 workpieces (216 cuts)

Figure 6.3 Top and Side Views of the Progressive Ramp Cut Tools with SEM and Microscope

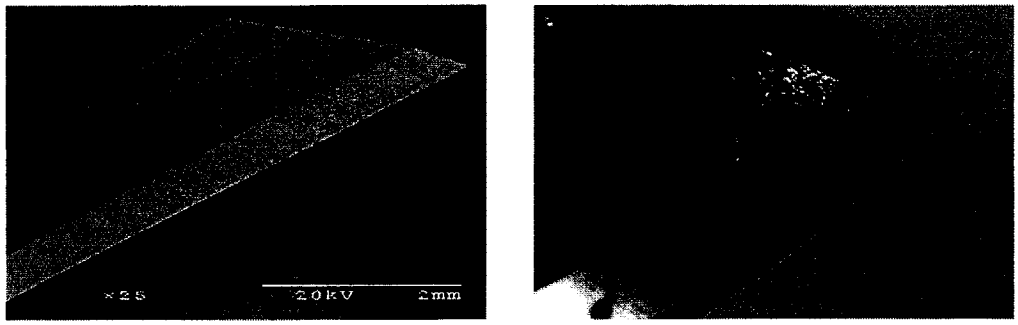

(a) Brand new tool

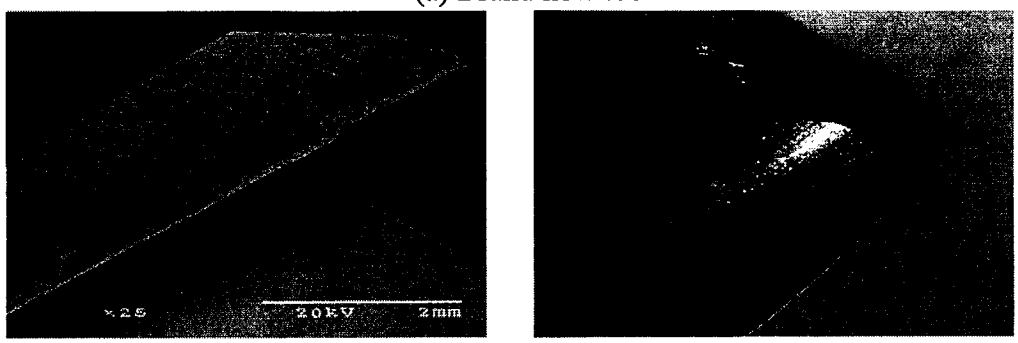

(b) Tool after machining 2 workpieces (72 cuts)

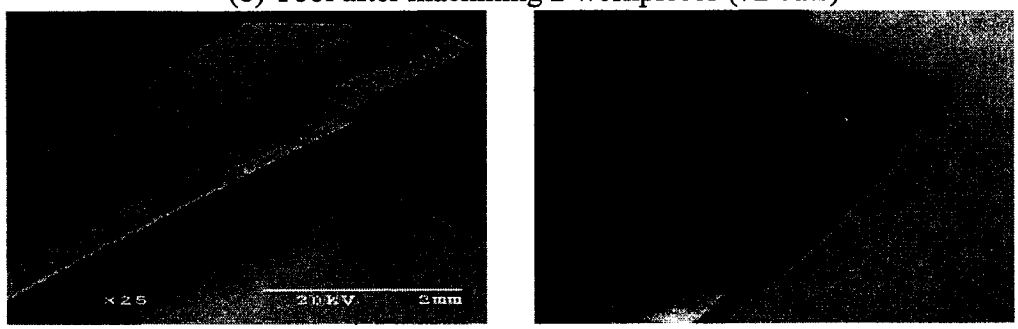

(c) Tool after machining 4 workpieces (144 cuts)

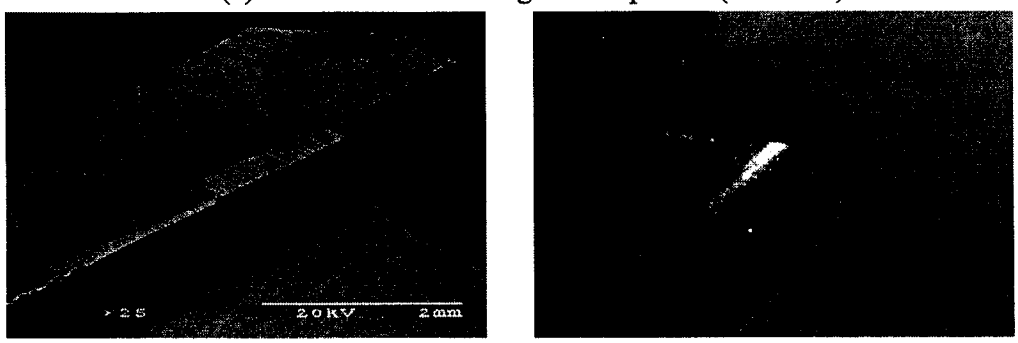

(d) Tool after machining 6 workpieces (216 cuts)

Figure 6.4 Top and Side Views of the Progressive Straight Cut Tools with SEM and Microscope

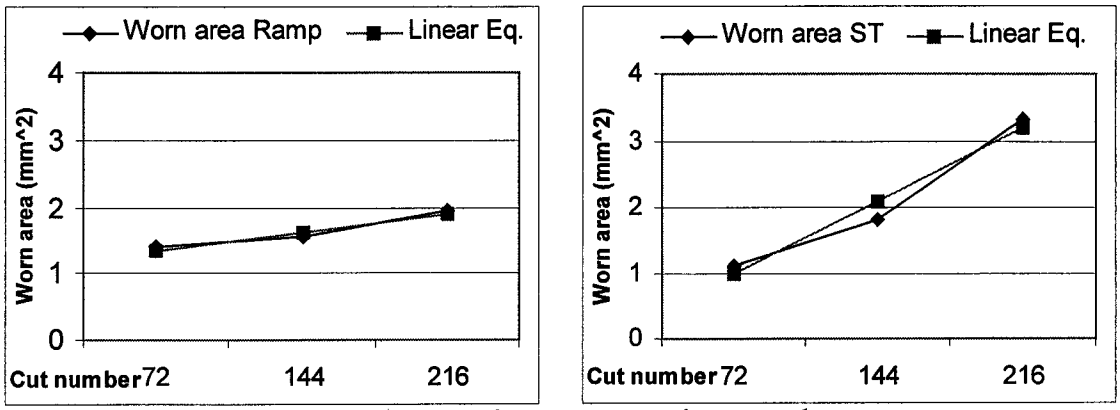

(a) Tool worn area and cut number

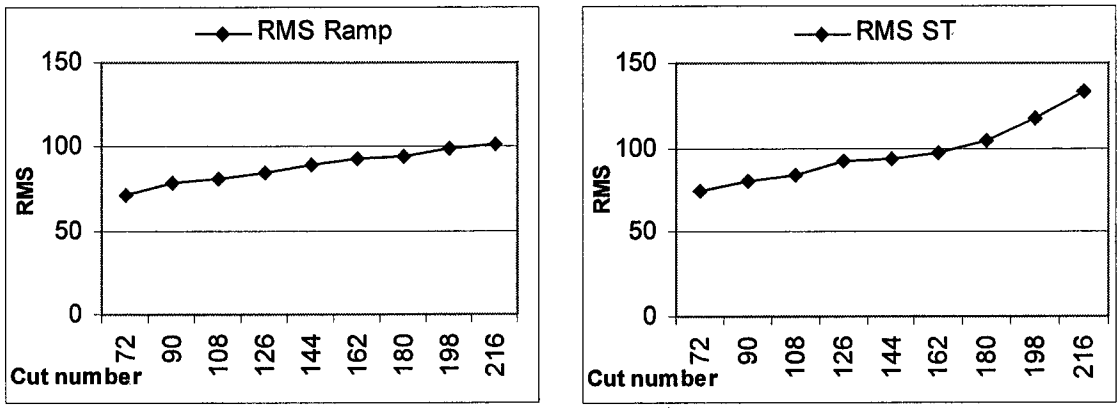

(b) RMS values of cutting forces and cut number

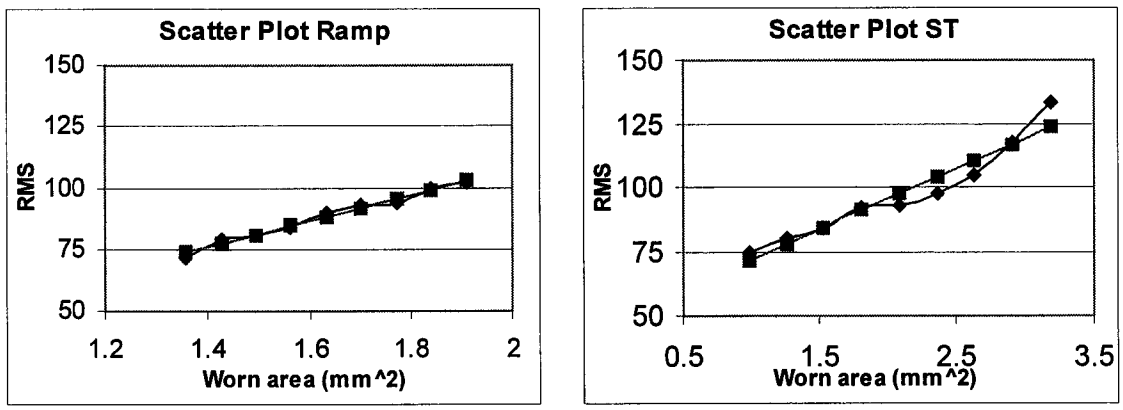

(c) Scatter plots of tool worn areas and RMS of cutting forces

Figure 6.5 Tool Wear Estimation with Tool Worn Area and RMS Values of Cutting Forces

Tool wear has been measured from the top view using Image Tool software. Worn area versus cut number is plotted in Figure 6.5(a) for each ramp and straight cut. Linear regression is used to fit those data and shows 0.96 R-squares on each. Figure 6.5(b) is about RMS values as cut number increases. Those are the same data as used in Figure 6.1(c) and 6.2(c). Scatter graphs are plotted in Figure 6.5(c) for each ramp and straight cut with those data used in Figure 6.5(a) and (b) and those R-squares are 0.98 and 0.92 respectively. Consequently, cutting force data can be drawn from measured worn tool area.

Worn area for the ramp cut is 1.94 mm^2 and 3.32 mm^2 for the straight cut. The reduced machined slot width between the beginning and last cut is 0.2388mm for ramp cut and 0.1575 mm for straight cut with CMM. The reason is the probe of the CMM used in this measurement has about 4 mm diameter. Because of the probe nose at the edge of the bottom inside the slot, the slot thickness could not be measured exactly. However, Those slot thickness has been measured by vernier calipers and showed reduced slot width 0.35 mm for ramp cut and 0.63 mm for straight cut. Table 6.1 shows the tool worn area and slot width for ramp and straight cuts as machining progresses.

Table 6.1 Tool Worn Area and Slot Width

Measured new tool diameter 12.67mm	**Ramp cut**		**Straight cut**	
	Worn area (mm^2)	**Slot width (mm)**	**Worn area (mm^2)**	**Slot width (mm)**
At first	-	12.75	-	12.85
After machining 2 wkpcs	1.39	12.57	1.12	12.55
After machining 4 wkpcs	1.57	12.45	1.82	12.45
After machining 6 wkpcs	1.94	12.40	3.32	12.22

6.2 Monitoring Spindle Motor Current

Spindle motor current has been measured to monitor ramp and straight cut in the different way. The spindle motor in a CNC machine is a 3- phase AC motor. In this type of motor 3-phase alternating currents are generated when a magnet rotates inside a generator with three coils positioned at 120 degrees from each other. There will be a rotating magnetic field, which causes an induced current in the rotor and creates a torque to rotate the rotor when the 3-phase AC motor runs. A power meter is used to measure spindle motor current as shown in Figure 6.6.

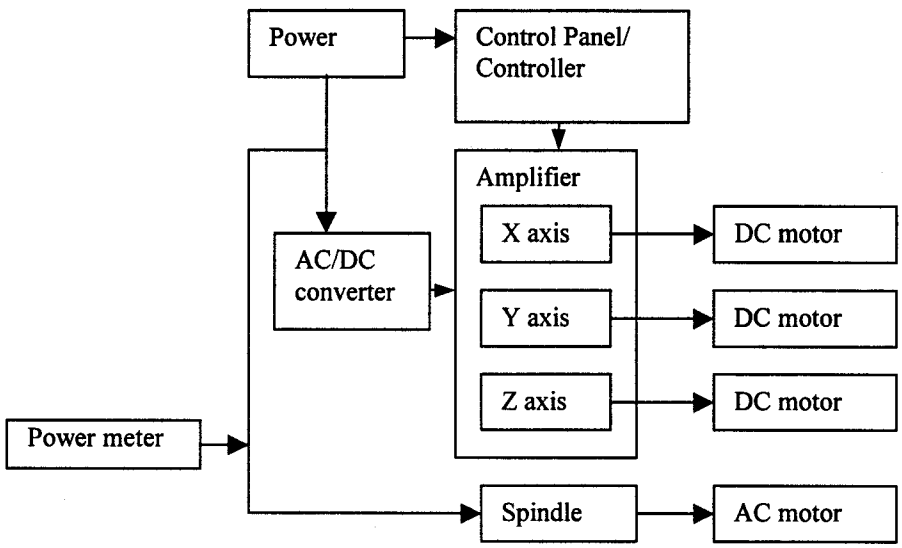

Figure 6.6 Schematic Control Diagram of CNC Machining Center

Voltage values measured during machining are almost constant at 225 volts. To ensure experimental setup consistency alternate ramp and straight cut are made repeatedly as the case of feed motor currents in Chapter 5. In each cut, data was measured at 5 locations. Since the length of workpiece is 3 inches, measured locations were decided at 0.25, 0.75, 1.5,

2.25, and 2.75 inches at the center of the tool. In Figure 6.7 ramp and straight cut signals are plotted for spindle motor current signals on each forward and backward machining.

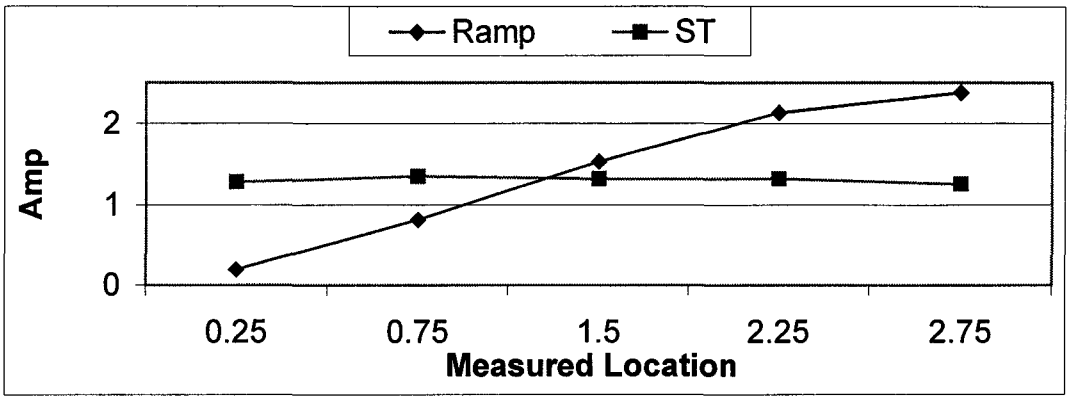

(a) Forward spindle motor currents in ramp and straight cuts

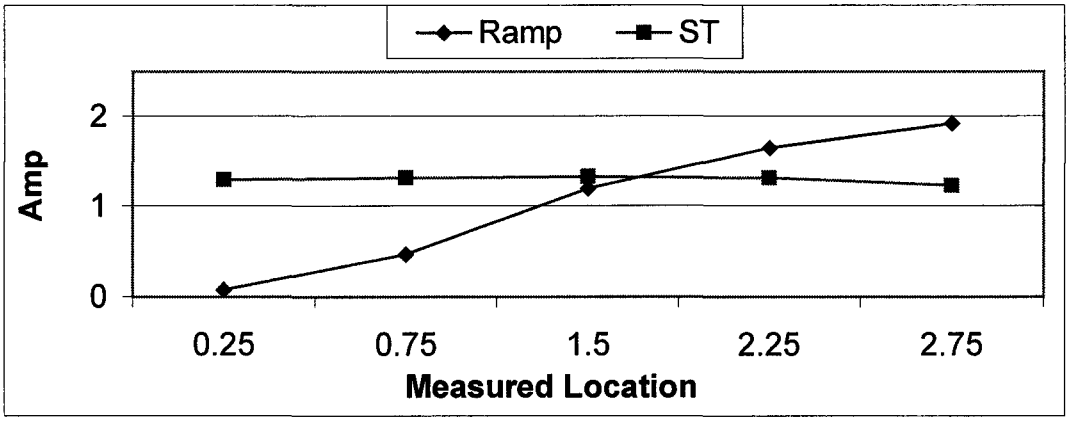

(b) Backward spindle motor currents in ramp and straight cuts

Figure 6.7 Spindle Motor Currents in Ramp and Straight Cuts

Table 6.2 Percentage Difference of Area of Spindle Motor Current Signals Between Ramp and Straight Cuts

	Fwd ramp	Fwd st.	Bwd ramp	Bwd st.	Comb. ramp	Comb. st.
Area	3.64	3.30	2.71	3.26	6.35	6.56
% diff.		10.2%		-20.1%		-3.3%

In Figure 6.7, it is noticed that the ramp cuts show higher values of spindle motor current at the middle of the cut for forward cut and show lower values for backward cuts compared to straight cuts. This is because the tool presses down on the workpiece as machining goes on while the tool moves straight back for backward ramp cut. Spindle motor current signals for the straight cuts are almost the same and consistent for forward and backward cuts. Because the only difference is moving direction. Table 6.2 shows area calculations for spindle motor current signals to compare ramp and straight cuts for forward as well as backward cuts. The area for a forward ramp cut is more by about 10 % compared to a forward straight cut. The area for a backward ramp cut is less by about 20 % compared to backward straight cut. Combined forward and backward cuts show the ramp cut is less by about 3.3 %. Consequently, the power consumption for straight cuts is expected to be higher than ramp cuts since power is multiplication of voltage and current.

6.3 Physical Insight

In this research, one type of the tool and workpiece is used. It is recommended to use lower speed ranges for hard, tough, and abrasive materials and higher speed ranges for soft materials, better finishes, smaller diameter cutters. It is better to use higher feeds for heavy, roughing cuts, high tensile strength materials, abrasive materials, and lower feeds for light, and finishing cuts, deep slots, low tensile strength materials. EMSIM simulation shows how different materials affect on cutting forces and those are displayed in Table 6.3.

It is clearly noticed that cutting forces were getting higher as the hardness of workpiece increases. If harder material need to be used, such as gray cast iron (150- 220 BHN), it is better to use a harder tool like carbide.

Table 6.3 Effect of Material Types on the Cutting Forces (lb) with HSS Tool

Types of wkpc	Avg. X force	Avg. Y force	Avg. Z force	Avg. R- force
2024 aluminum	-8.64	22.07	-6.67	24.69
1018 steel	-19.15	43.64	-5.14	48.22
1048 steel	-41.95	74.03	-8.11	87.55

Xu and Geng (2002) used Ti Beta 21S which is generally known to be one of the most difficult materials to machine because of its high hardness, high strength at high temperature, affinity to react with the tool materials, and low thermal diffusivity. They suggested that Ti Beta 21S, as a difficult–to-cut material, should be milled with a sharp-edged tool at lower cutting parameters to avoid severe wear of the tool. Coolant should be used to conduct away the cutting heat. A proper tool material should be selected.

According to Ozel and Altan (2000), chip and tool temperatures increase with increasing cutting speed. It is found that the temperatures on the tool rake face are much higher than the temperatures in the shear zone. Predicted maximum tool temperatures are located near to the tool tip but not on the tool tip. This proves that the chip–tool interface friction elevates the temperatures on the rake face as the chip continues to slide on this surface. The highest tool temperatures were predicted on the rake face at the primary (side) cutting edge of the flat end mill insert regardless of cutting conditions. This is due to the additional heat generated by the chip sliding mechanism on the rake face. Those temperatures play a major role in crater wear development at the primary cutting edge.

An important parameter influencing the machining temperature is the form stability of the tool wedge. As the tool wears out, the geometry of the cutting wedge changes, influencing the machining performance. As the tool wear progresses, frictional heating due to the sliding of the material over the cutting zone increases, resulting in the observed rise in the cutting temperature with flank wear (Sreejith et al. 1999).

Cooling influences machining in various ways. At the contact between the chip and tool, cooling can reduce the chip temperature and, thus, affect directly the friction force between the chip and tool. Contact area for ramp cut is twice larger than for straight cut and because depth of cut is keep changing, it allows the tool to cool down faster than the tool for straight cut and generates less cutting force.

CHAPTER 7. CONCLUSIONS

Conclusions of this research are based on the experimental observations and results that have been presented and discussed on three individual journal papers that are included in this dissertation as Chapters 3, 4, and 5 and additional Chapter 6. Each of three journal papers focuses on the experimental observations of cutting force and tool wear effects in ramp cut, tool wear monitoring in ramp cut, and comparison of ramp and straight cuts in end milling.

Experimental cutting force data in ramp cuts in end milling were generated and analyzed for tool wear effects. The ramp cuts are unique in that they have a changing depth of cut. The wavelet transform was used to generate a multilevel decomposition of the cutting force signal and was very useful. The RMS value of the approximation coefficients of the wavelet transformed resultant cutting force signal was used to model and estimate tool wear. For smaller depth of cut a linear regression fit of the RMS value of the approximation coefficients was obtained. Under these conditions tool wear was estimated within an error of maximum 6%. Metrology was also used and useful to estimate the tool wear. The slot thickness is continuously reduced as the tool is worn and can serve as another indicator for tool wear estimation.

Cutting force data in ramp and straight cuts is measured with a dynamometer and current sensors were compared for the trends in the X, Y and Z signals. It was observed that ramp cuts needed less cutting forces and power consumption than straight cut. Percentage difference of RMS values of the approximation coefficients between ramp and straight cuts is about 30% and cutting force difference at the middle is about 20%. Area comparison of X

feed current signals from the table motor between ramp and straight cuts shows that the forward ramp cut is less than the forward straight cut by about 10 % and 28 % for the backward cut. Combined forward and backward cut areas show that the ramp cut is less by about 3.3% than the straight cut with spindle motor current.

The ramp cut shows less RMS values than the straight cut except for the forward Z force attributed to geometric reasons. However, X and Y forces are lower and consequently the resultant force is lower for ramp cuts. In the mid point comparison, ramp cuts also shows slightly smaller or about same values of forces compared to the straight cuts. Comparing table and spindle motor currents also shows that ramp cuts use less cutting force than straight cuts. Picture analysis with a SEM and microscope for tool wear estimation also shows clearly that the tool used for straight cuts has worn more than the tool used to make ramp cuts. The estimation of tool wear can be used to plan optimal tool replacement.

Cooling influences machining in various ways. At the contact between the chip and tool, cooling can reduce the chip temperature and, thus, affect directly the friction force between the chip and tool. Contact area for ramp cut is twice larger than for straight cut and because depth of cut is keep changing, it allows the tool to cool down faster than the tool for straight cut and generates less cutting force.

Generally, it is recommended to use lower speed ranges for hard, tough, and abrasive materials and higher speed ranges for soft materials, better finishes, smaller diameter cutters. It is better to use higher feeds for heavy, roughing cuts, high tensile strength materials, abrasive materials, and lower feeds for light, and finishing cuts, deep slots, low tensile strength materials to make efficient machining.

The research done in Chapter 3 had been published in the *Transactions of NAMRI/SME*, Vol. 30, the work in Chapter 4 had been accepted by *International Journal of Advanced Manufacturing Technology*, and Chapter 5 will be submitted to the Journal Publication. Based upon this research, process monitoring in micro machining is suggested as future work.

REFERENCES

Altintas, Y. and Engin, S. (2001), "Generalized Modeling of Mechanics and Dynamics of Milling Cutters," *Annals of the CIRP*, Vol. 50, no. 1, pp. 25-30.

Boothroyd, G. and Knight, W. A. (1989), "Fundamentals of Machining and Machine Tools", Second Edition, *Marcel Dekke, Inc.*

Braghini, A. Jr and Coelho, R. T. (2001), "An Investigation of the Wear Mechanisms of Polycrystalline Cubic Boron Nitride (PCBN) Tools When End Milling Hardened Steels at Low/Medium Cutting Speeds", *International Journal of Advanced Manufacturing Technology*, Vol. 17, pp. 244-257.

Devor, R.E., Kline, W. A. and Zdeblick, W. J. (1980), "A Mechanistic Model of the Force System in End Milling with Application to Machining Airframe Structures," *Proceedings of the 8th North American Metalworking Research Conference*, pp. 297-303.

Ehmann, K. F., Kapoor, S. G., DeVor, R. E., and Lazoglu, I. (1997), "Machining Process Modeling: A Review," *Journal of Manufacturing Science and Engineering*, Vol. 119, Nov., pp. 655-663.

Elanayar, S. and Shin, Y. C. (1996), "Modeling of Tool Forces for Worn Tools: Flank Wear Effects," *Journal of Manufacturing Science and Engineering,* Vol. 118, No. 3, pp. 359-366.

El - Wardany, T. I. and Elbestawi, M. A. (1997), "Prediction of Tool Failure Rate in Turning Hardened Steels", *International Journal of Advanced Manufacturing Technology*, Vol. 13, pp. 1-16.

"EMSIM" (2002), http://mtamri.me.uiuc.edu, simulation software at University of Illinois at Urbana-Champaign, accessed on Jan. 2002.

Gong, W., Obikawa, T., and Shirakashi, T. (1997), "Monitoring of Tool Wear States in Turning Based on Wavelet Analysis," *JSME International Journal*, Vol. 40, No. 3, pp. 447-453.

Huang, P. (1998), "A Fuzzy Logic Approach to Detect Tool Breakage using a Dynamometer", *M.S. Thesis*, Iowa State University.

Lee, B. Y. and Tarng, Y. S. (1999), "Application of the Discrete Wavelet Transform to the Monitoring of Tool Failure in End Milling Using the Spindle Motor Current," *International Journal of Advanced Manufacturing Technology*, Vol. 15, pp. 238-243.

Li, X. (1998), "Real-time Detection of the Breakage of Small Diameter Drills with Wavelet Transform," *International Journal of Advanced Manufacturing Technology*, Vol. 14, pp. 539-543.

Li, X. (1999), "On-Line Detection of the Breakage of Small Diameter Drills using Current Signature Wavelet Transform", *International Journal of Machine Tools and Manufacture,* Vol. 39, pp. 157-164.

Li, X. (2002), "A brief review: Acoustic Emission Method for Tool Wear Monitoring during Turning", *International Journal of Machine Tools and Manufacture*, Vol. 42, pp. 157-165.

Li, X., Djordjevich, A., and Venuvinod, P.K. (2000), "Current Sensor Based Feed Cutting Force Intelligent Estimation and Tool Wear Condition Monitoring", IEEE Transactions of Industrial Electronics, Vol. 47, No. 3, pp. 697-701.

Li, X., Dong, S., and Yuan, Z. (1999), "Discrete Wavelet Transform for Tool Breakage Monitoring", *International Journal of Machine Tools and Manufacture*, Vol. 39, pp. 1935-1944.

Li, X., Tso, S., and Wang, J. (2000), "Real-Time Tool Condition Monitoring using Wavelet Transforms and Fuzzy Techniques", *IEEE Transactions on Systems, Man, and Cybernetics - Part C: Applications and Reviews*, Vol. 30, no. 3, pp. 352-357.

Li, X. and Wu, J. (2000), "Wavelet Analysis of Acoustic Emission Signals in Boring", *Proceedings of the Institution of Mechanical Engineers, Part B: Journal of Engineering Manufacture*, Vol. 214, no. 5, pp. 421-424.

Misiti, M., Misiti, Y., Oppenheim, G., and Poggi, J. (1996), "Wavelet Toolbox," *The Mathworks. Inc.*

Mori, K., Kasashima, N., Fu, J.C., and Muto, K. (1999), "Prediction of Small Drill Bit Breakage by Wavelet Transforms and Linear Discriminant Functions" *International Journal of Machine Tools and Manufacture*, Vol. 39, pp. 1471-1484.

Ozel, T. and Altan, T. (2000), "Process Simulation using Finite Element Method – Prediction of Cutting Forces, Tool Stresses and Temperatures in High Speed Flat End Milling", *International Journal of Machine Tools and Manufacture*, Vol. 40, pp. 713-738.

Smithey, D. W., Kapoor, S. G., and DeVor, R. E. (2000), "A Worn Tool Force Model for Three-Dimensional Cutting Operations," *International Journal of Machine Tools and Manufacture*, Vol. 40, pp. 1929-1950.

Sreejith, P. S., Krishnamurthy, R., Narayanasamy, K., and Malhotra, S. K. (1999), "Studies on the Machining of Carbon/Phenolic Ablative Composites", *Journal of Materials Processing Technology*, Vol. 88, pp 43-50.

Tansel, I. N., Arkan, T. T., Bao, W. Y., Mahendrakar, N., Shisler, B., Smith, D., and McCool, M., (2000), "Tool Wear Estimation in Micro-Machining. Part II: Neural-Network-Based Periodic Inspector for Non-Metals," Vol. 40, pp. 609-620.

Tansel, I. N., Mekdeci, C., and Mclaughlin, C. (1995), "Detection of Tool Failure in End Milling with Wavelet Transformations and Neural Networks," *International Journal of Machine Tools and Manufacture*, Vol. 35, No. 8, pp. 1137-1147.

Tansel, I., Rodriguez, O., Trujillo, M., Paz, E., and Li, W. (1998), "Micro-end-milling - I. Wear and Breakage," *International Journal of Machine Tools and Manufacture*, Vol. 38, pp. 1419-1436.

Trent, E. M. and Wright, P. K. (2000), "Metal Cutting", Fourth Edition, *Butterworth Heinemann.*

Wang, L., Mehrabi, M. G., and Kannatey-Asibu, E., Jr. (2001), "Tool Wear Monitoring in Machining Processes Through Wavelet Analysis," *Transactions of NAMRI/SME*, Vol. 29, pp. 399-406.

Xu, J. H. and Geng, G. S. (2002), "Experimental Study on the Milling of a Ti Beta 21S", *Journal of Materials Processing Technology*, Vol. 129, pp. 190-192.

ACKNOWLEDGEMENTS

First and foremost, I would like to express my greatest gratitude to my major professor, Dr. Ranga Narayanaswami. He has been most influential in my achievements during my graduate studies, as he helped me to grow professionally and become a better researcher. I consider myself very fortunate and privileged to have him as my major professor, since without his academic guidance, personal, and financial support, my past years here at Iowa State would not have been such a pleasant and memorable experience.

I also would like to thank my committee members, Dr. Douglas Gemmill, Dr. Timothy Van Voorhis, Dr. Abhijit Chandra, and Dr. Palaniappa A. Molian for their academic guidance and support. My special appreciation goes to Jim Dautremont in Mechanical Engineering and Kevin Brownfield in Industrial and Manufacturing Systems Engineering for their assistance and expertise with the instrumentation and machining experiments. These experiments could not have been possible without their generous time and effort given in setting up in the lab.

I'd especially like to thank my mother who has endured countless number of emotional and financial sacrifices and difficulties for me to have the best education possible. Without her love and support, I certainly would not be where I am today.